European Research Council
Established by the European Commission

SAPIENZA
UNIVERSITÀ DI ROMA

Lesson 2
jet substructure

Leticia Cunqueiro Mendez

GDR-QCD:HIC in the QCD phase diagram,
Nantes 4th July 2022

Jet substructure

Jets play a central role at the LHC

Jet substructure exploits info on internal radiation pattern, many scopes:

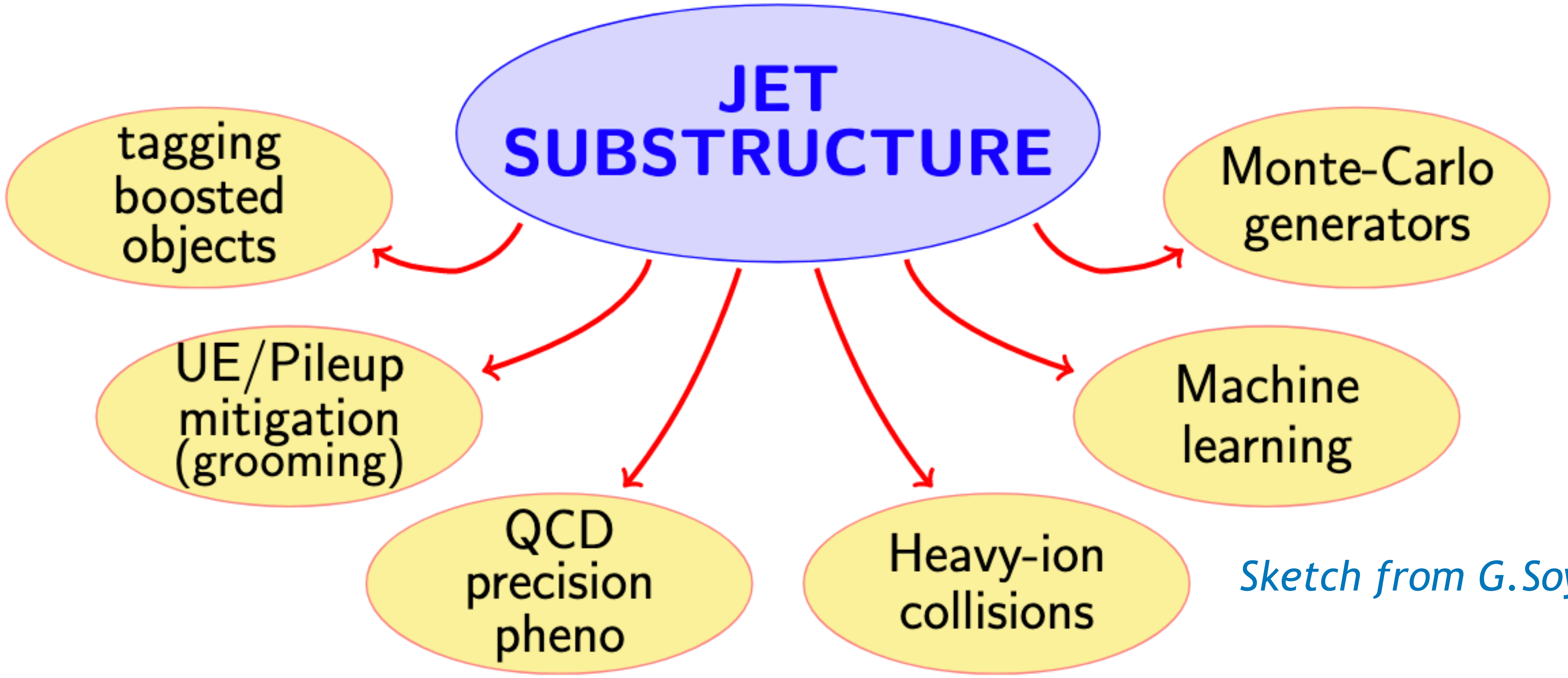

Sketch from G.Soyez

Here:

- Recent results that constrain the parton shower modelling and fixed-order calculations
- Few examples where quantum properties are exposed in new ways

Jet substructure using the clustering history

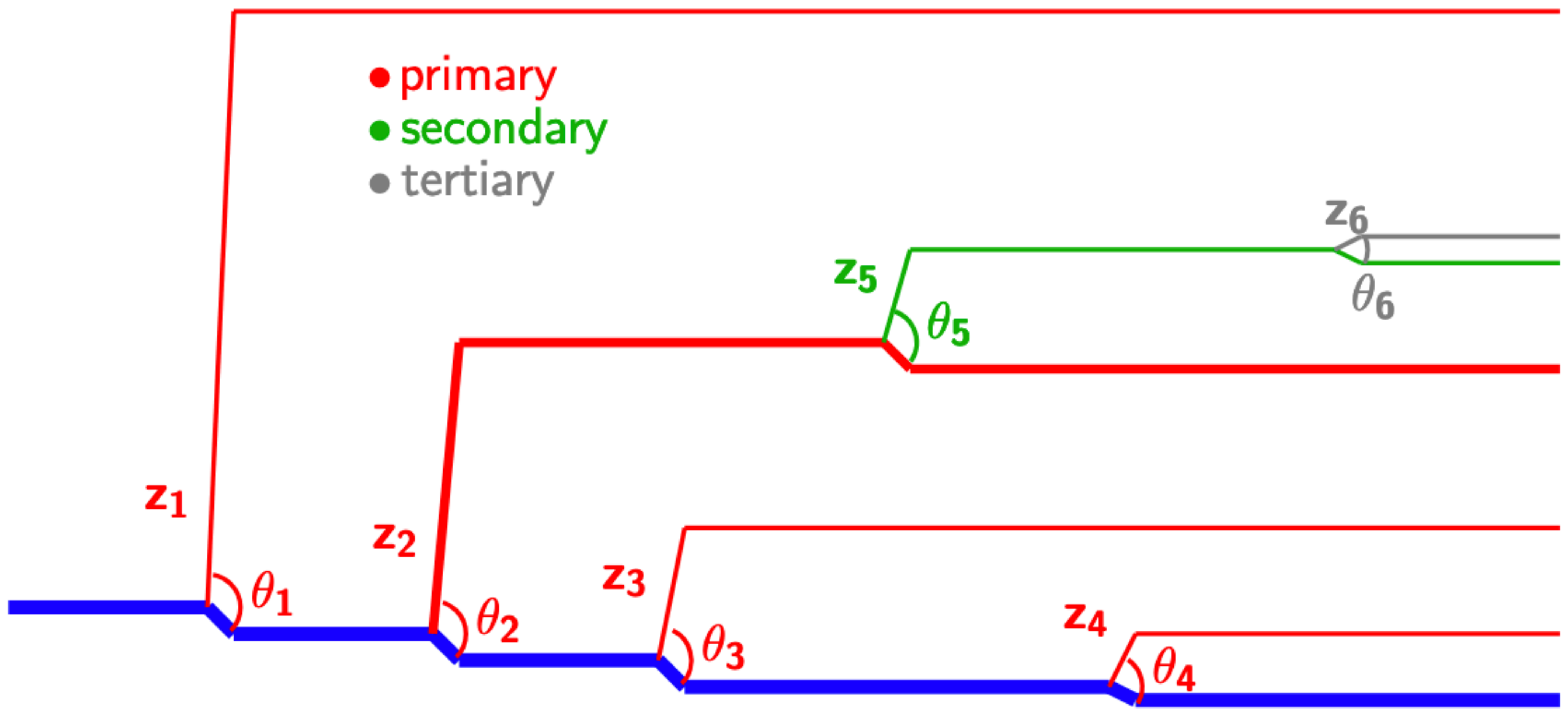

Another sketch from G.Soyez

The Cambridge/Aachen algorithm sequentially combines the closest pairs

The clustering history can be undone iteratively, following always the hardest branch

At each step, two subjet prongs are obtained, **j1** and j2 , with $p_{T,1} > p_{T.2}$

where θ is the angle between the prongs,
$k_T = \theta p_{T,2}$
and $z = p_{T,2}/(p_{T,1} + p_{T,2})$

The iterative declustering proceeds until substructure is found (grooming)
or the jet can be fully declustered to study the kinematics of all the emissions (Lund jet plane)

The primary Lund plane: visualizing the parton shower

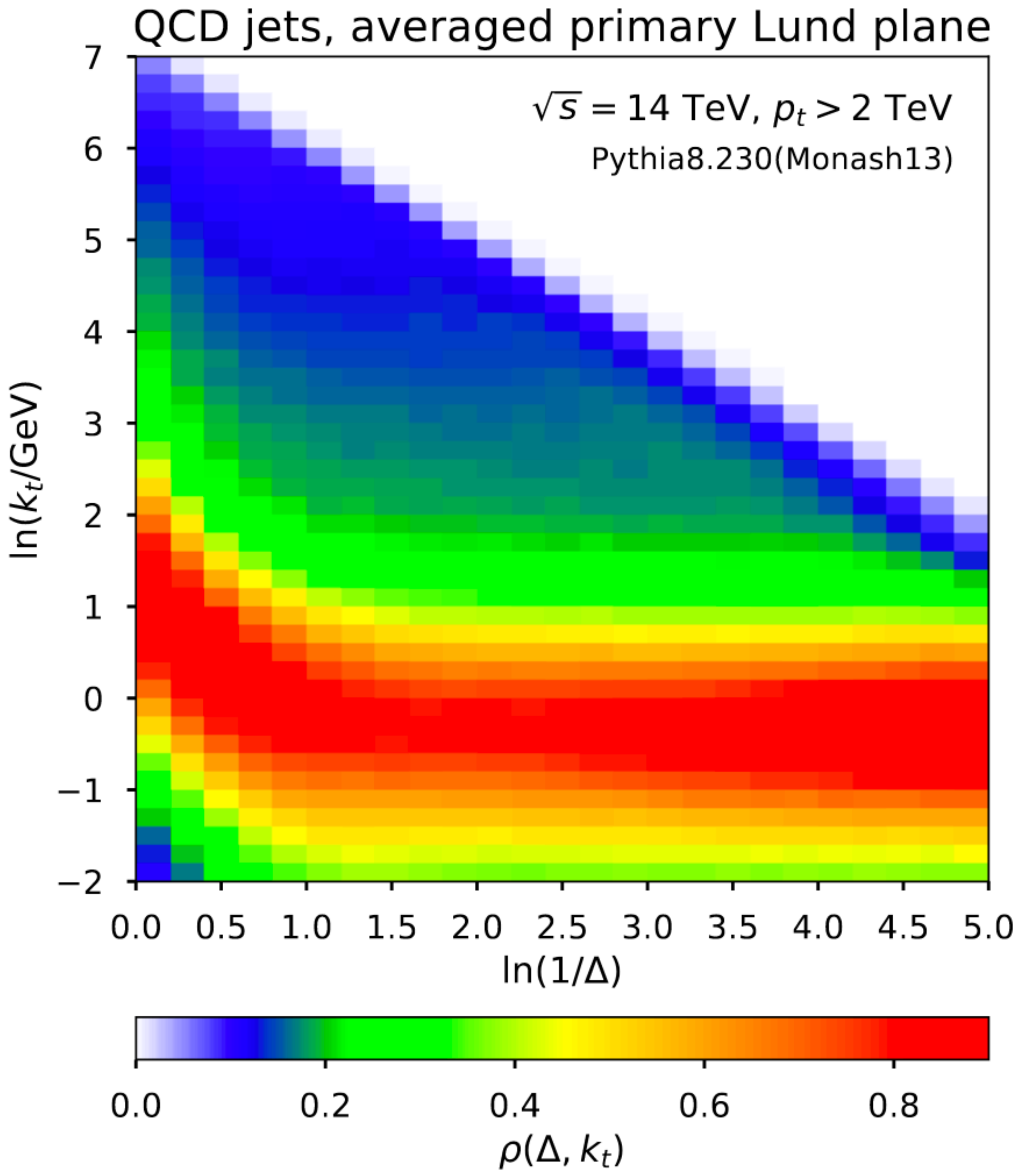

At leading order, emissions populate the plane uniformly and the running of the coupling sculpts the plane

QCD Splitting probability

$$d^2P = 2\frac{\alpha_s(k_\perp)C_R}{\pi}dln(z\theta)dln(\frac{1}{\theta})$$

An all-order calculation is available: *Lifson et al, JHEP 10 (2020) 170*

Vast applications, as a tagger and as an observable!

Dreyer et al, JHEP 12 (2018) 064

The primary Lund plane with ATLAS

ATLAS, Phys.Rev.Lett. 124 (2020) 22, 222002

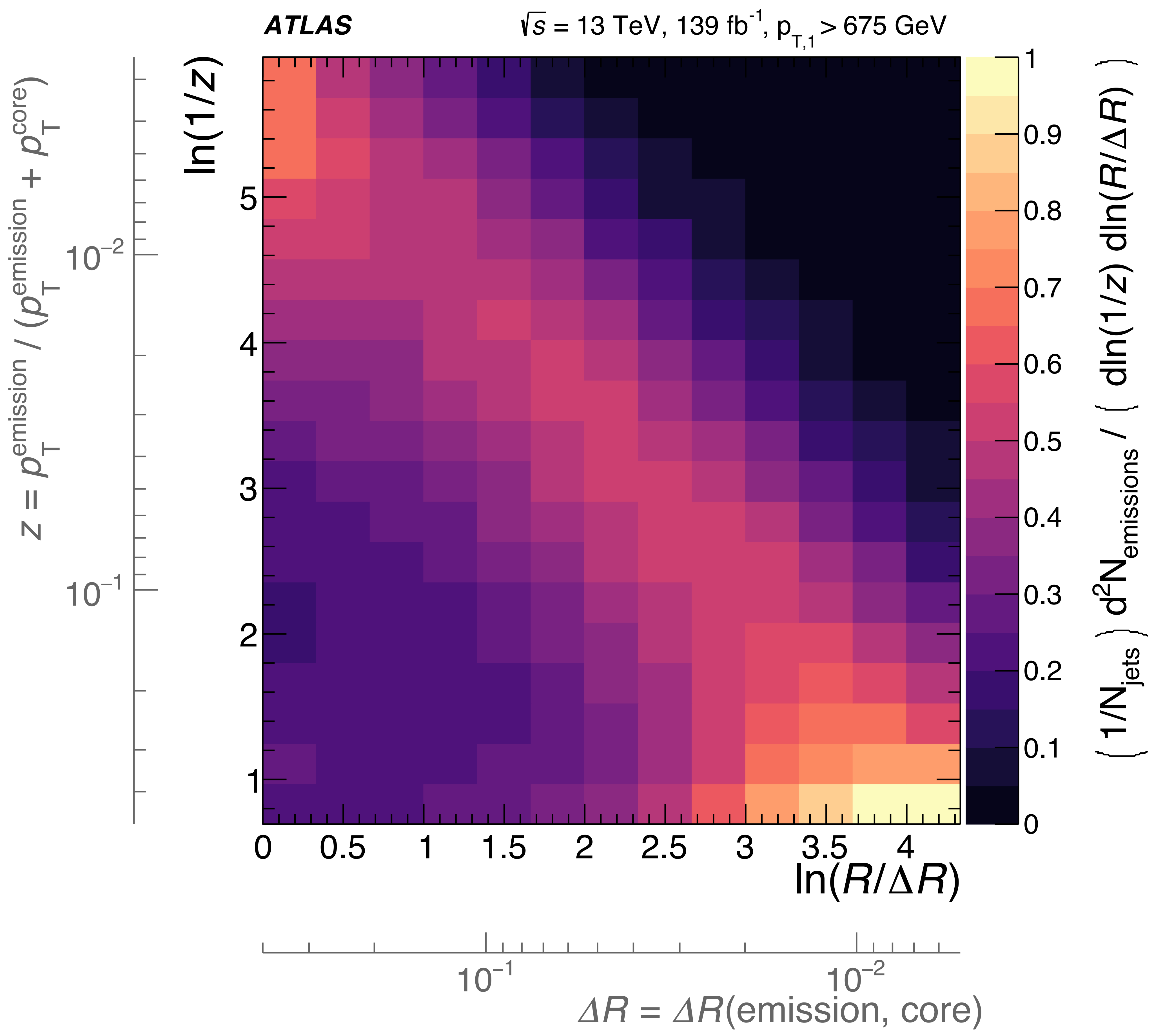

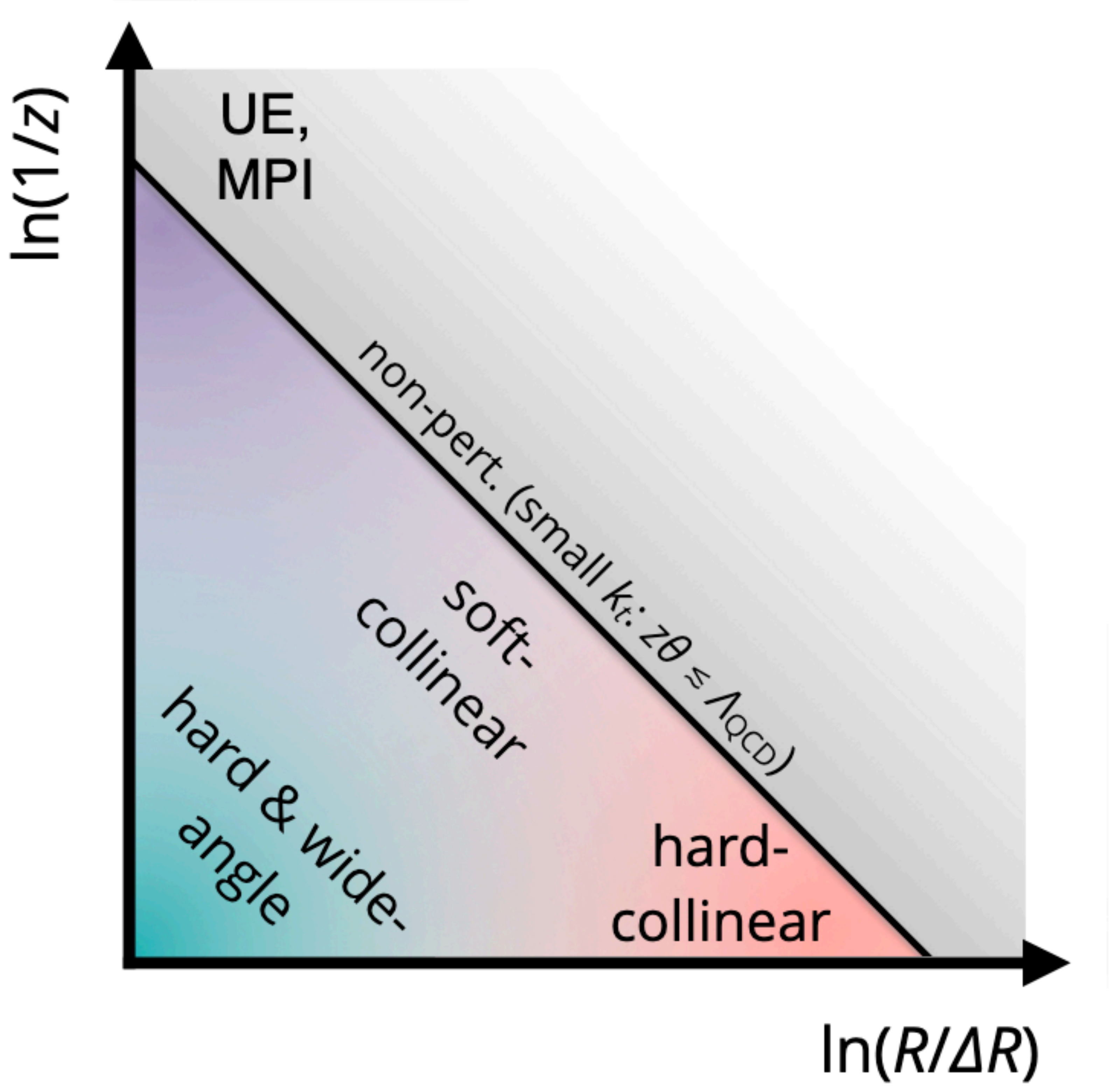

The primary Lund plane with ATLAS

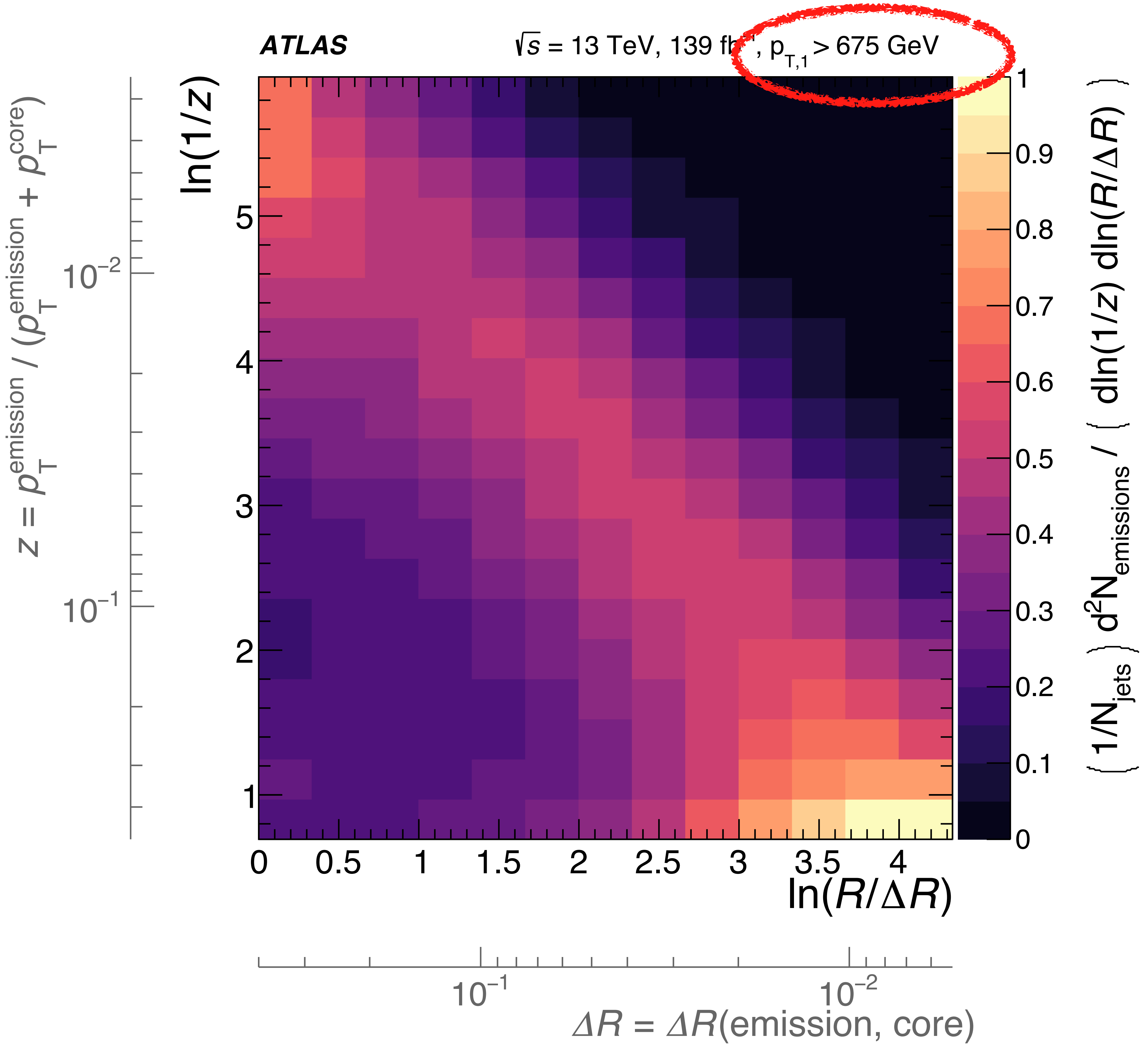

Hadronization

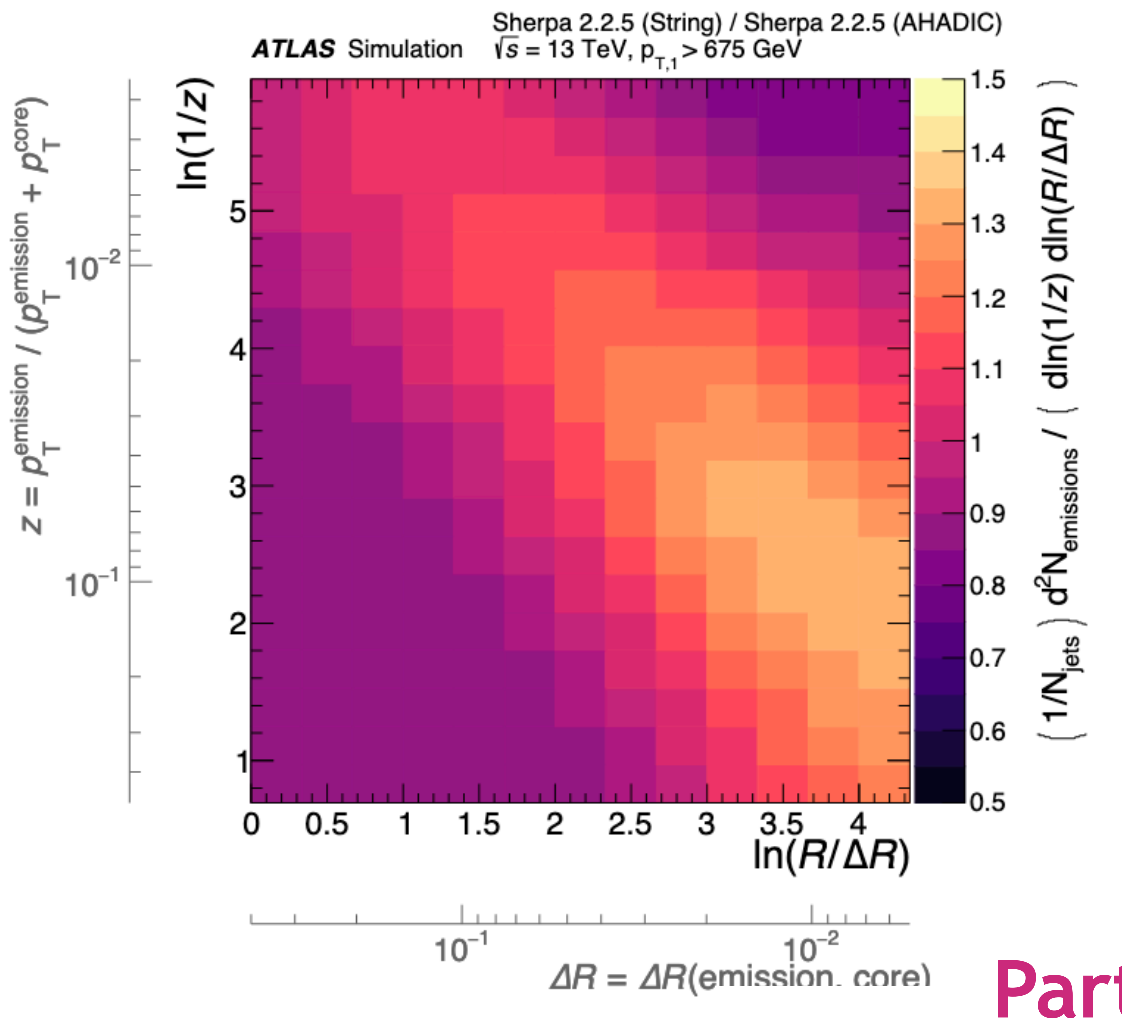

Matrix elements

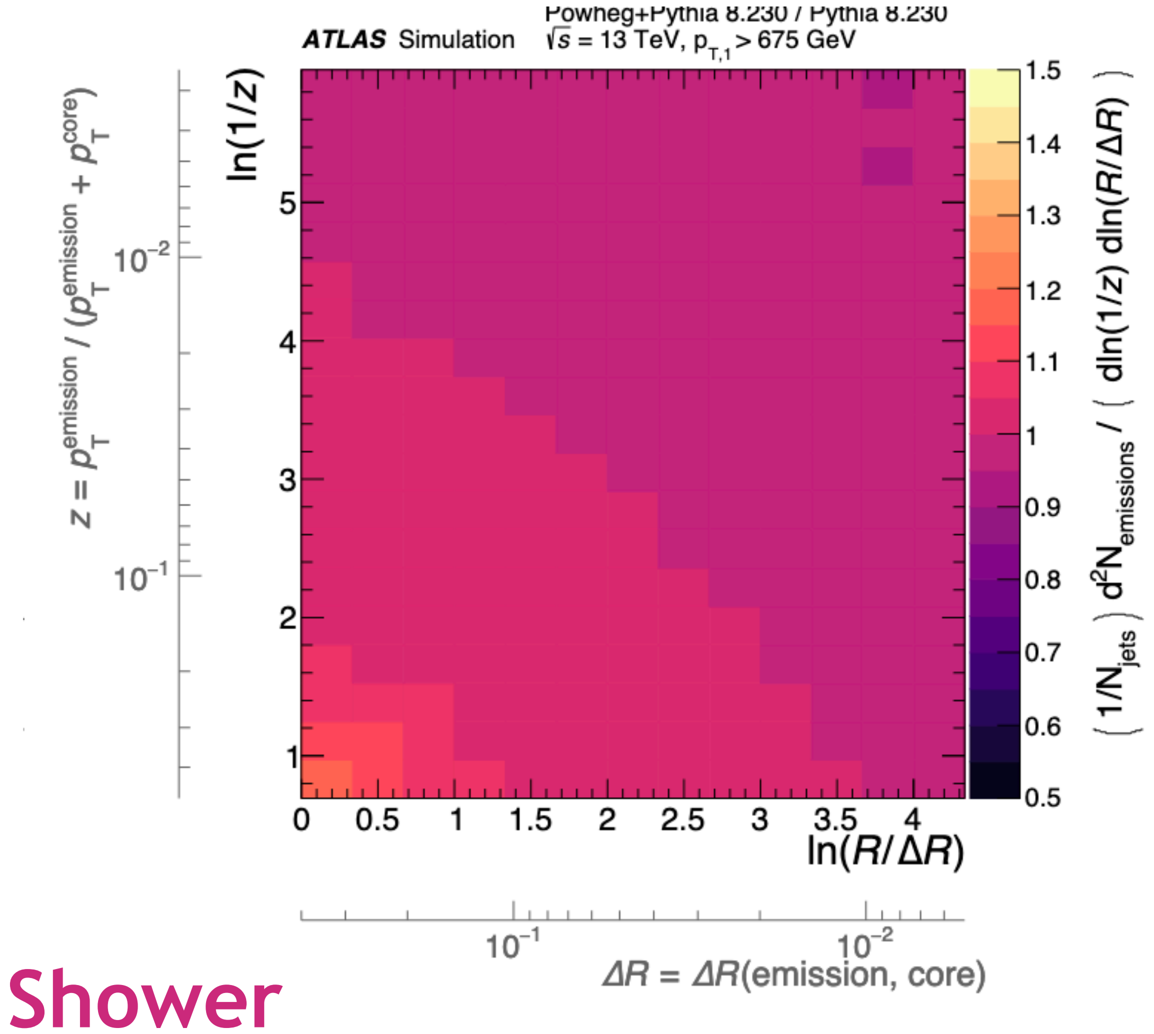

Parton Shower

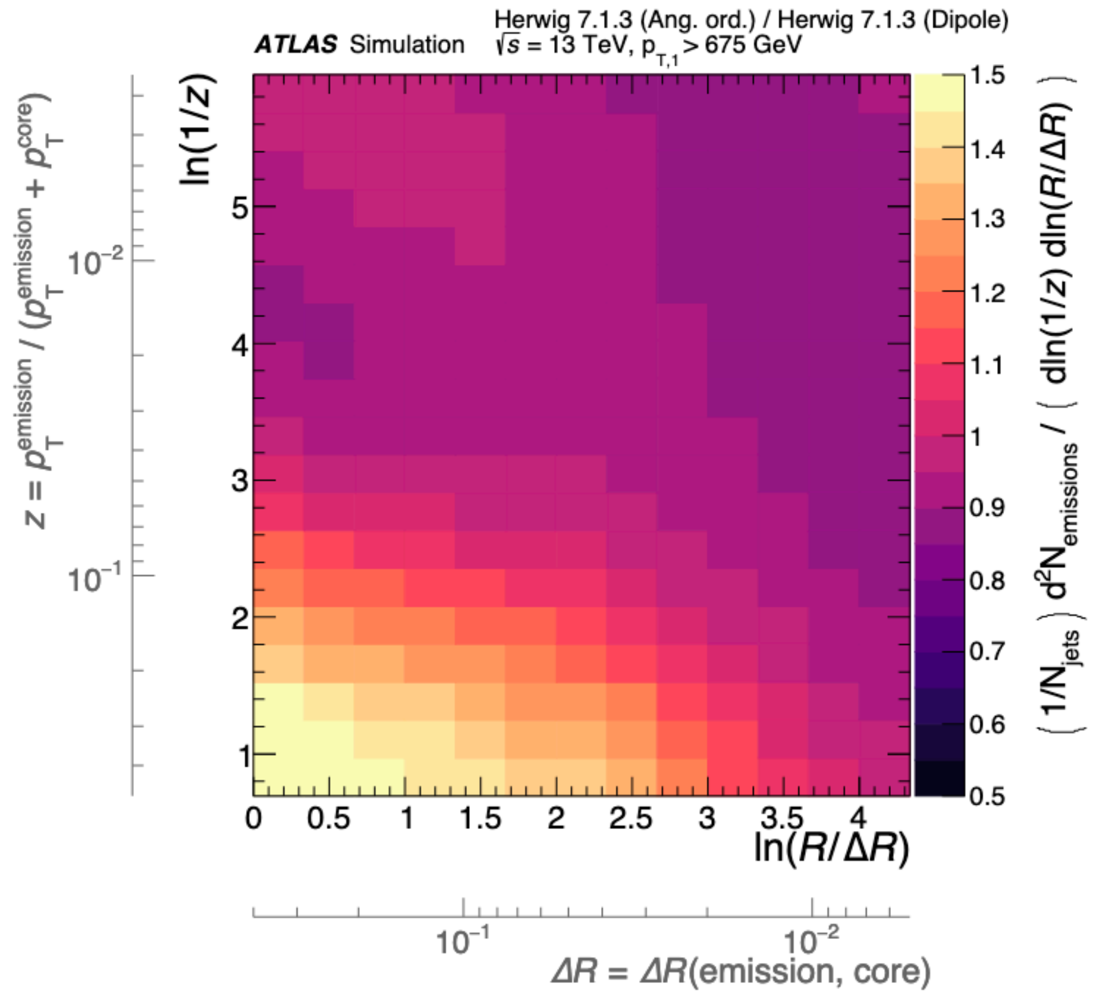

- Multiple physics effects contribute beyond the LO uniformly-filled plane
- However the measurement captures salient features of the q/g parton shower: the running of the coupling sculpts the plane

[ATLAS, Phys.Rev.Lett. 124 (2020) 22, 222002](#)

The primary Lund plane with ATLAS

Comparisons to MC generators

Parton shower ⟷ Hadronisation

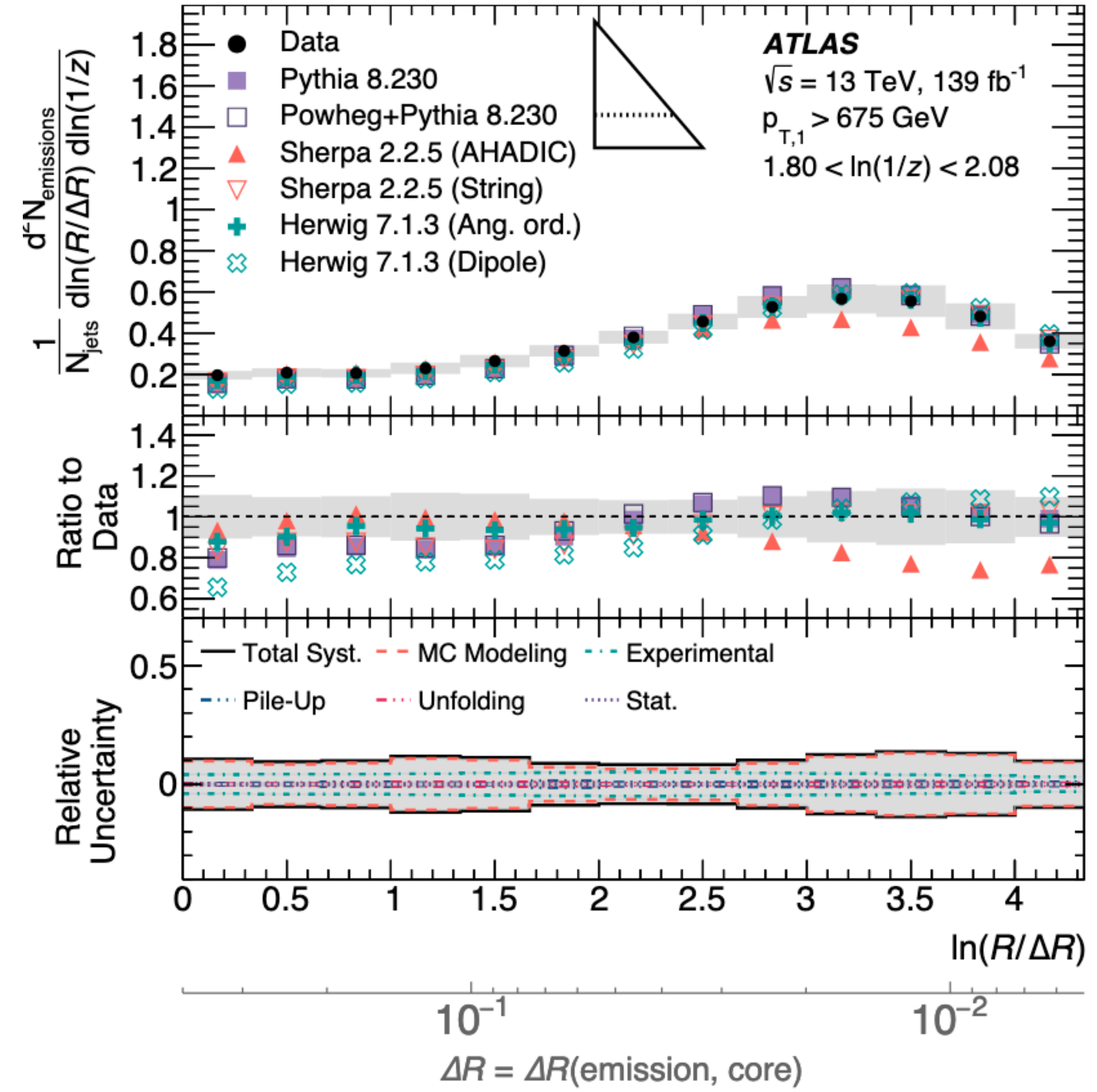

Ability of the Lund Plane to isolate physics effects:

- PS effects (wide angles)
- hadronisation (collinear splits).

Input to (non)perturbative model development and tuning

Comparison to analytical calculations

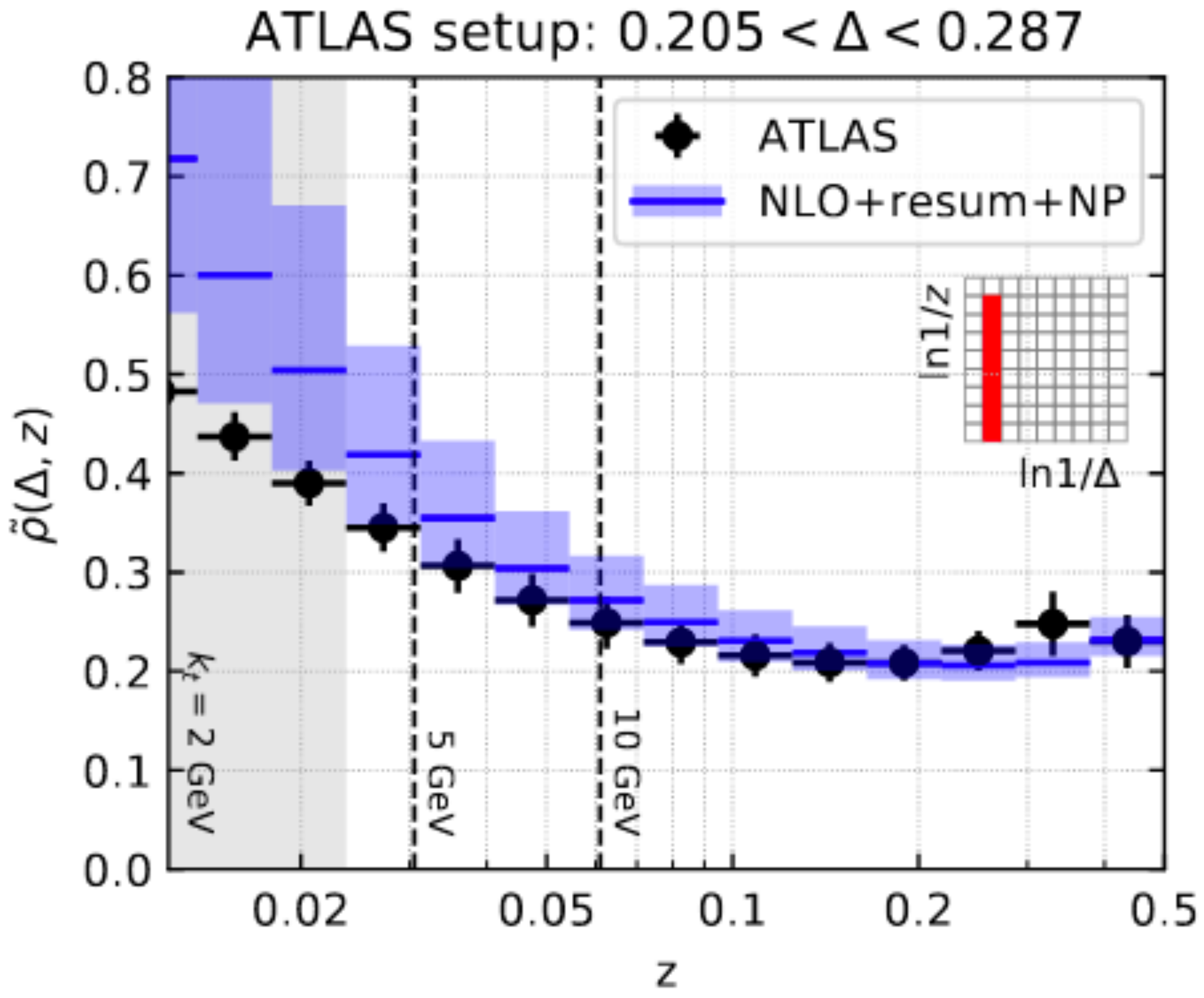

New all-order single log calculation of the Lund plane density including [Lifson et al, JHEP 10 (2020) 170]

Precision of the Lund plane density 5-7% at high k_T while ~20% at the edge of the perturbative region (k_T~5 GeV)

The primary Lund plane with ALICE

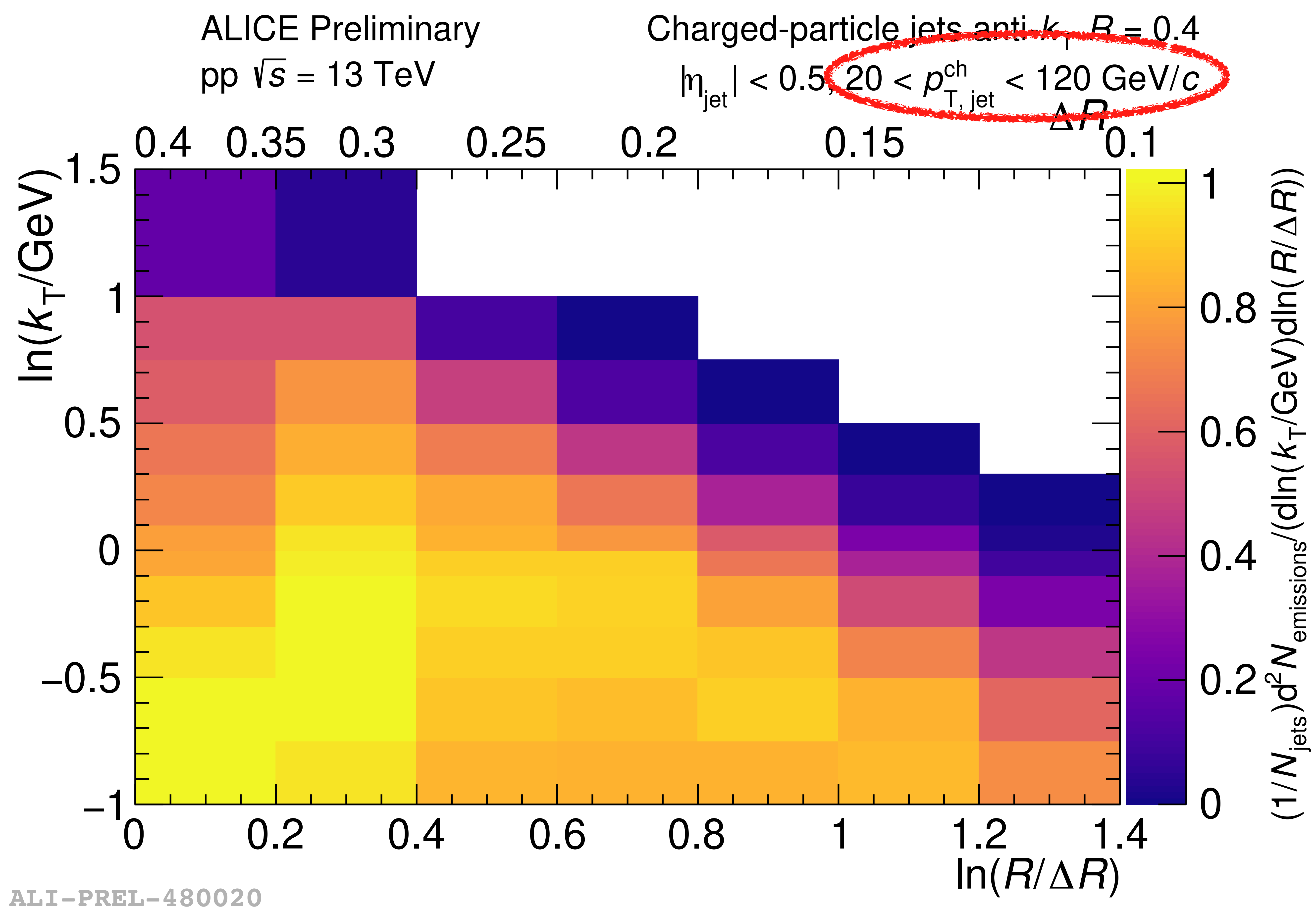

	ALICE	ATLAS
$p_{T,jet}$ (GeV)	20-120	>675
max k_T (GeV)	5	>135
ΔR (rad)	0.1-R	0.005 - R

ALICE-PUBLIC-2021-002.

The primary Lund plane with ALICE

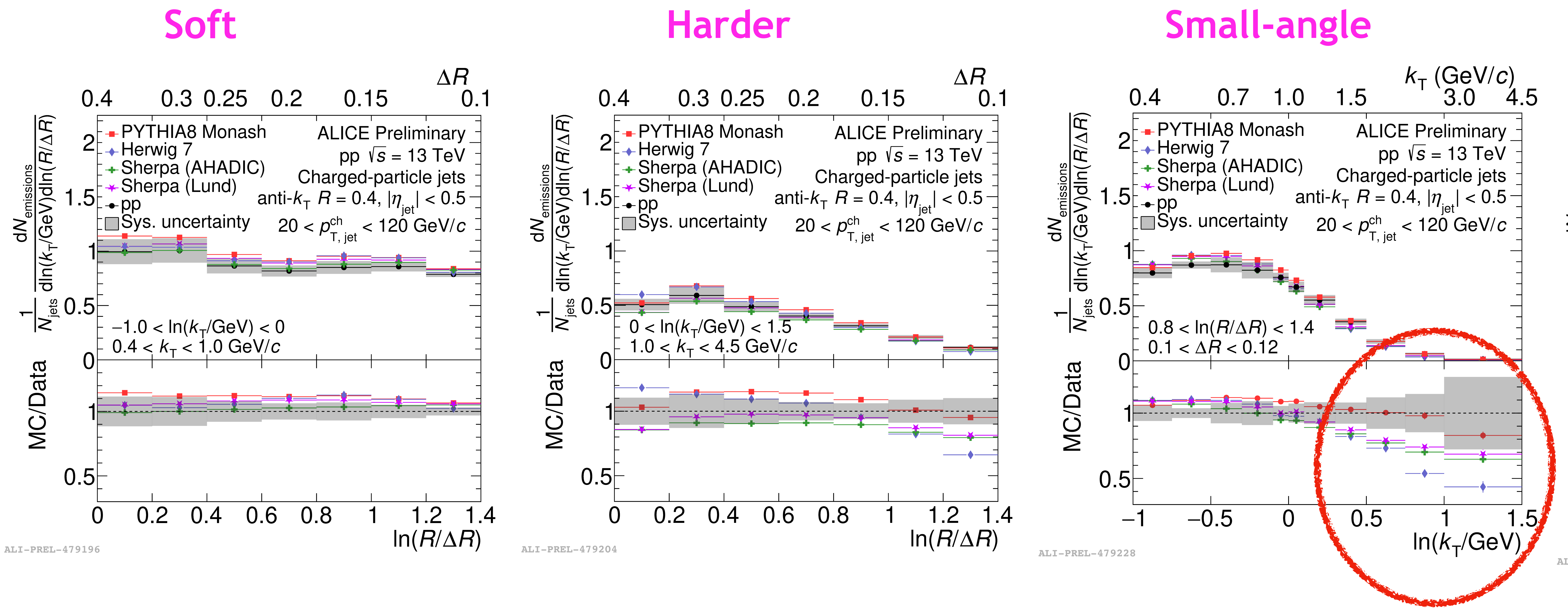

- Similarly to ATLAS measurement, model uncertainties (Herwig vs PYTHIA in the response and matching purity/efficiency corrections) are dominant
- Some tensions in the moderately hard, moderately low angles (0.1-0.2 rad)
- Perturbative reach to be extended with triggered samples

ALICE-PUBLIC-2021-002.

Grooming

Groom away branches in order to **access hard parts of the jet that are under better theoretical control**

- **mMDT/SofDrop grooming**

Remove branches of an angular-ordered clustering tree until you find a splitting that satisfies:

$$z_g = \frac{\min(p_{t,1}, p_{t,2})}{p_{t,1} + p_{t,2}} > z_{\text{cut}} \left(\frac{\Delta R_{12}}{R_0} \right)^{\beta}$$

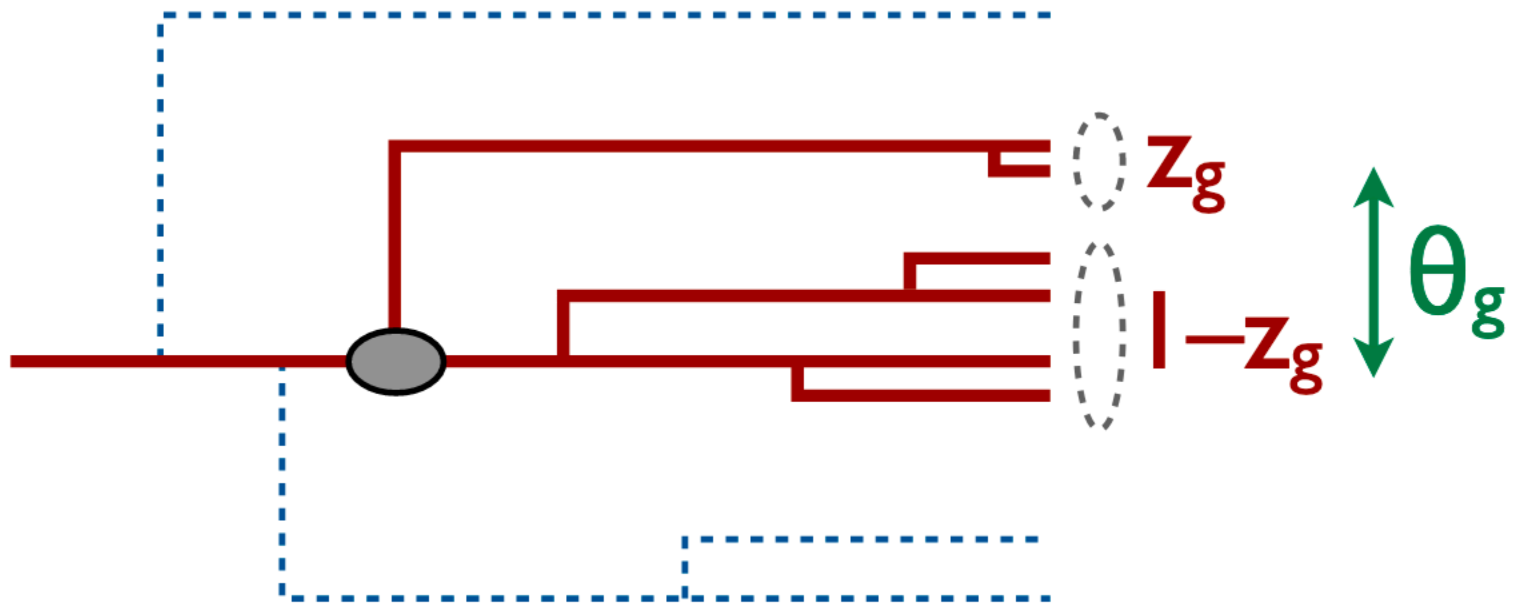

Larkoski et al, JHEP 05 (2014) 146
(Recursive SD) Dreyer et al, JHEP 06 (2018) 093
Butterworth et al,Phys.Rev.Lett. 100 (2008) 242001

- **New: Dynamical Grooming**

1. Select the hardest branch in the C/A sequence
2. Drop all branches at larger angles

$$\kappa^{(a)} = \frac{1}{p_T} \max_{i \in \text{C/A}} z_i (1 - z_i) p_{T,i} (\theta_i / R)^a$$

More aggressive grooming with decreasing parameter a

Mehtar-Tani et al, Phys.Rev.D 101 (2020) 3, 034004

DyG:

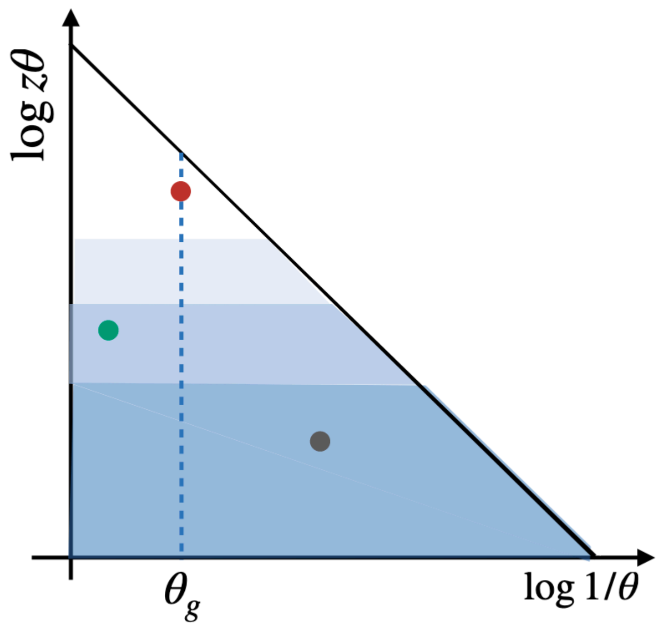

SD:

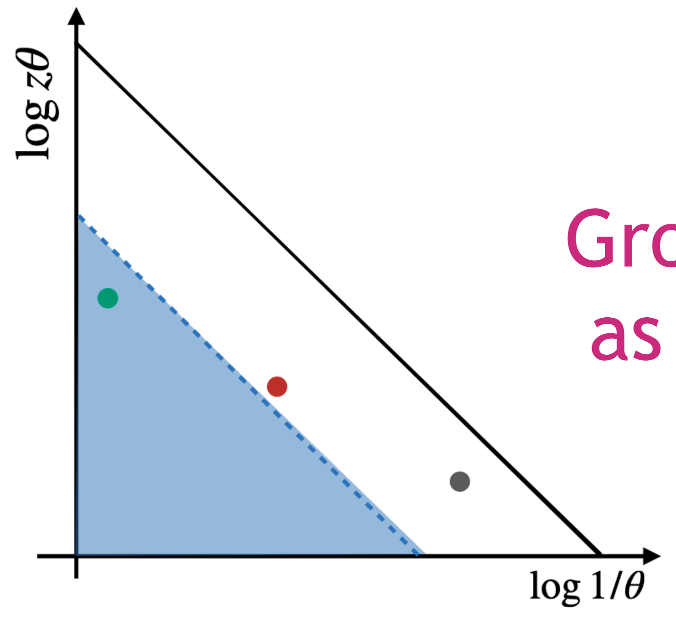

Groomed-away areas can we drawn as exclusion regions in the Lund Jet Plane

The groomed momentum balance

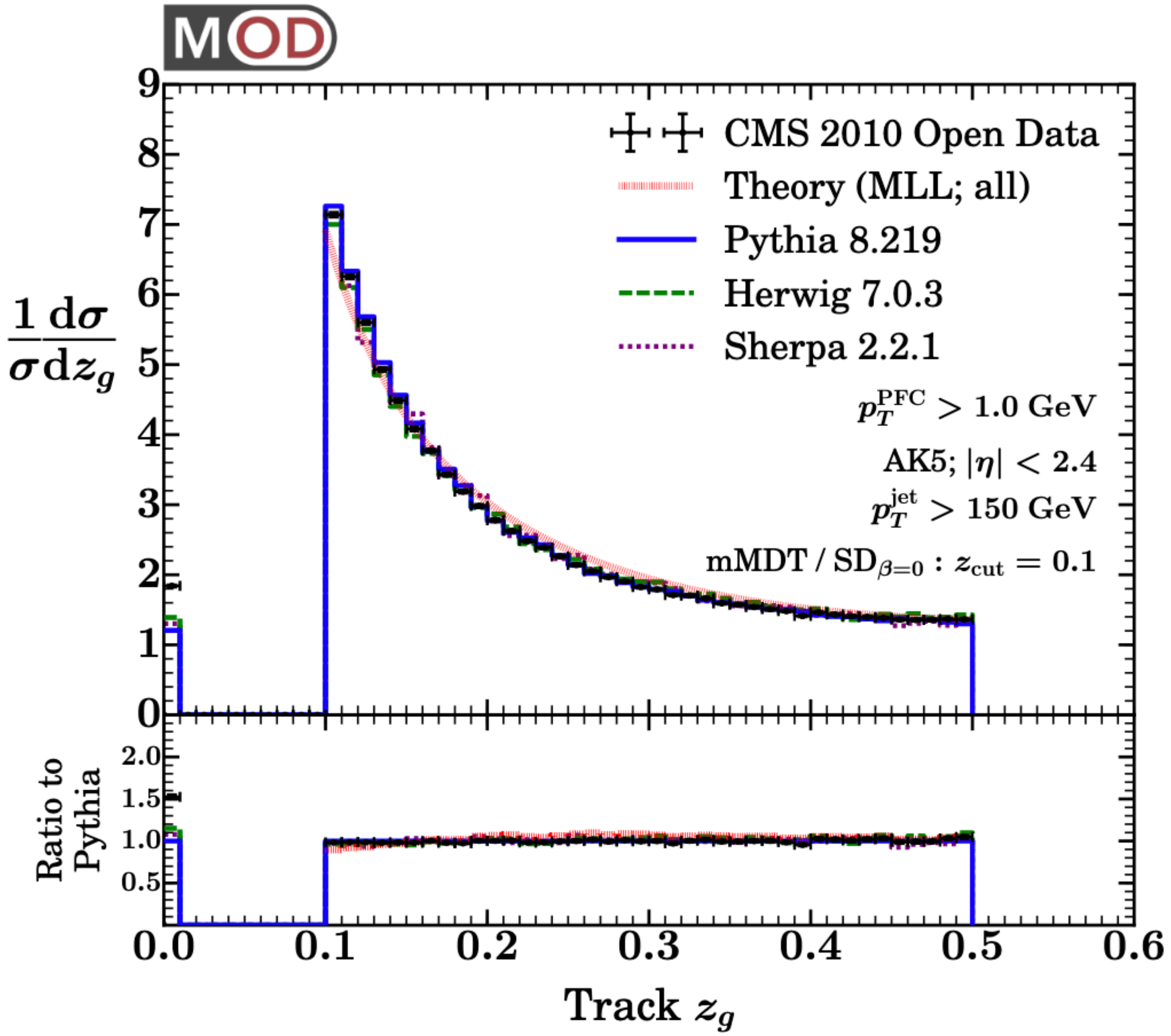

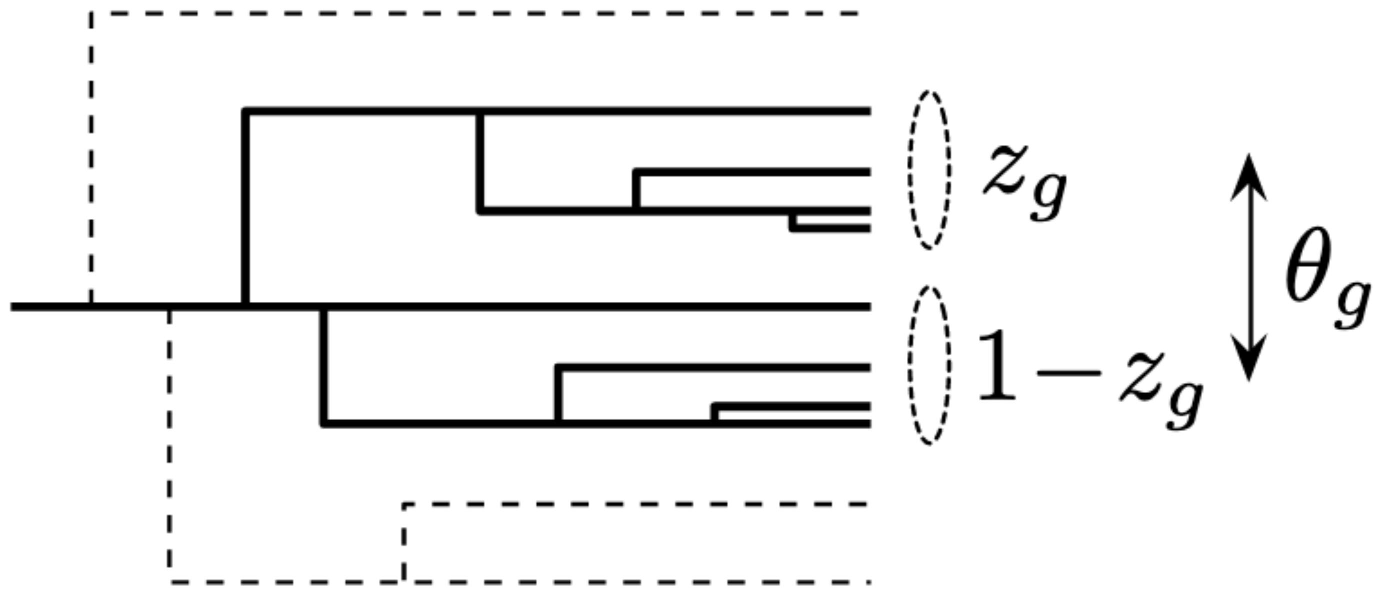

$$\overline{P}_i(z) = \sum_{j,k} \left[P_{i\to jk}(z) + P_{i\to jk}(1-z)\right]$$

recovers the 1/z universal dependence of the z-kernel in QCD

(2017)

Thaler et al, Phys.Rev.Lett 119, 12003 (2017)

The groomed momentum balance

$$z_g = \frac{p_{T2}}{p_{T1} + p_{T2}}$$

Low p_T, R dependence

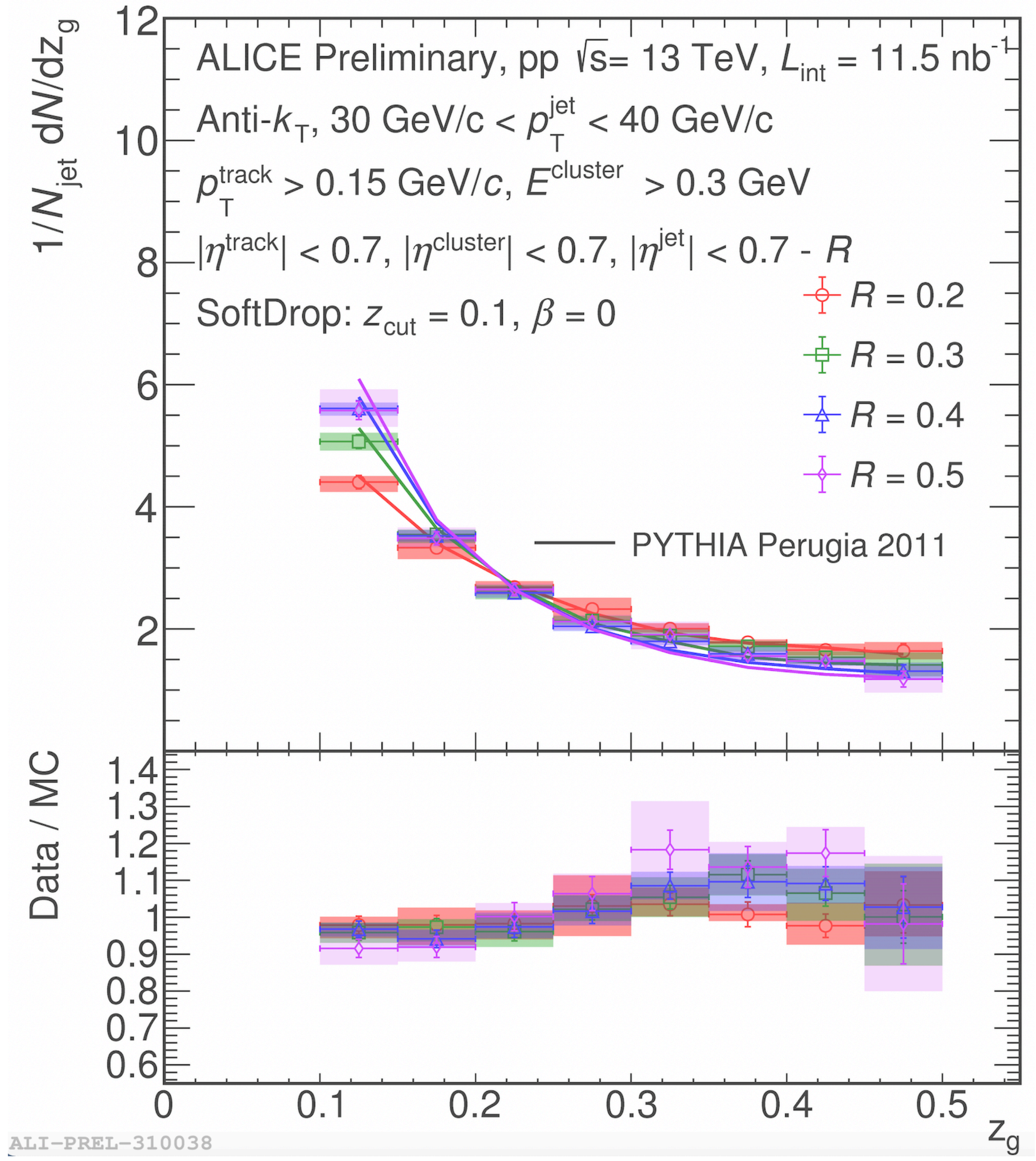

High p_T, large R=0.8, more grooming

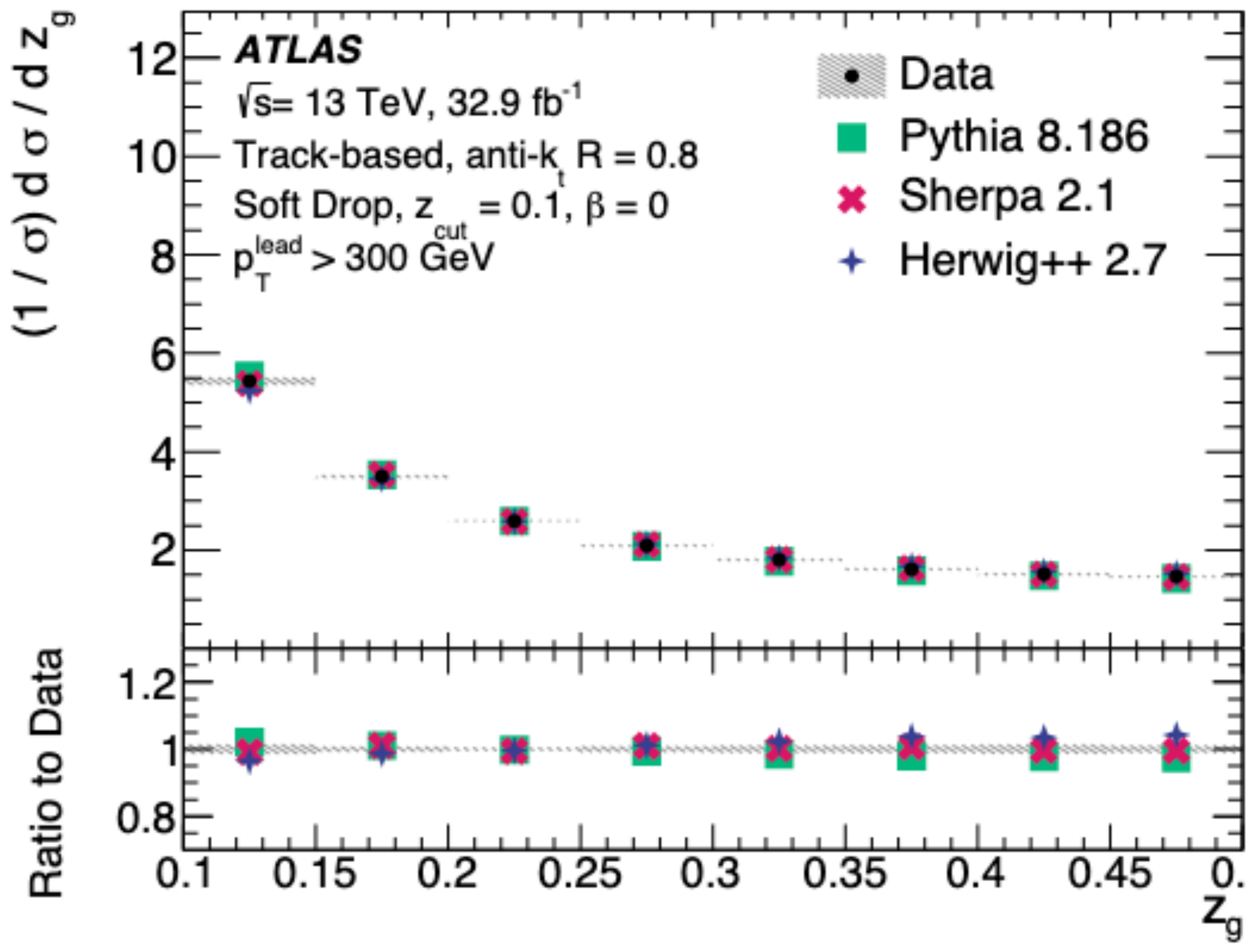

High p_T, large R=0.8, less grooming

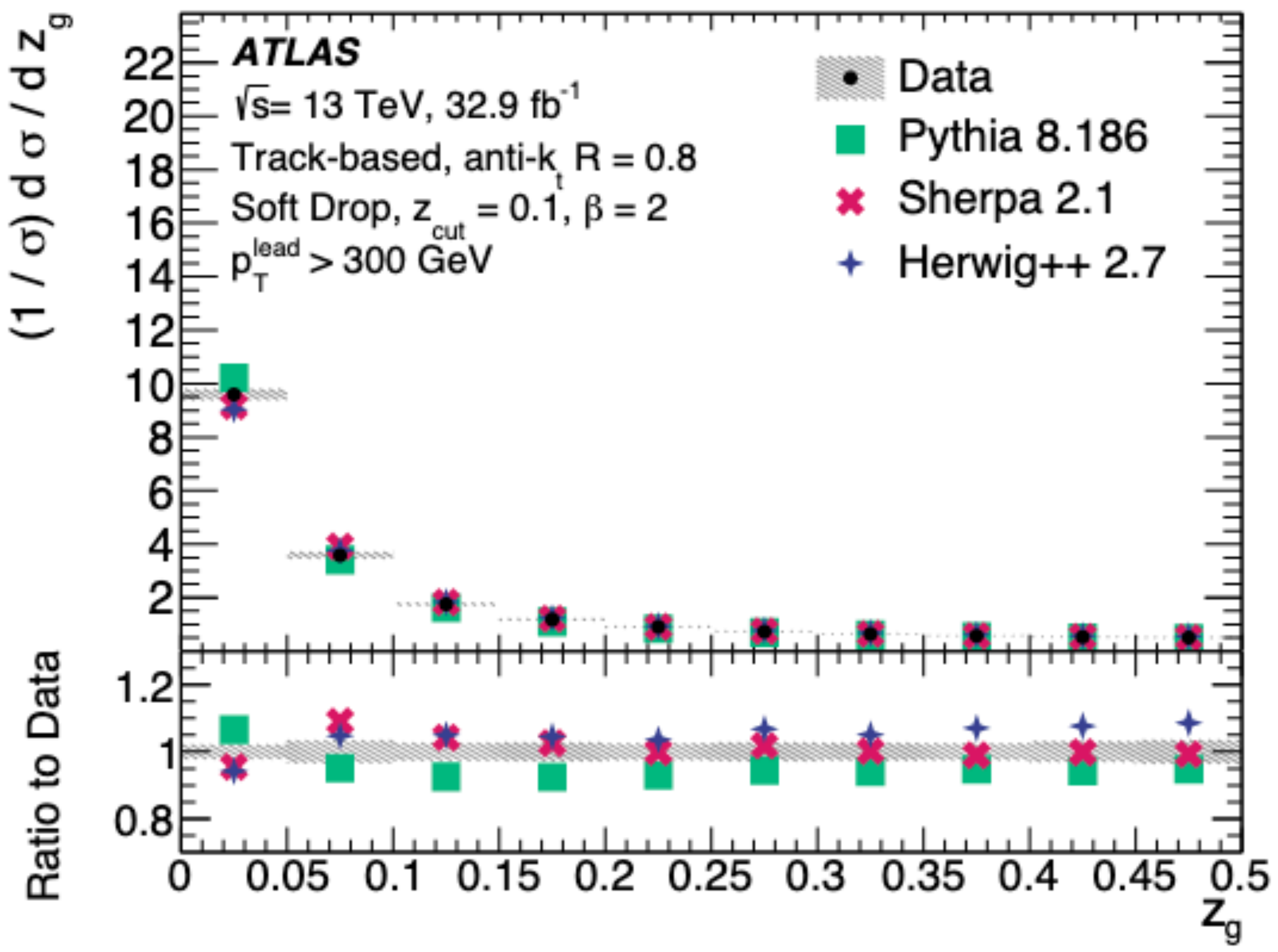

Phys. Rev. D 101, 052007 (2020)

Low z_g affected by non pert. effects (UE)
More soft subleading prongs at large R

Good description by MC generators
Largest discrepancies in the regions most affected by non pert. effects (higher β, low z_g)

The groomed jet radius

$$\theta_g = \frac{\Delta R(j_1, j_2)}{R_0}$$

Low p_T, R=0.4

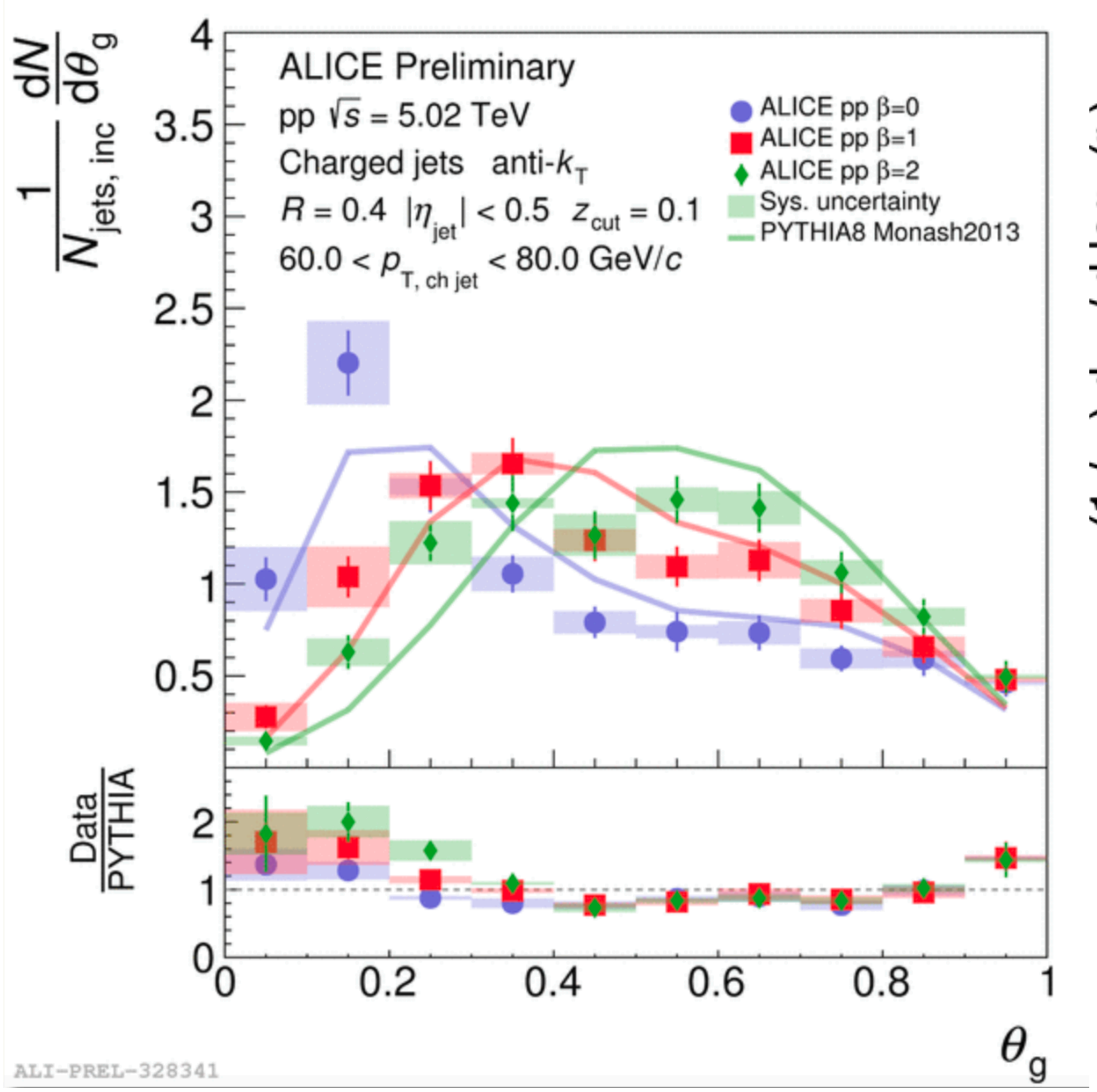

High p_T, large R=0.8, more grooming

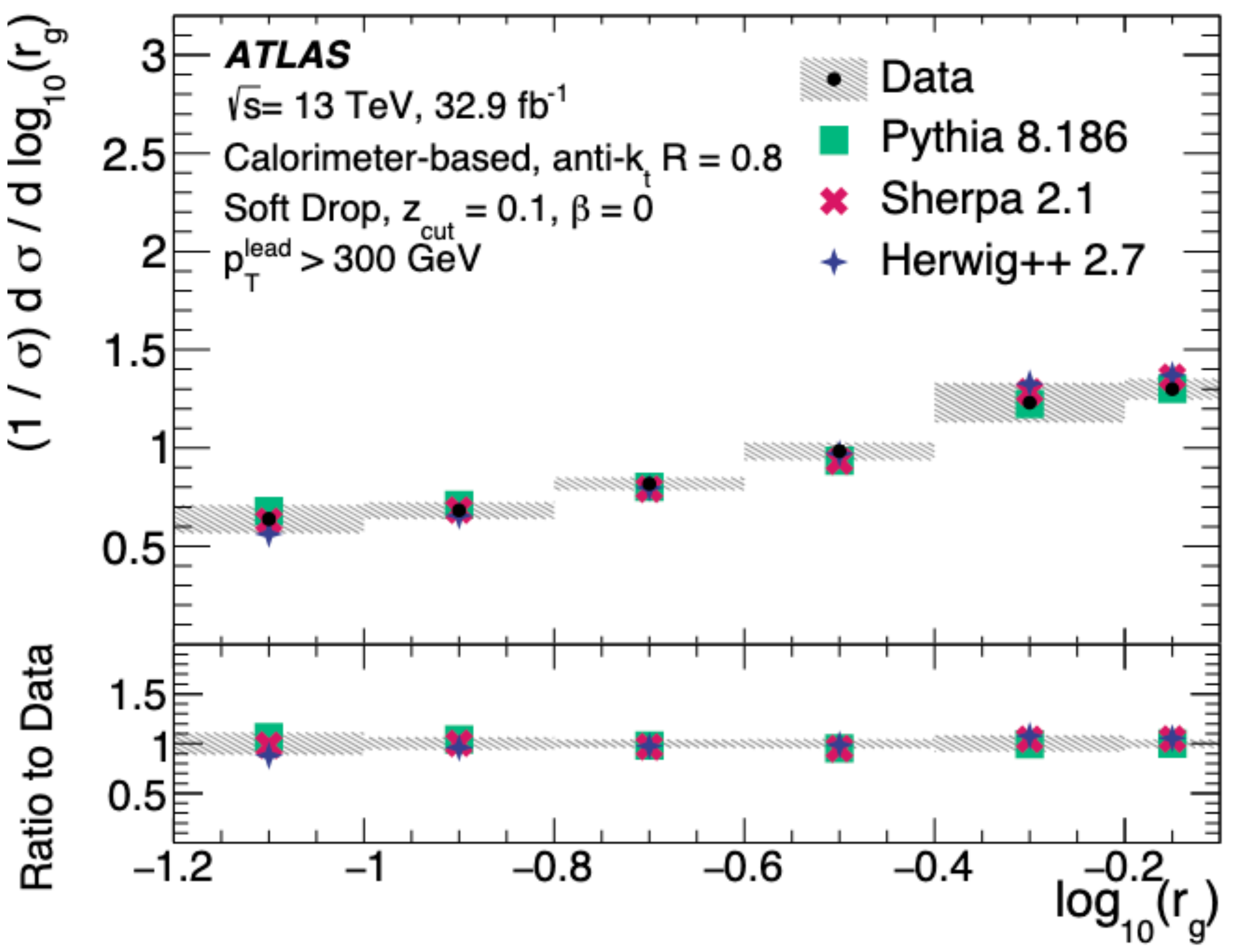

High p_T, large R=0.8, less grooming

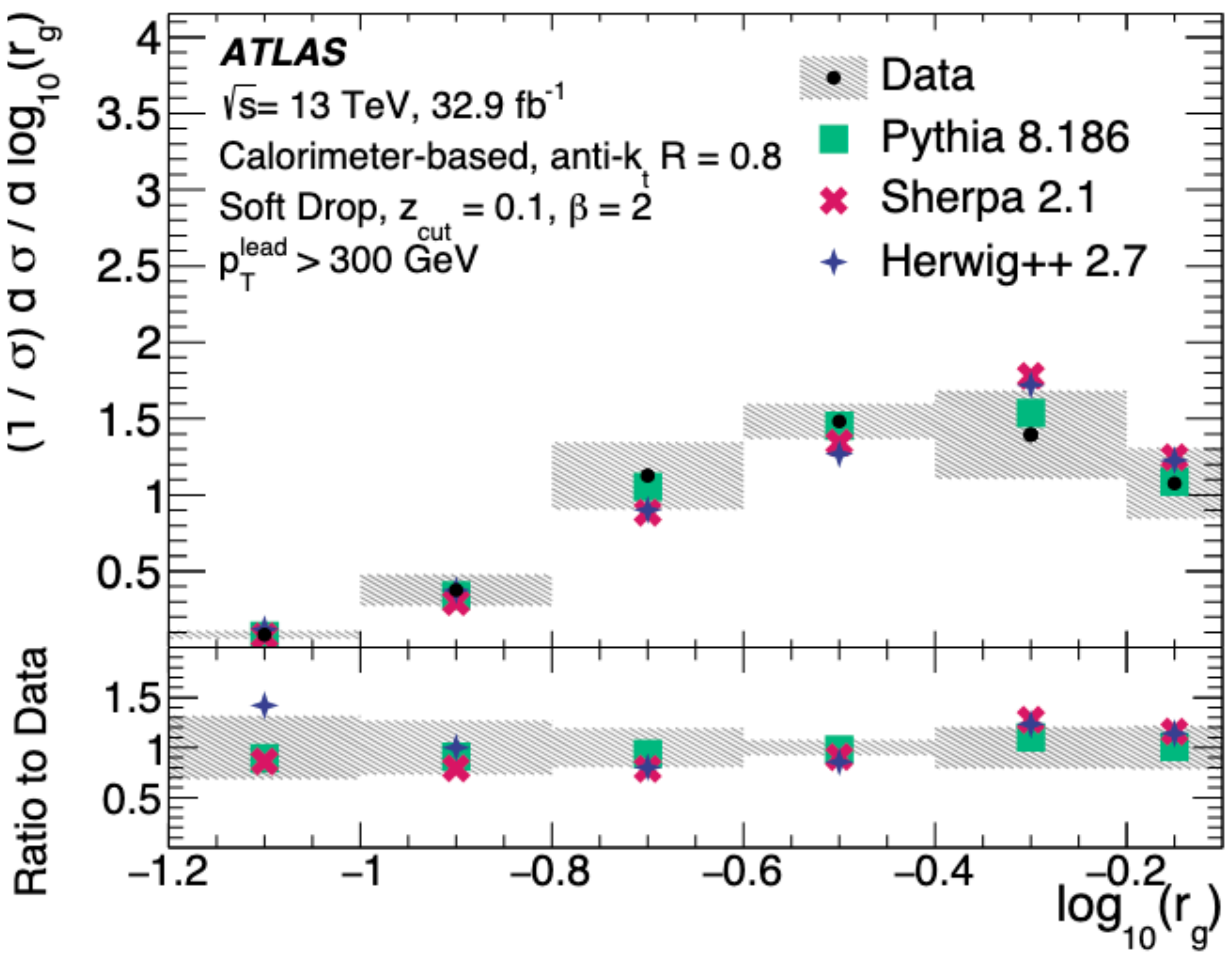

Phys. Rev. D 101, 052007 (2020)

Good description by MC generators
Largest discrepancies with less grooming in the regions most affected by non-perturbative effects (collinear splits)

Dynamical grooming

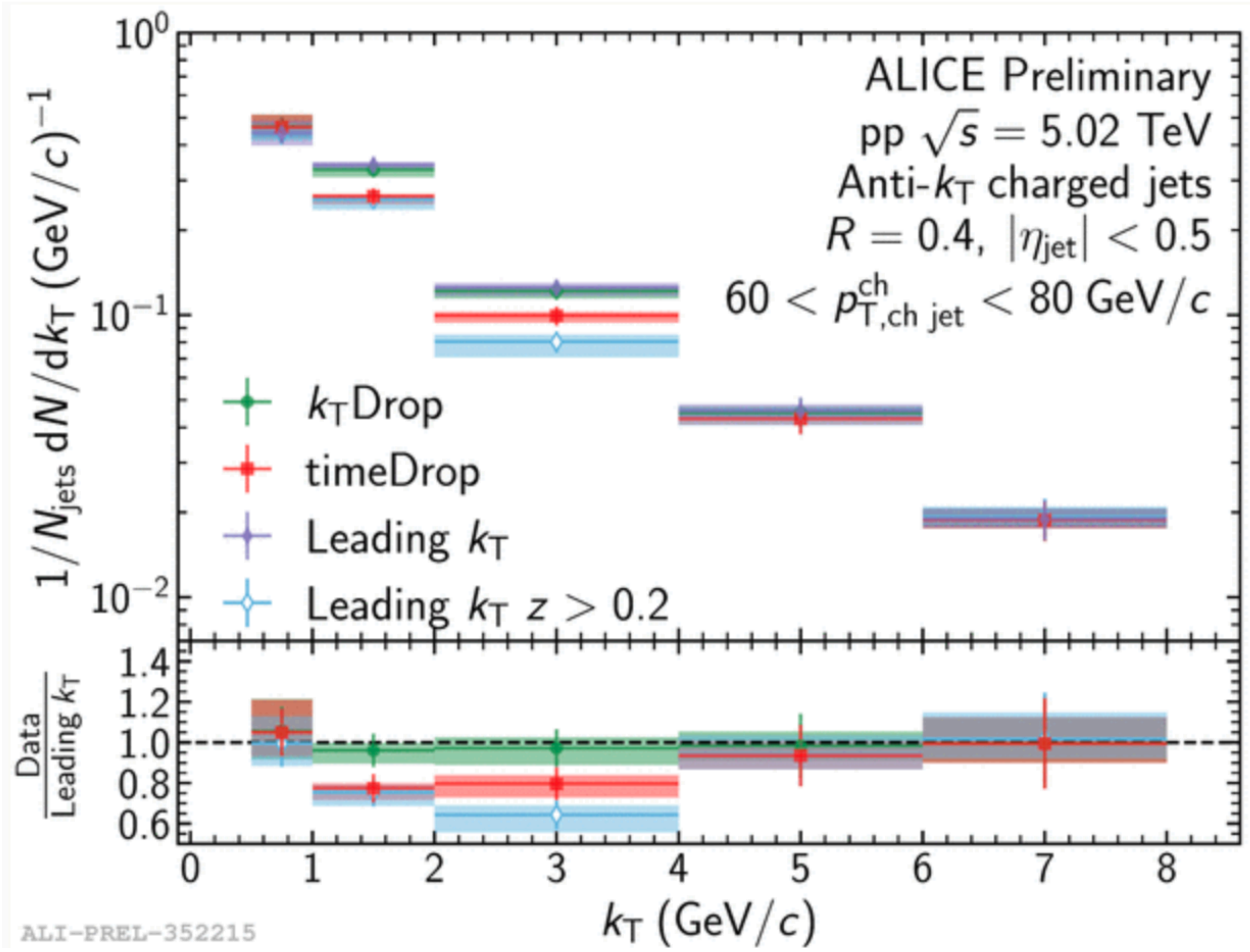

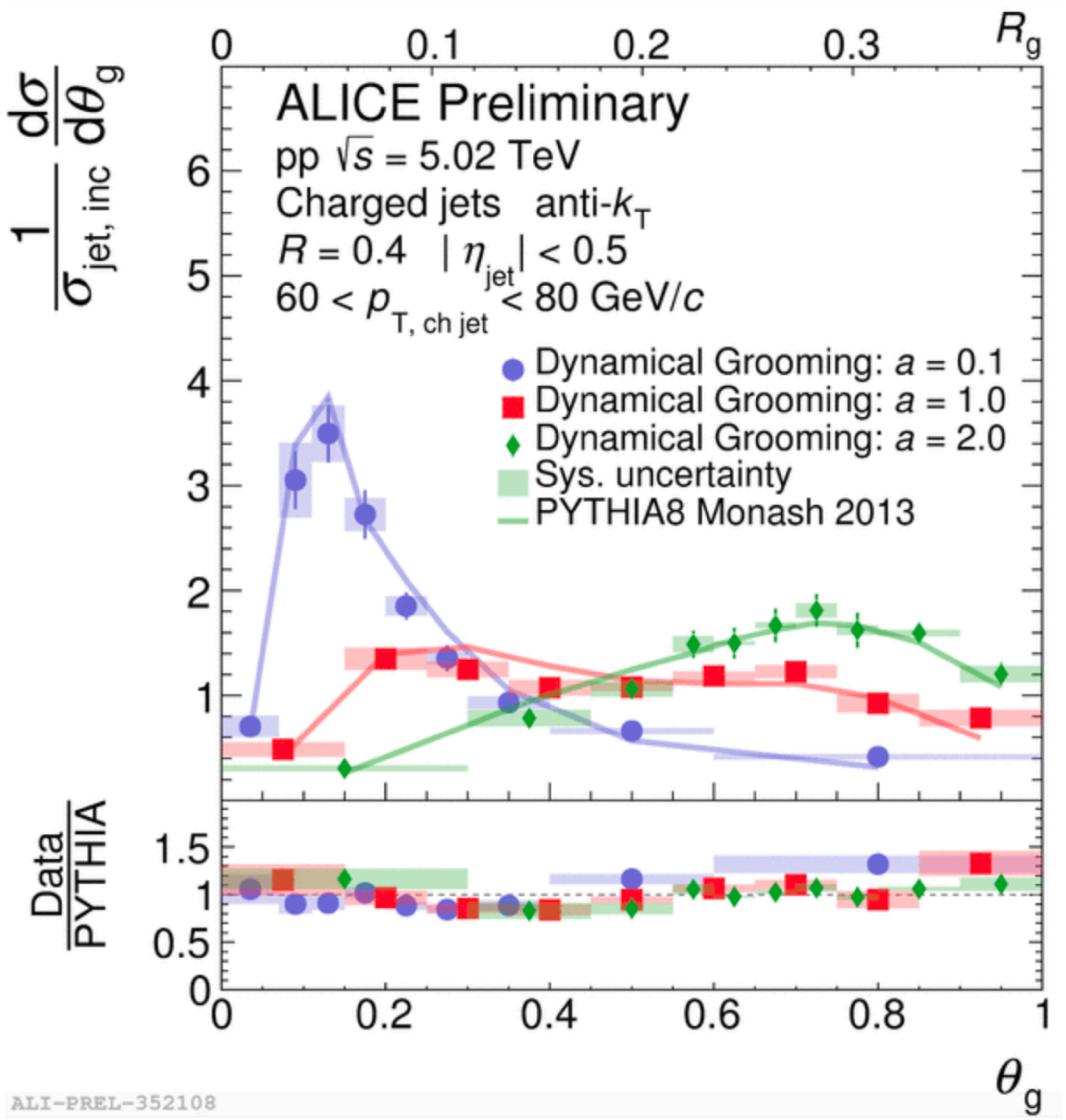

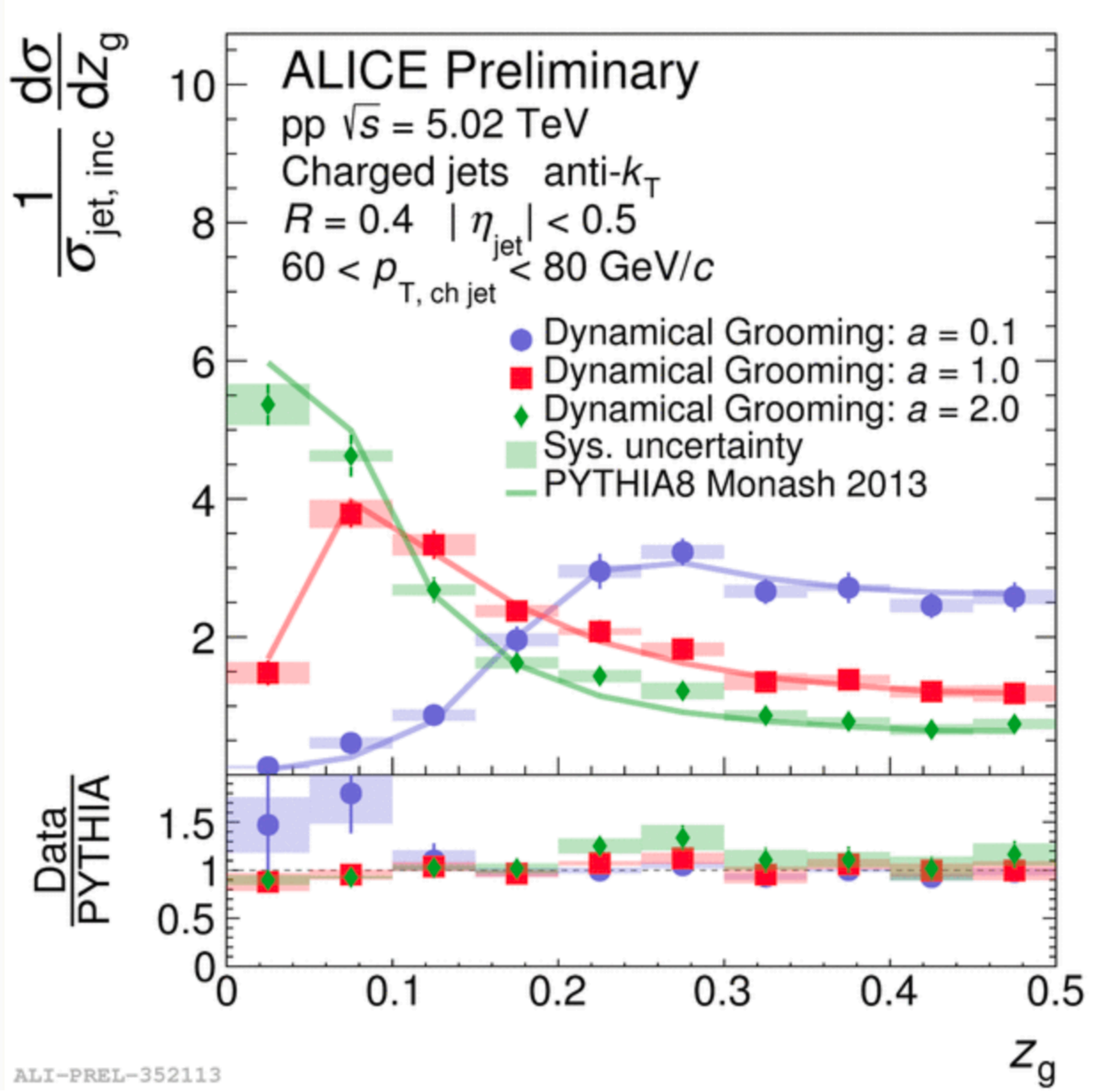

- First measurement of dynamical grooming
- Good agreement between PYTHIA and data
- At high k_T, different dyn grooming settings seem to select the same splitting
- First comparisons to analytical calculations at LO+N2DL accuracy *Caucal et al, arXiv:2103.06566*

Dynamical grooming

New at LHCP

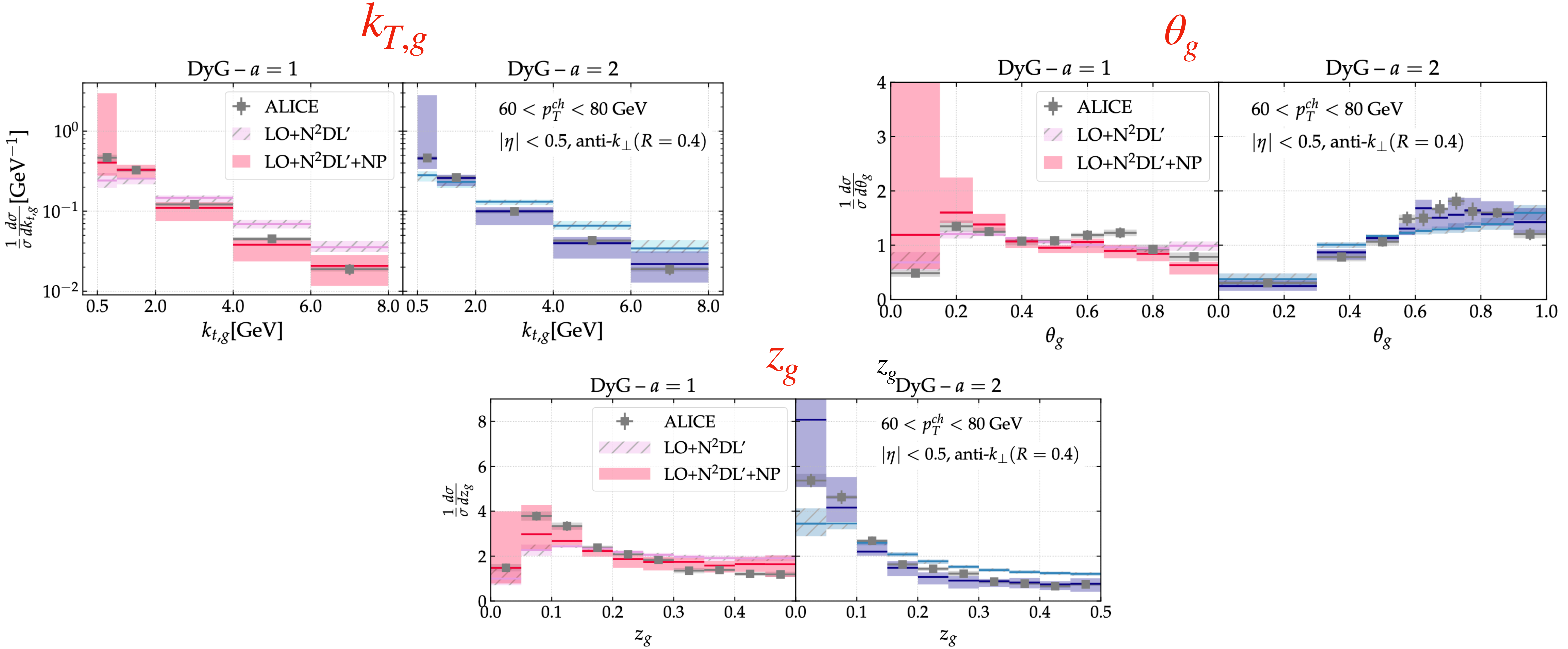

- First measurement of dynamical grooming
- Good agreement between PYTHIA and data
- At high k_T, different dyn grooming settings seem to select the same splitting
- First comparisons to analytical calculations at LO+N2DL accuracy Caucal et al, arXiv:2103.06566

The groomed jet mass: precision QCD

$$\rho = 2log_{10}(\frac{m_j}{p_{T,j}R})$$

Phys. Rev. D 101, 052007 (2020)

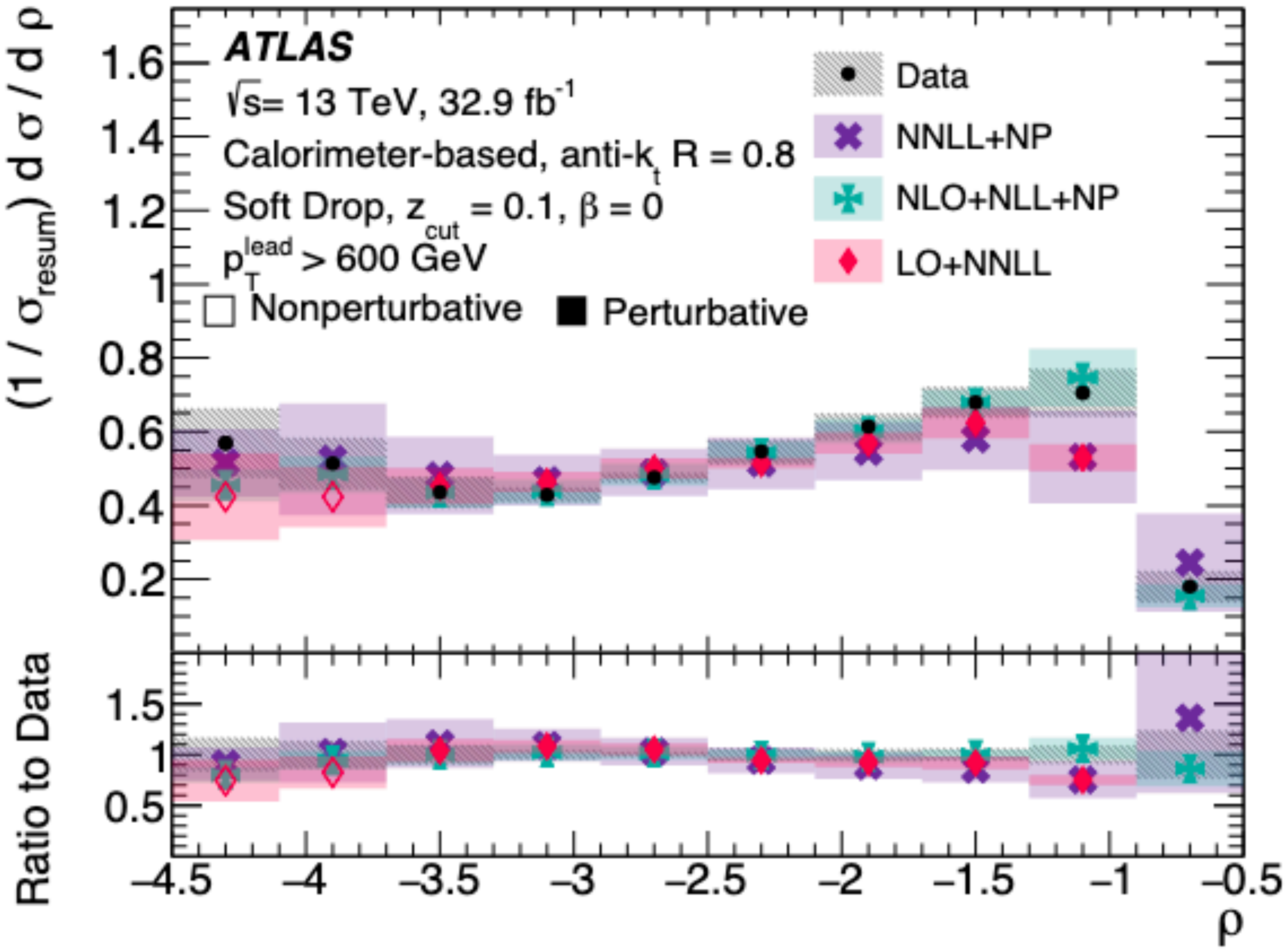

less aggressive grooming

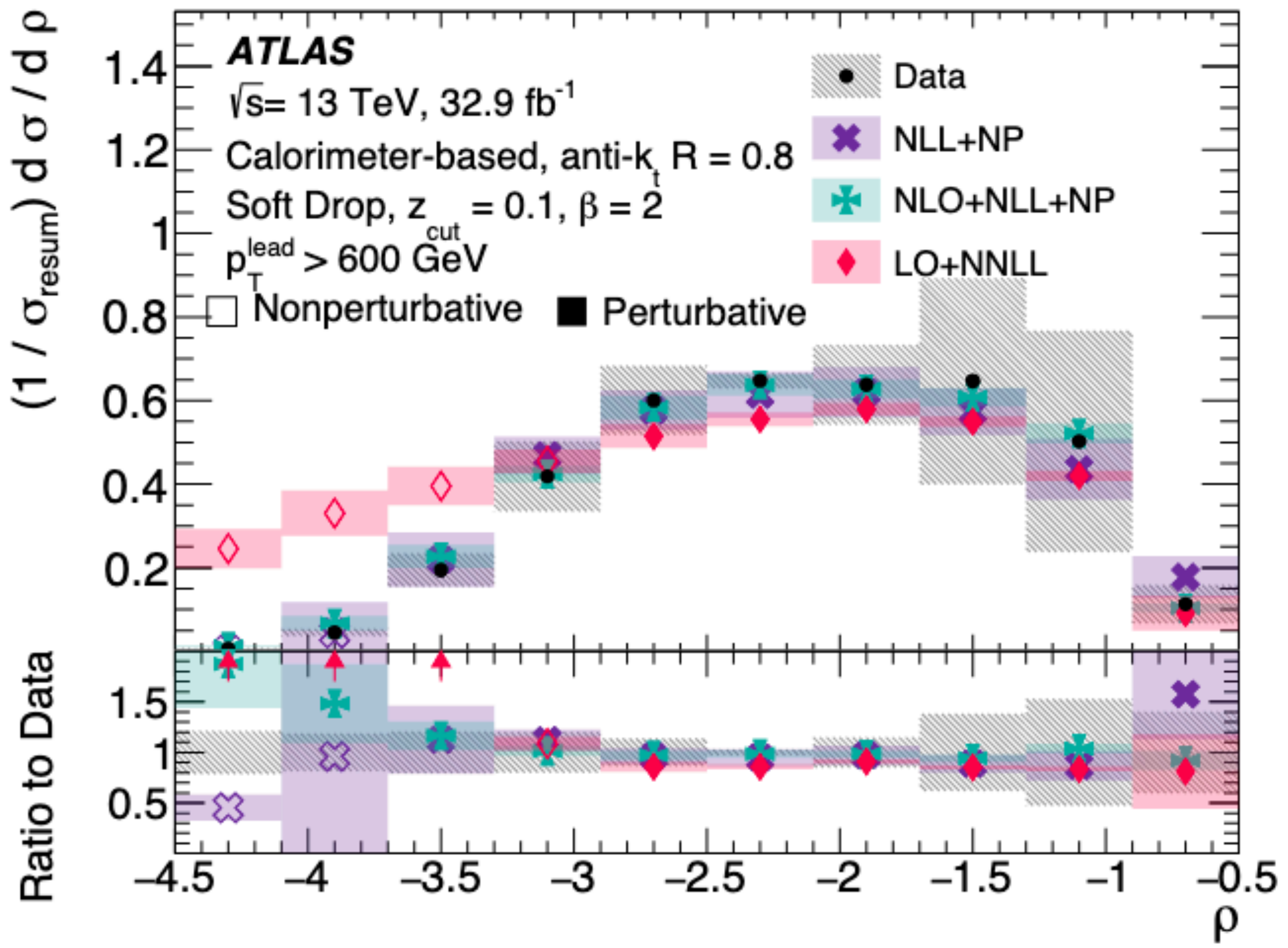

NP regime | Resummation regime | Fixed-order regime

- The calculations are able to describe the data in the resummation regime at the level of 10%
- See also CMS comparisons of groomed and ungroomed mass *CMS,JHEP 11 (2018) 113*
- *R*g comparison to NLL calculations also available (see backup)

Quark and gluon fragmentation

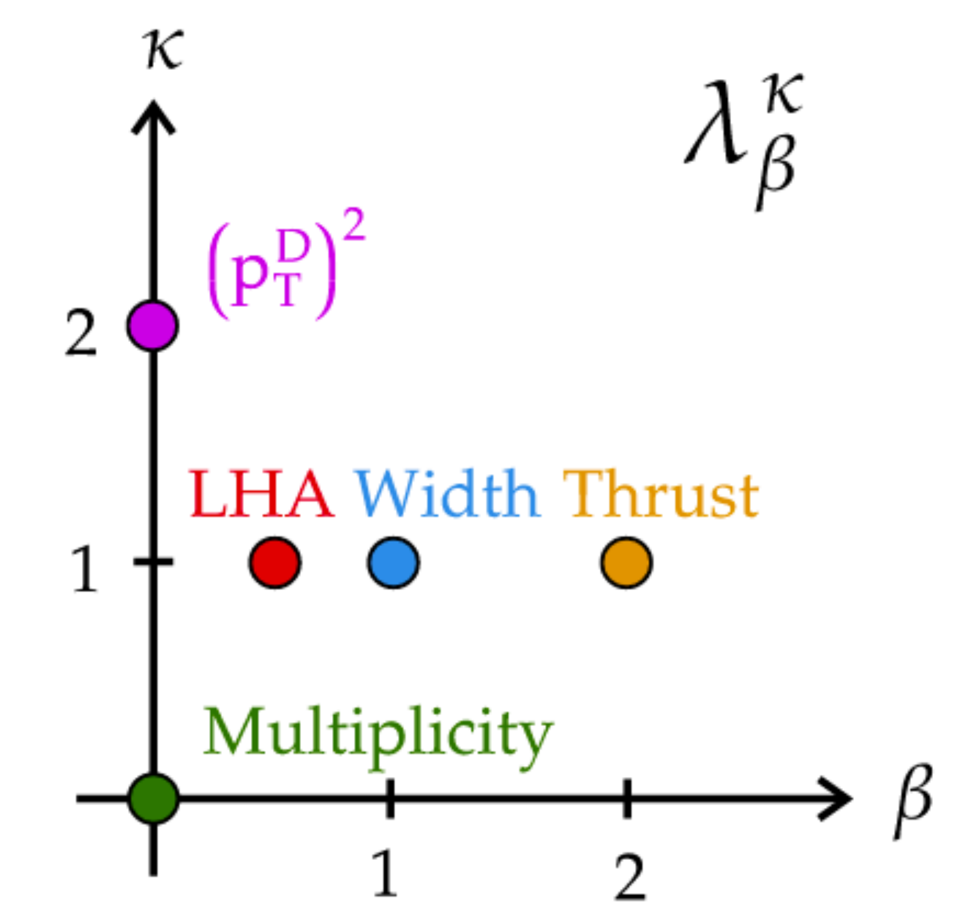

$$\lambda^{\kappa}_{\beta} = \sum_{i \in \mathrm{jet}} z_i^{\kappa} \left(\frac{\Delta R_i}{R} \right)^{\beta}$$

[*CMS PAS SMP-20-010*]

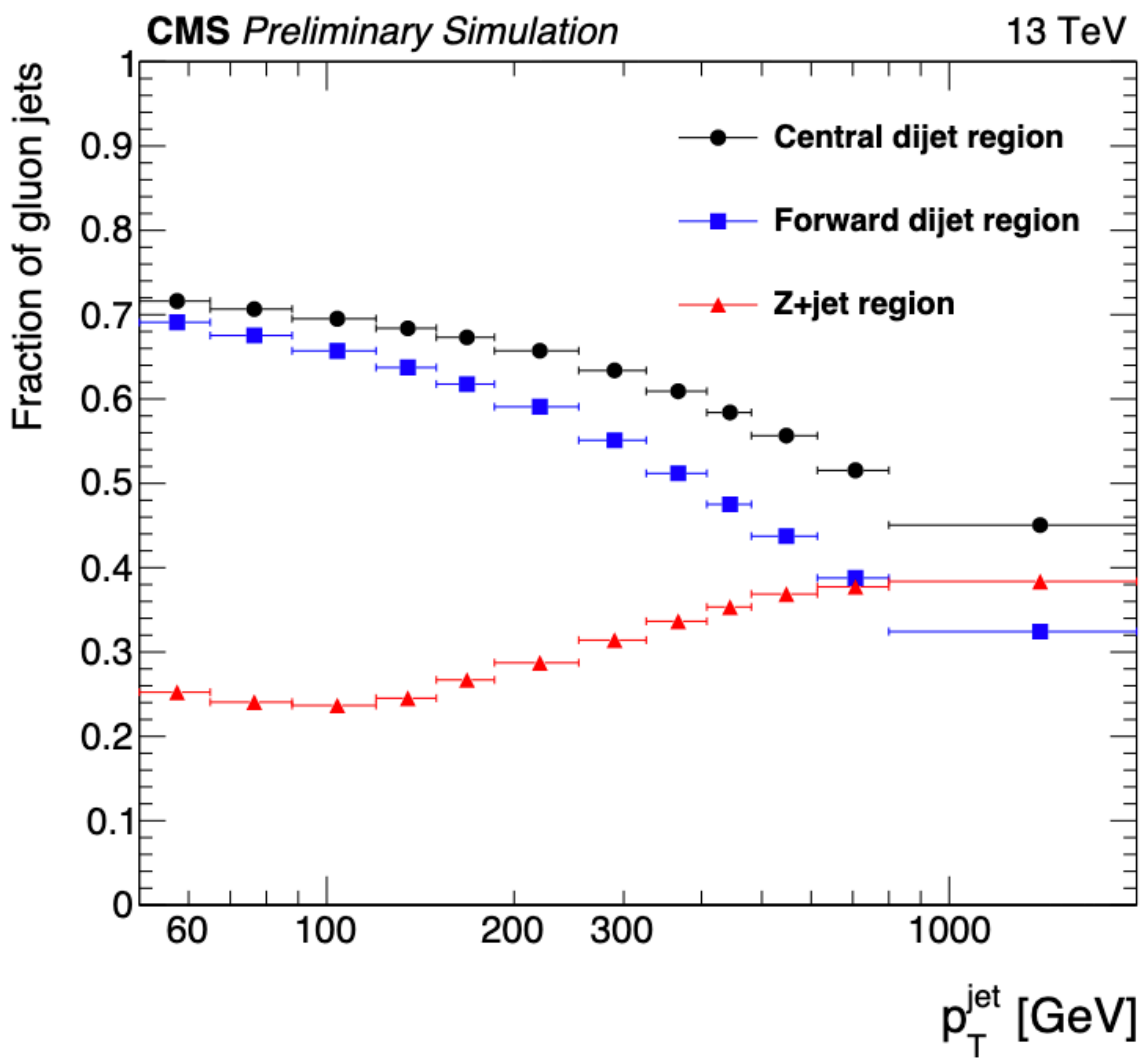

Quark fractions can be enhanced by selecting Z/γ-jet events

Quark and gluon fragmentation

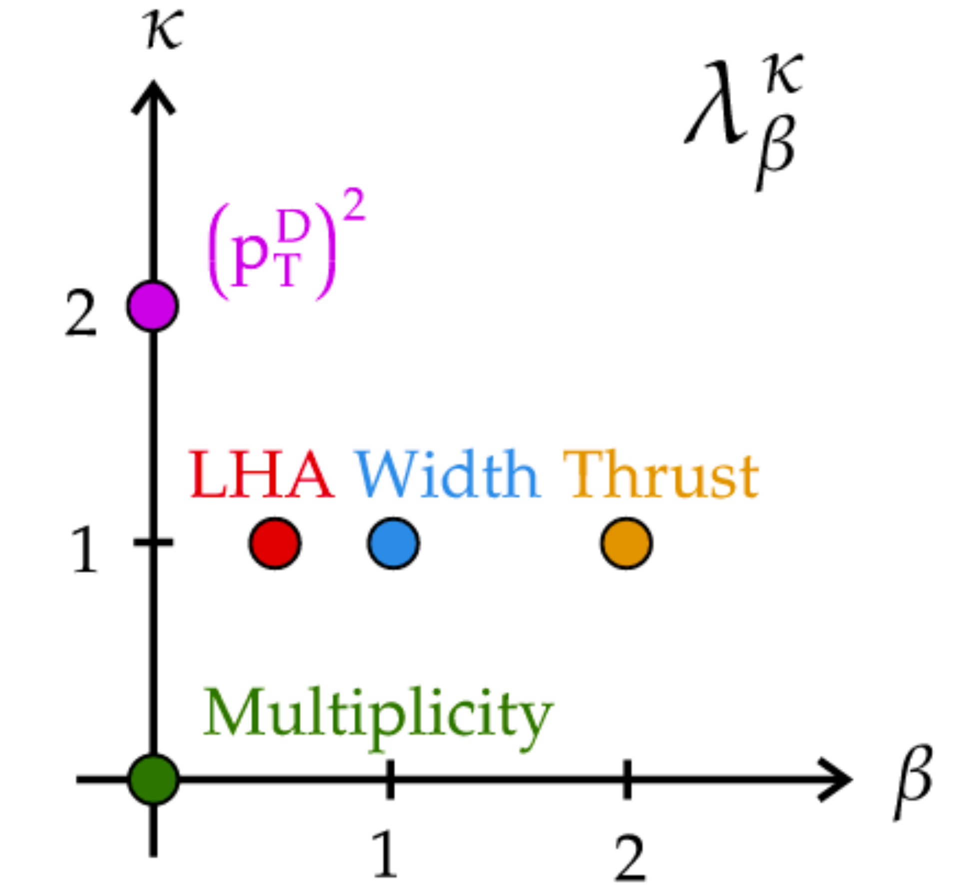

$$\lambda^{\kappa}_{\beta} = \sum_{i \in \text{jet}} z_i^{\kappa} \left(\frac{\Delta R_i}{R} \right)^{\beta}$$

[CMS PAS SMP-20-010](#)

Z+jet, quark-enriched

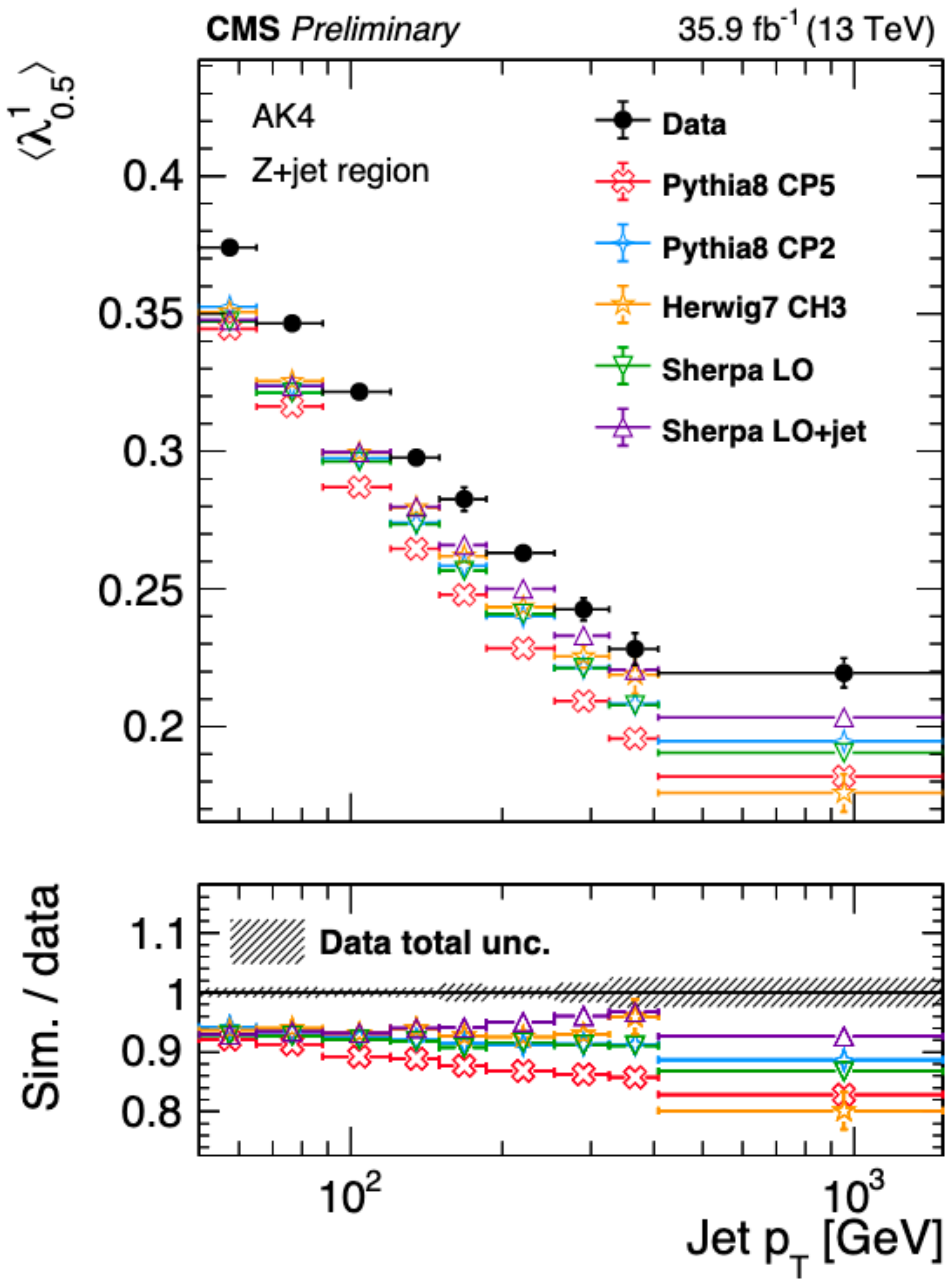

dijets, gluon-enriched

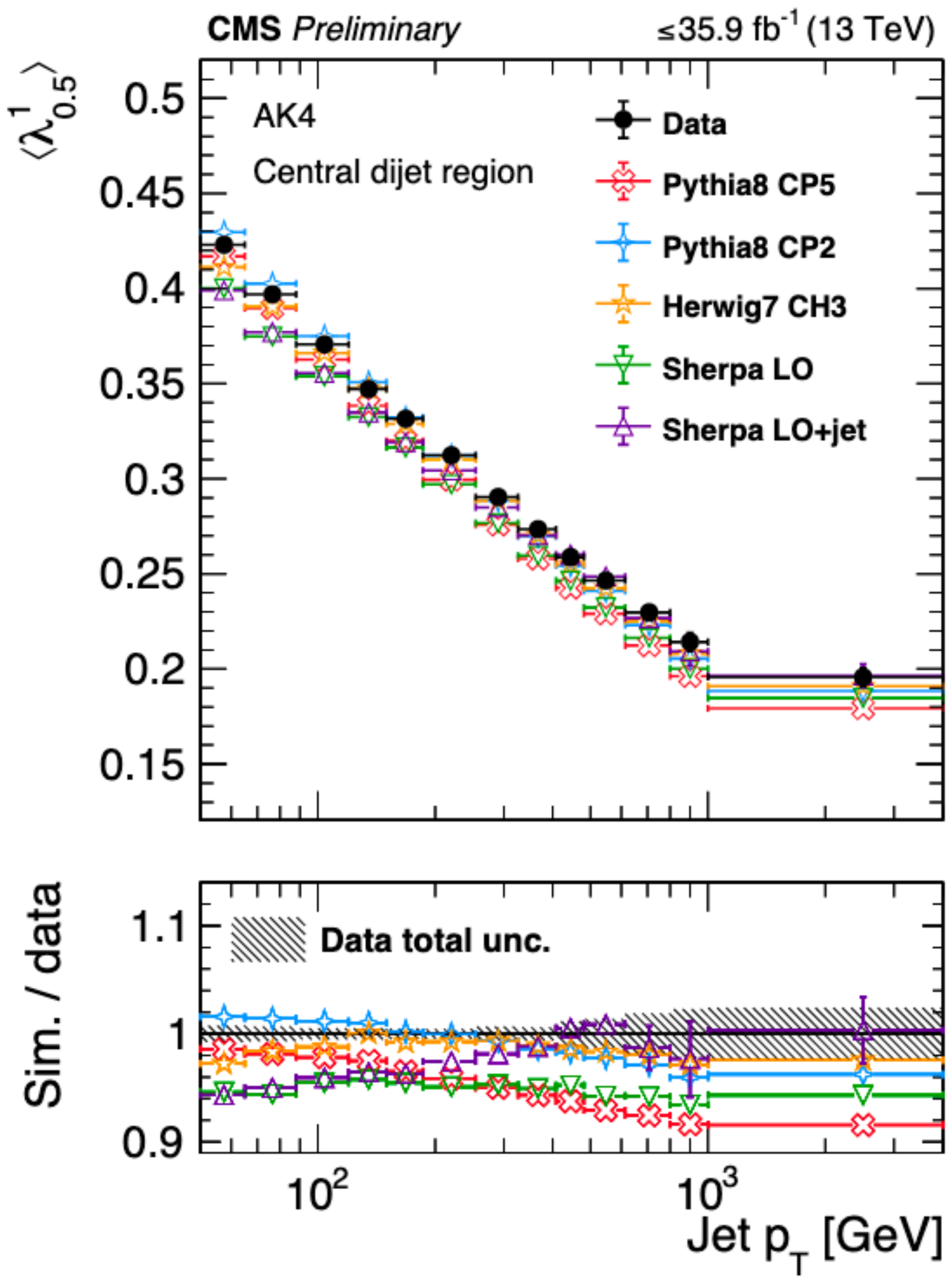

- At LO, LHA, Width, Thrust, Multiplicity, are expected to be higher in gluon-enriched samples
- Quark and gluon initiated jet showers not well described by generators, important consequences for taggers

Measuring the angle between different jet axes

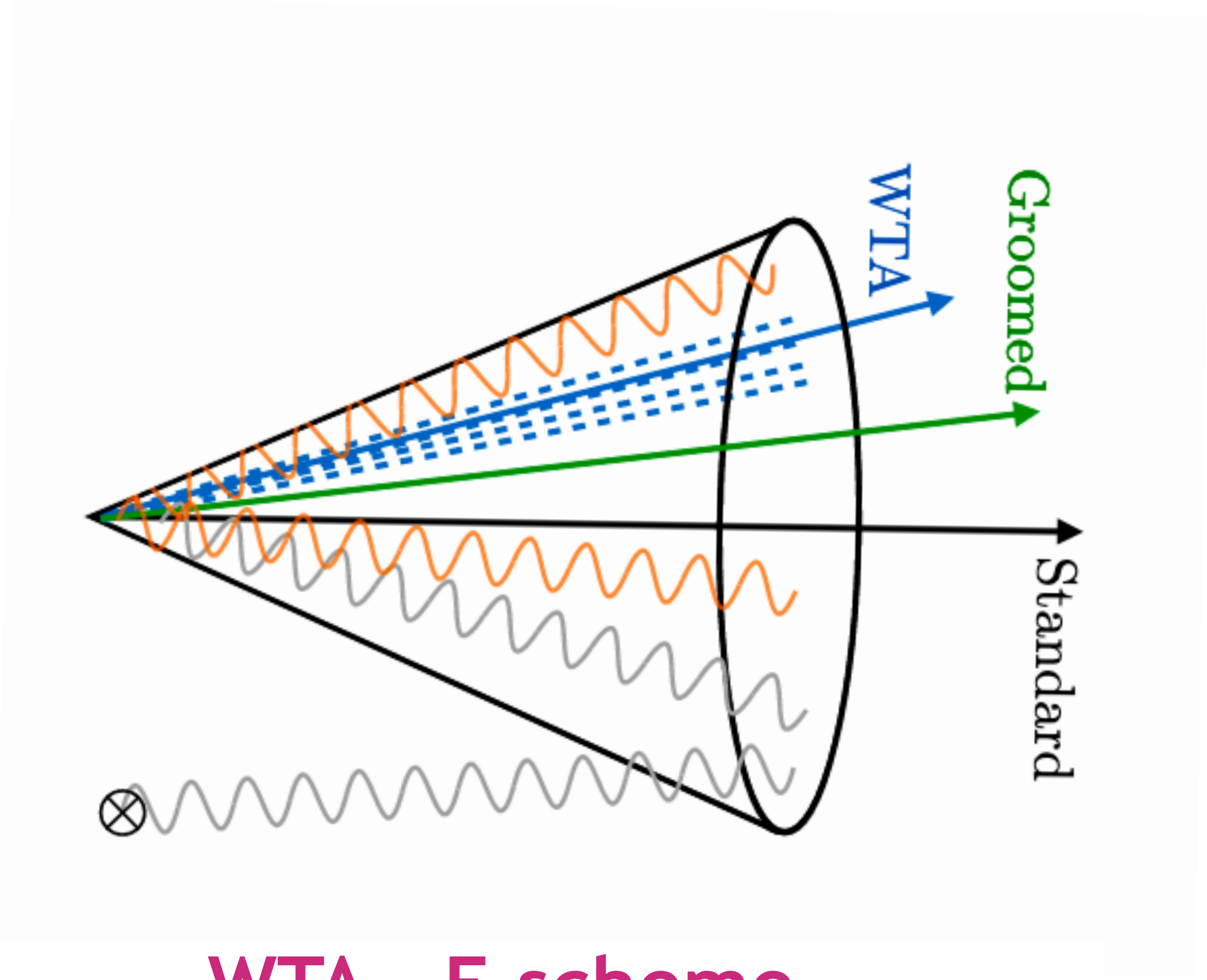

WTA —E-scheme

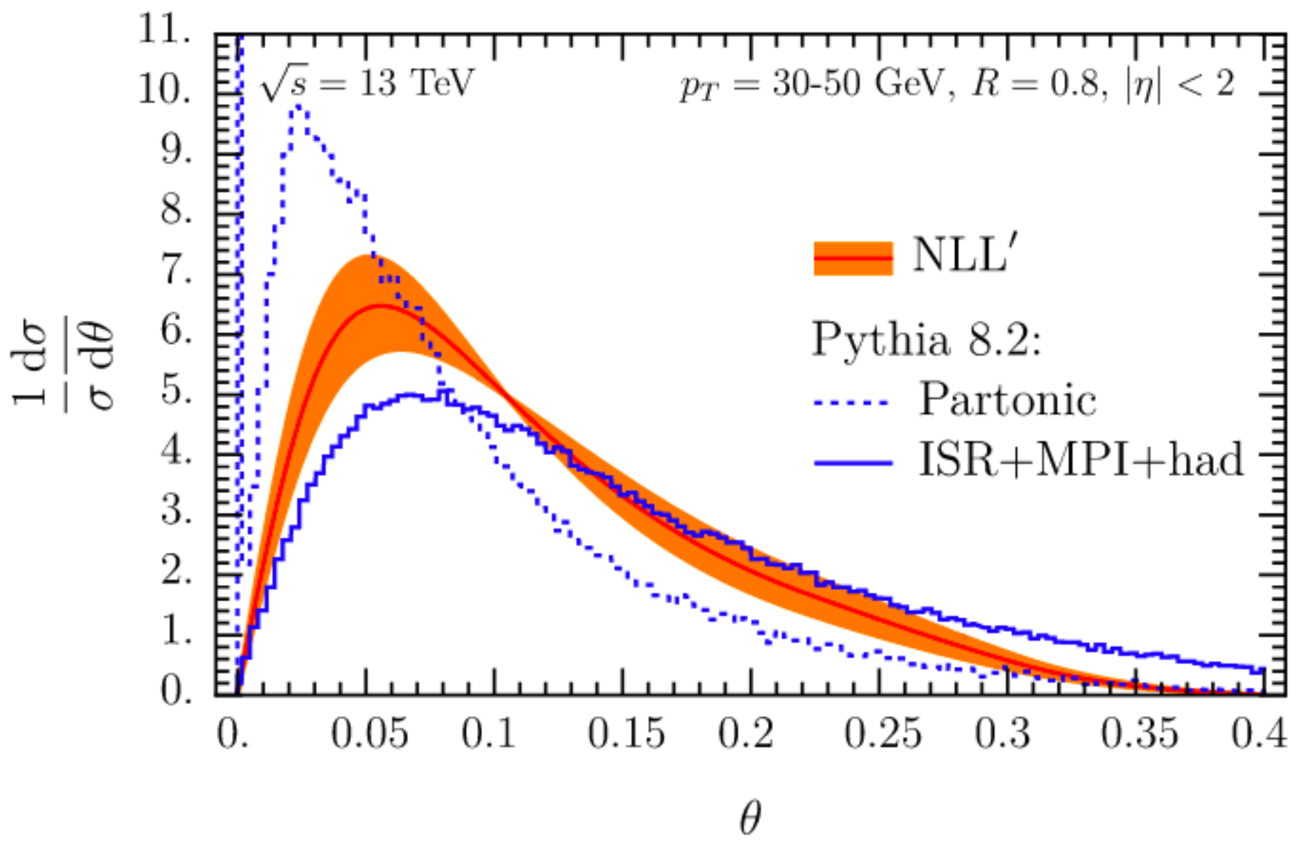

Cal et al, JHEP 04 (2020) 211

E-scheme — SD

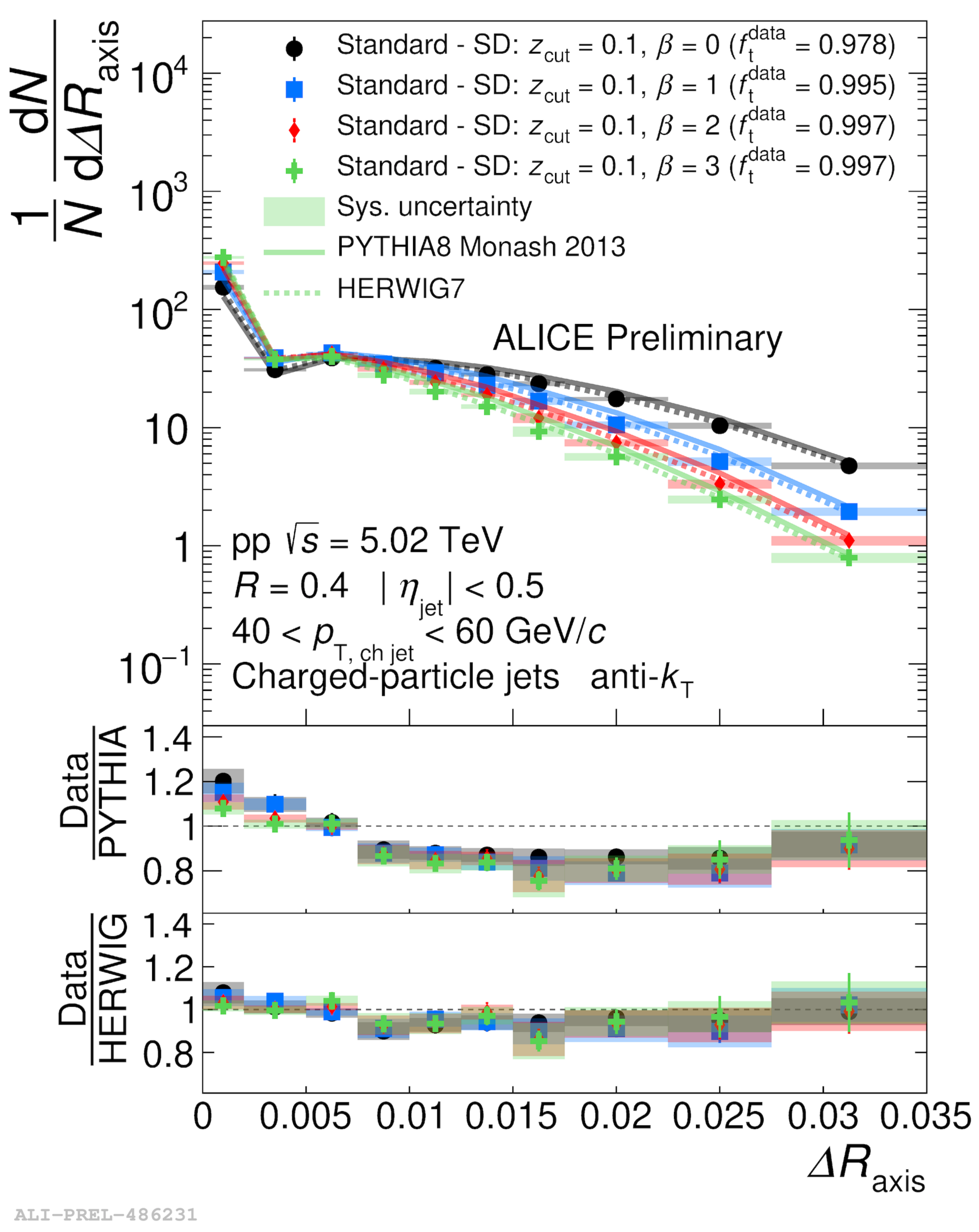

WTA —E-scheme

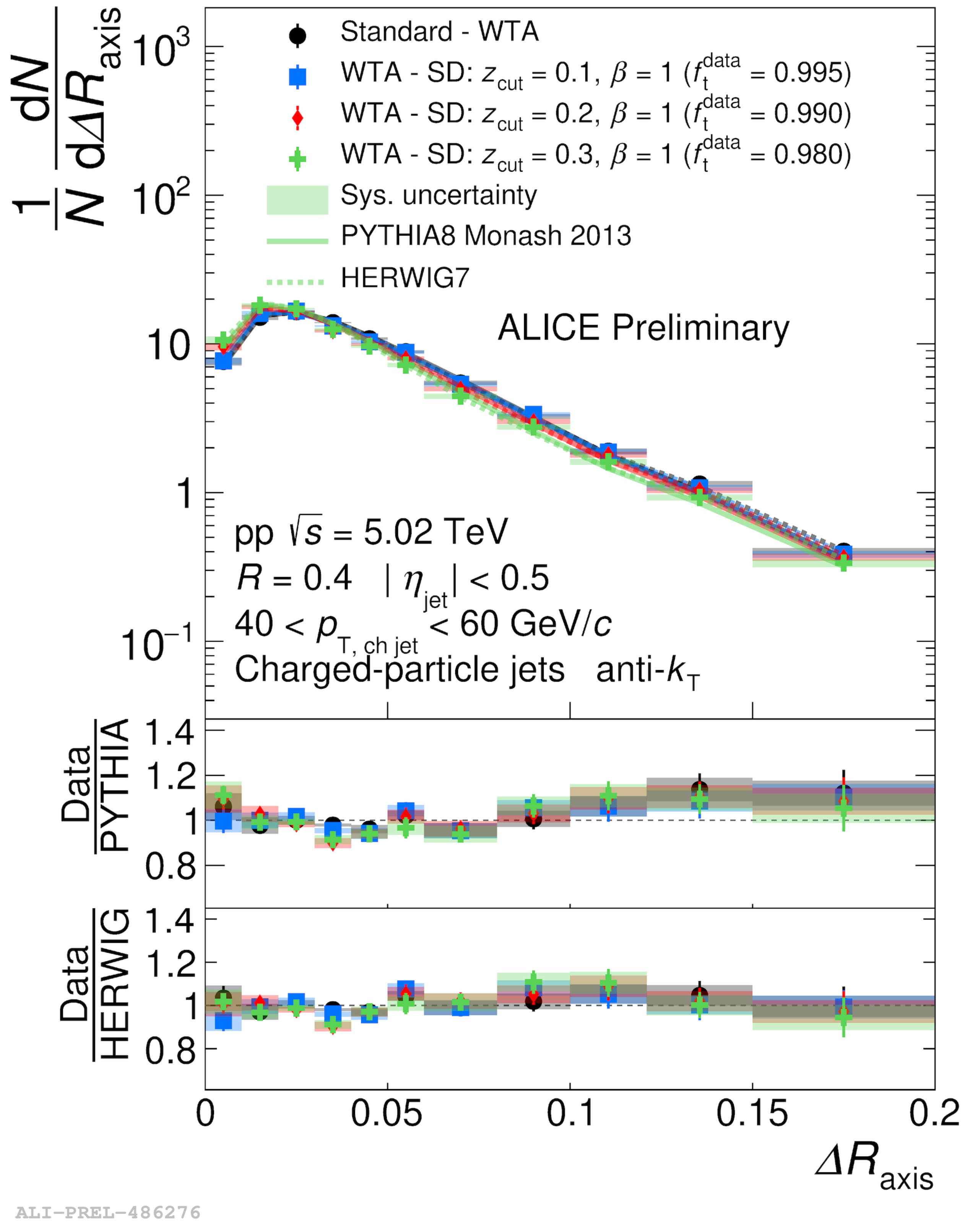

- Strong correlation between SD and E-scheme axes
- More aggressive grooming (β=0) ->larger ΔR_{axis} for SD and E-scheme
- Negligible dependence on grooming condition for WTA—E-scheme
- Differences sensitive to soft radiation pattern

Correlation of substructure observables

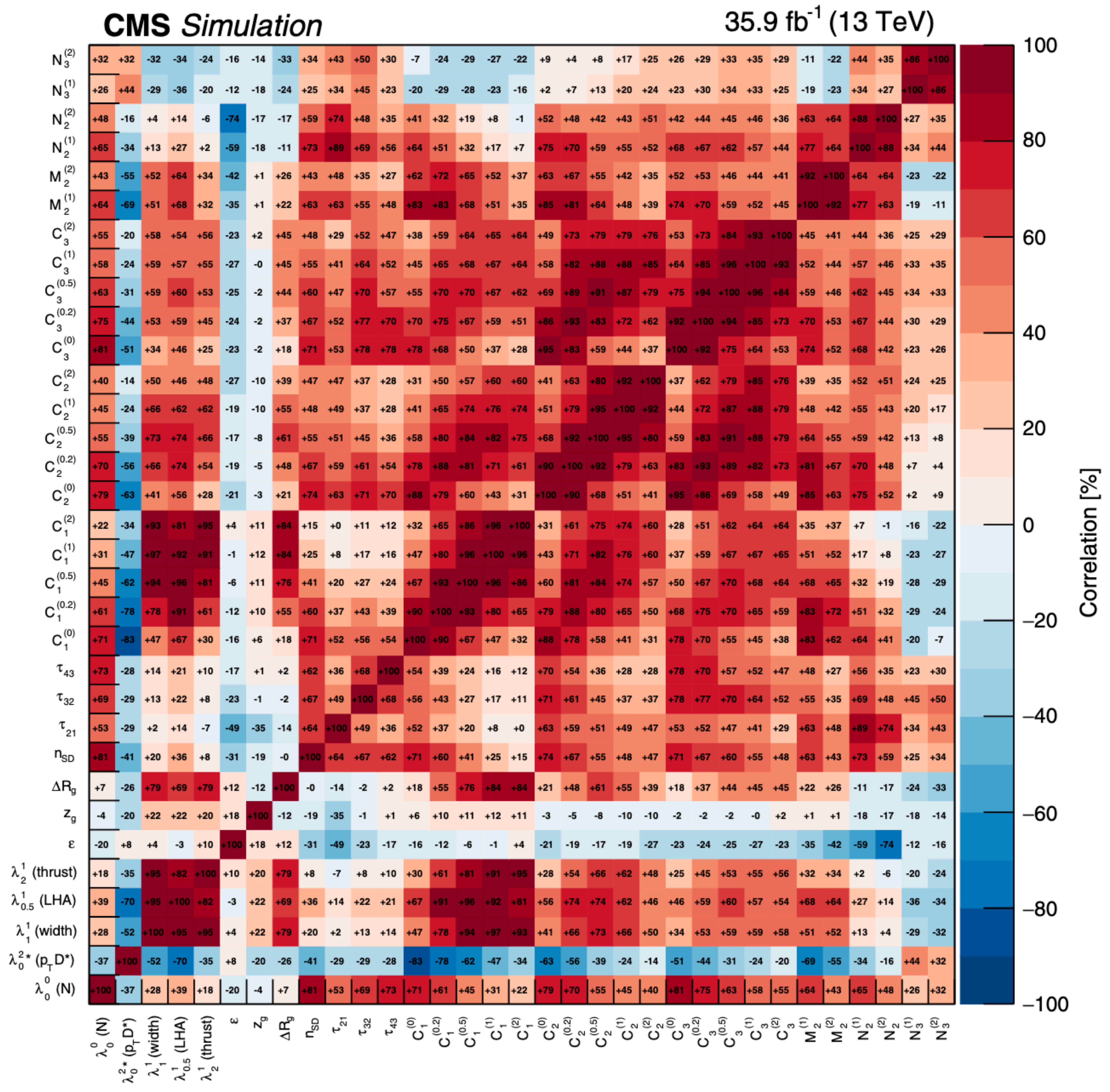

Most of the considered substructure observables are strongly correlated

Useful to select a set of minimally correlated variables:

R_g, z_g, multiplicity, ϵ

And study the best $\alpha_S(m_Z)$ that describes the data

This kind of consideration has broad scope!

CMS, Phys.Rev.D 98 (2018) 9, 092014

Correlation of substructure observables

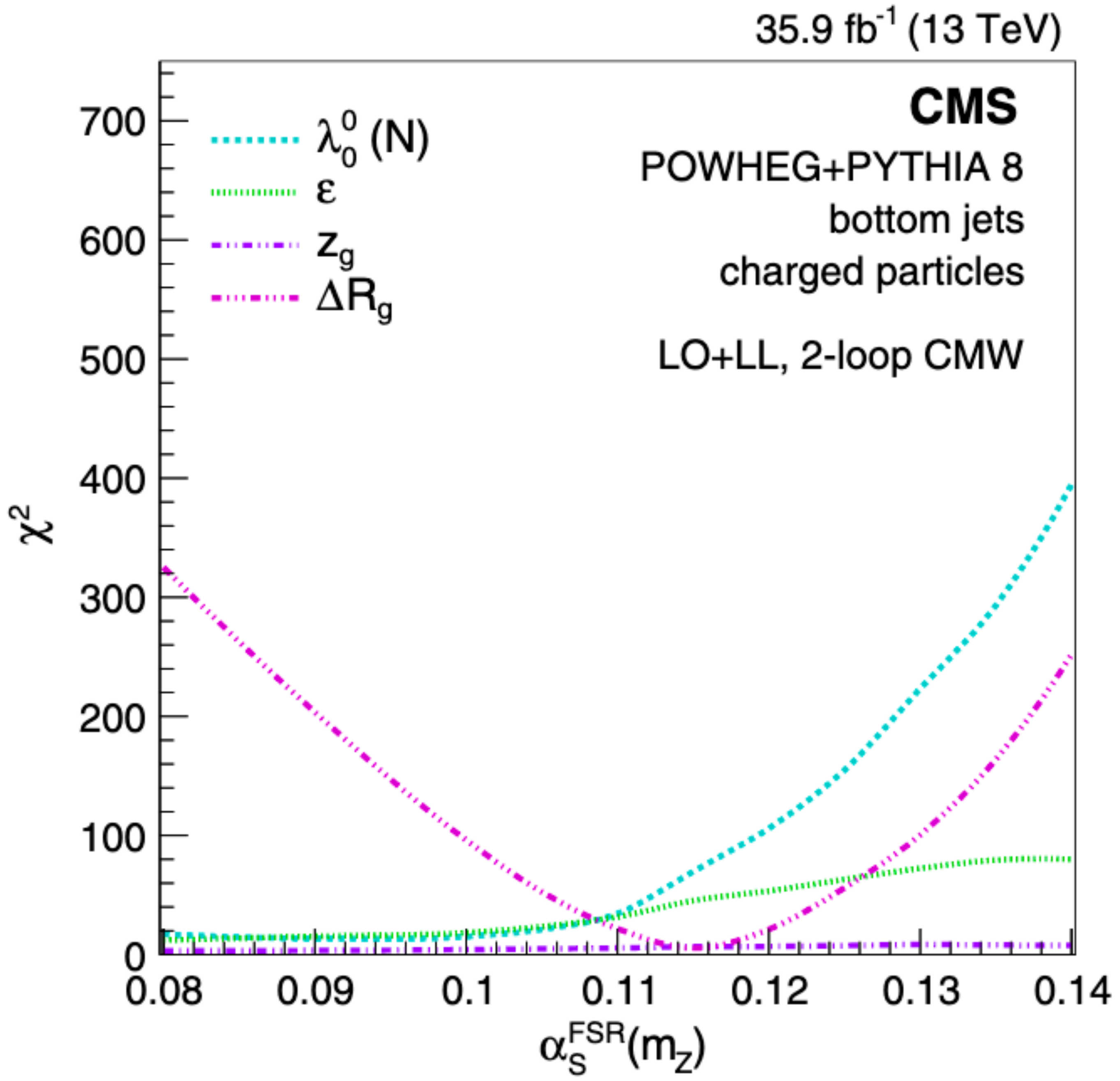

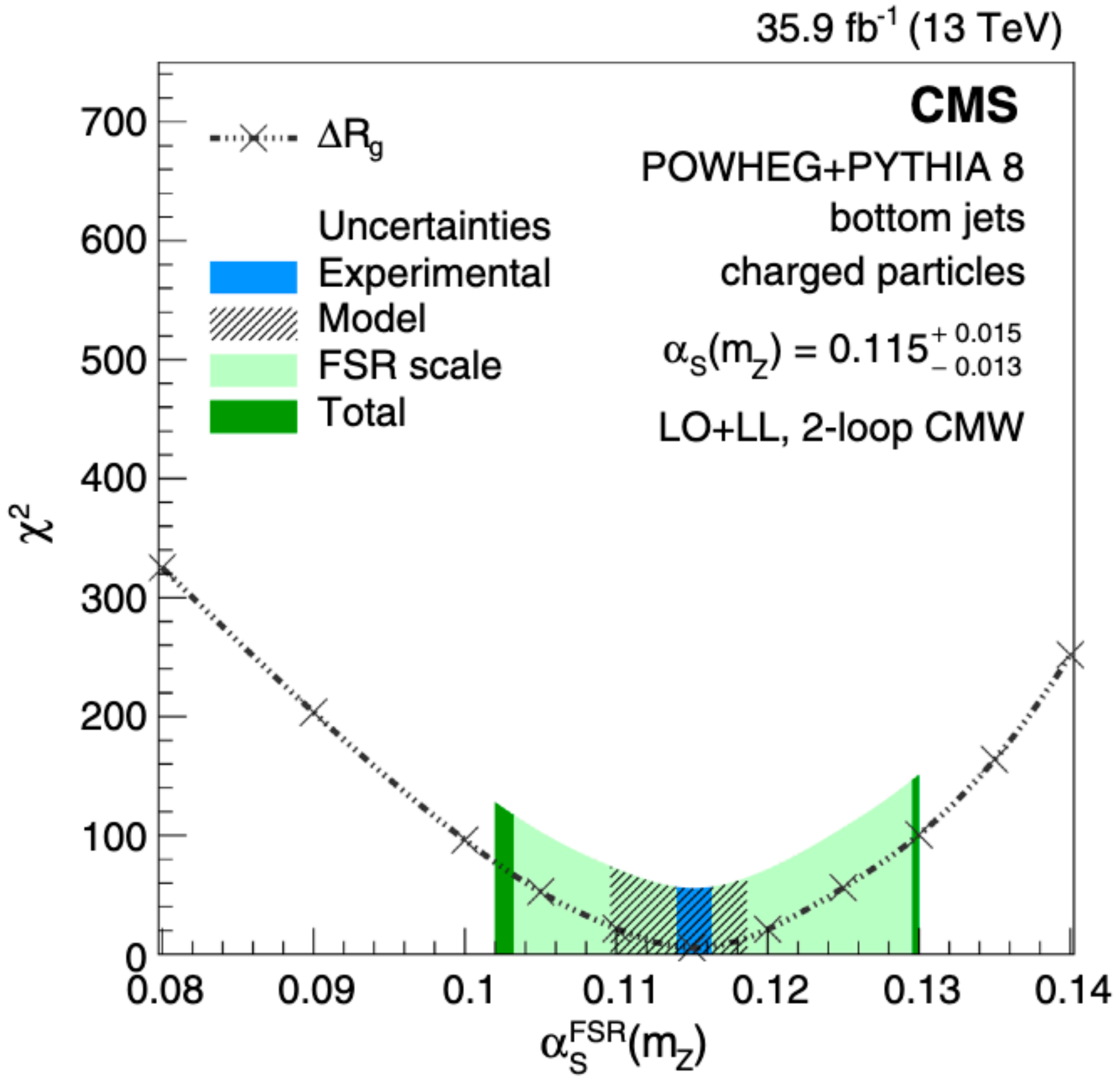

Most of the considered substructure observables are strongly correlated

Useful to select a set of minimally correlated variables:

<u>R_g, z_g, multiplicity, ϵ</u>

And study the best $\alpha_S(m_Z)$ that describes the data

- z_g independent on $\alpha_S(m_Z)$ (LO expectation)
- Multiplicity expected to be highly affected by non pert. effects
- $R_{g;}$ lower impact of non pert. radiation, sensitivity to $\alpha_S(m_Z)$

CMS, Phys.Rev.D 98 (2018) 9, 092014

What about colour flow?

Color singlet vs octet decays

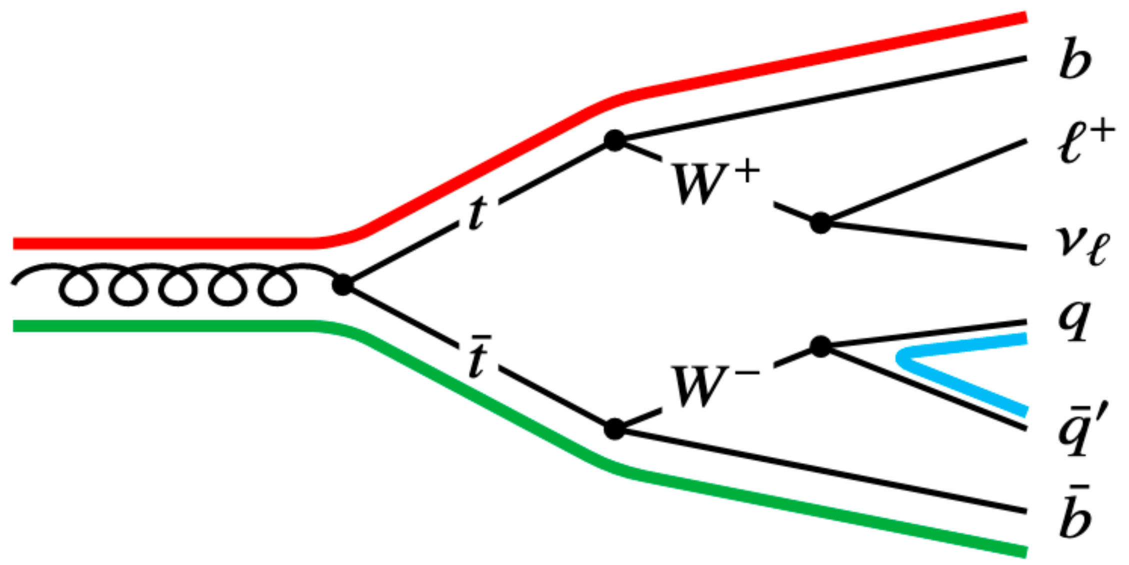

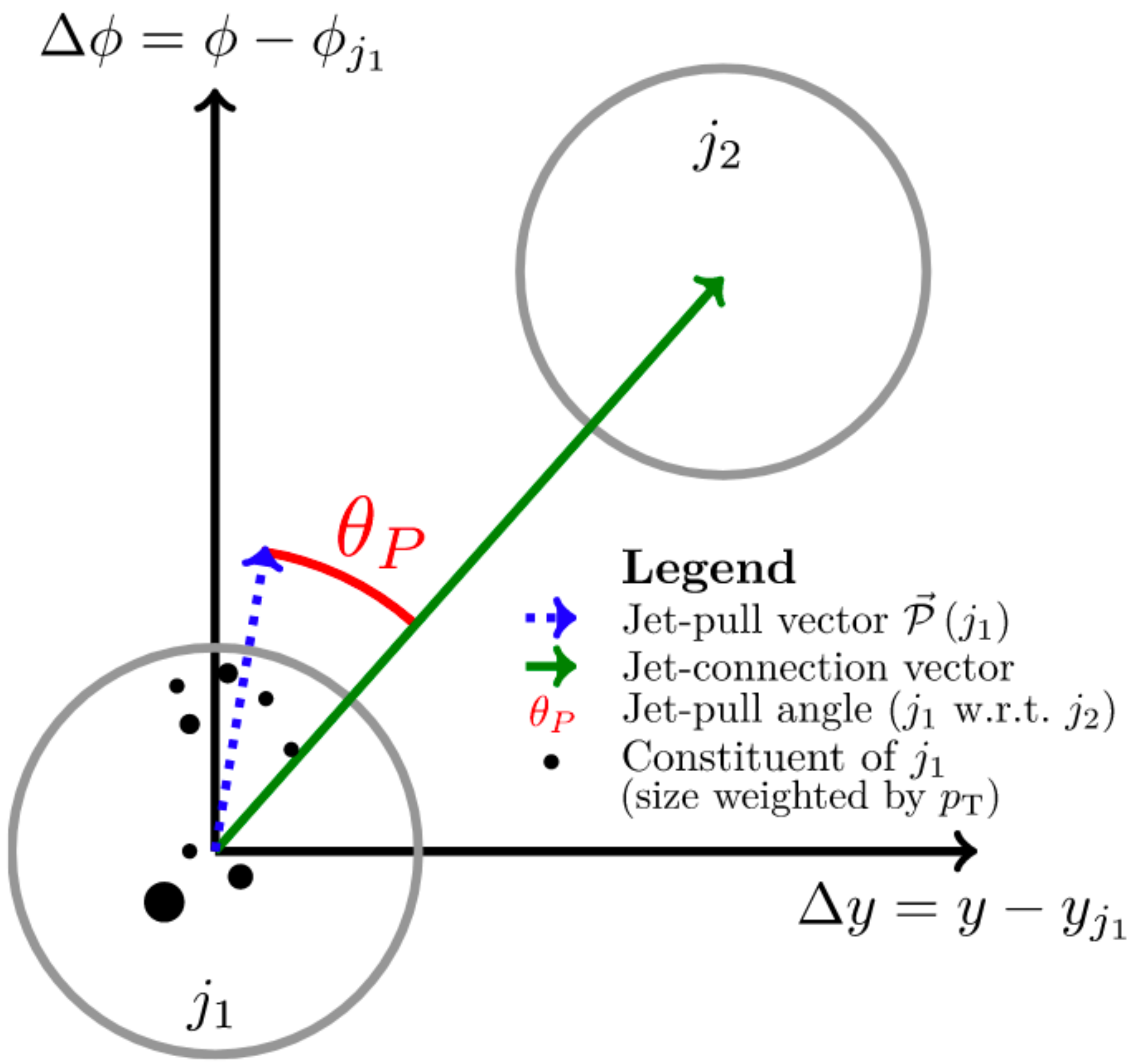

[ATLAS, Eur. Phys. J. C 78 (2018) 847]

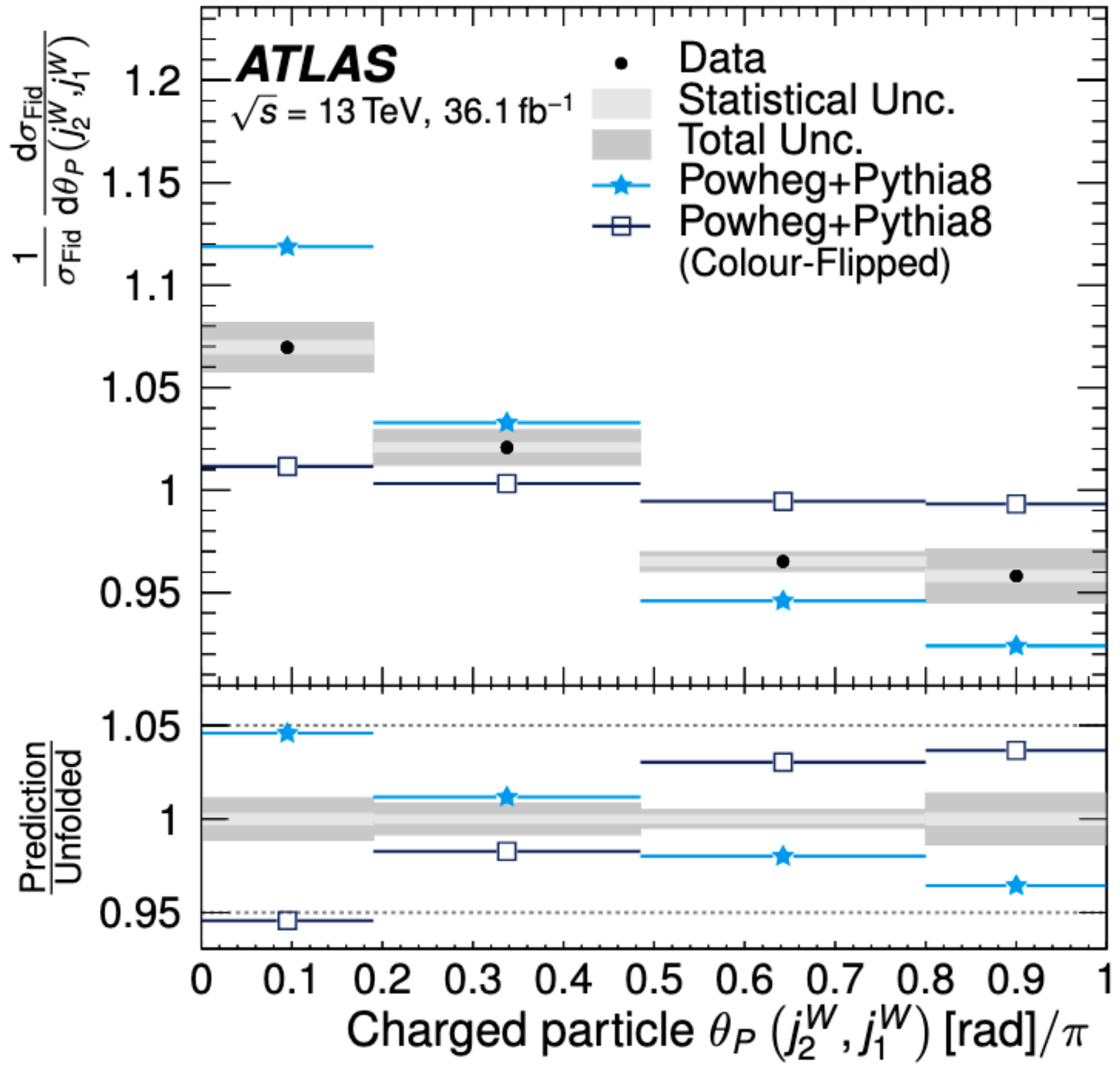

(b) θ_P (j_2^W, j_1^W)

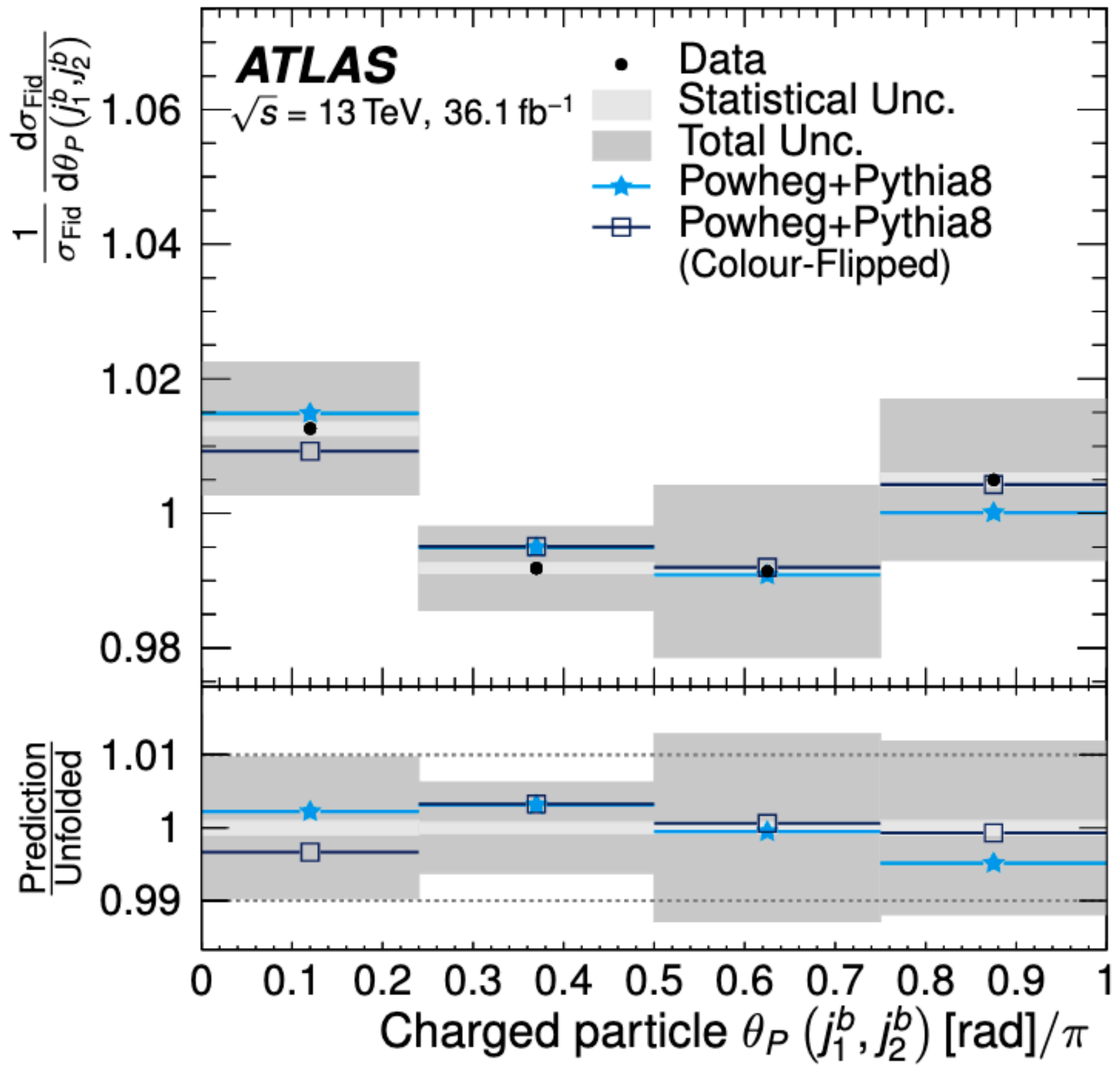

Pull angle: measurement of how much the radiation pattern from one jet leans towards another

Color flow not well constrained in QCD

Color info could complement kinematic properties to select specific topologies

New IRC-safe version (pull magnitude and projections)
Larkoski et al, JHEP 01 (2020) 104

A note on calorimetric vs track-based results

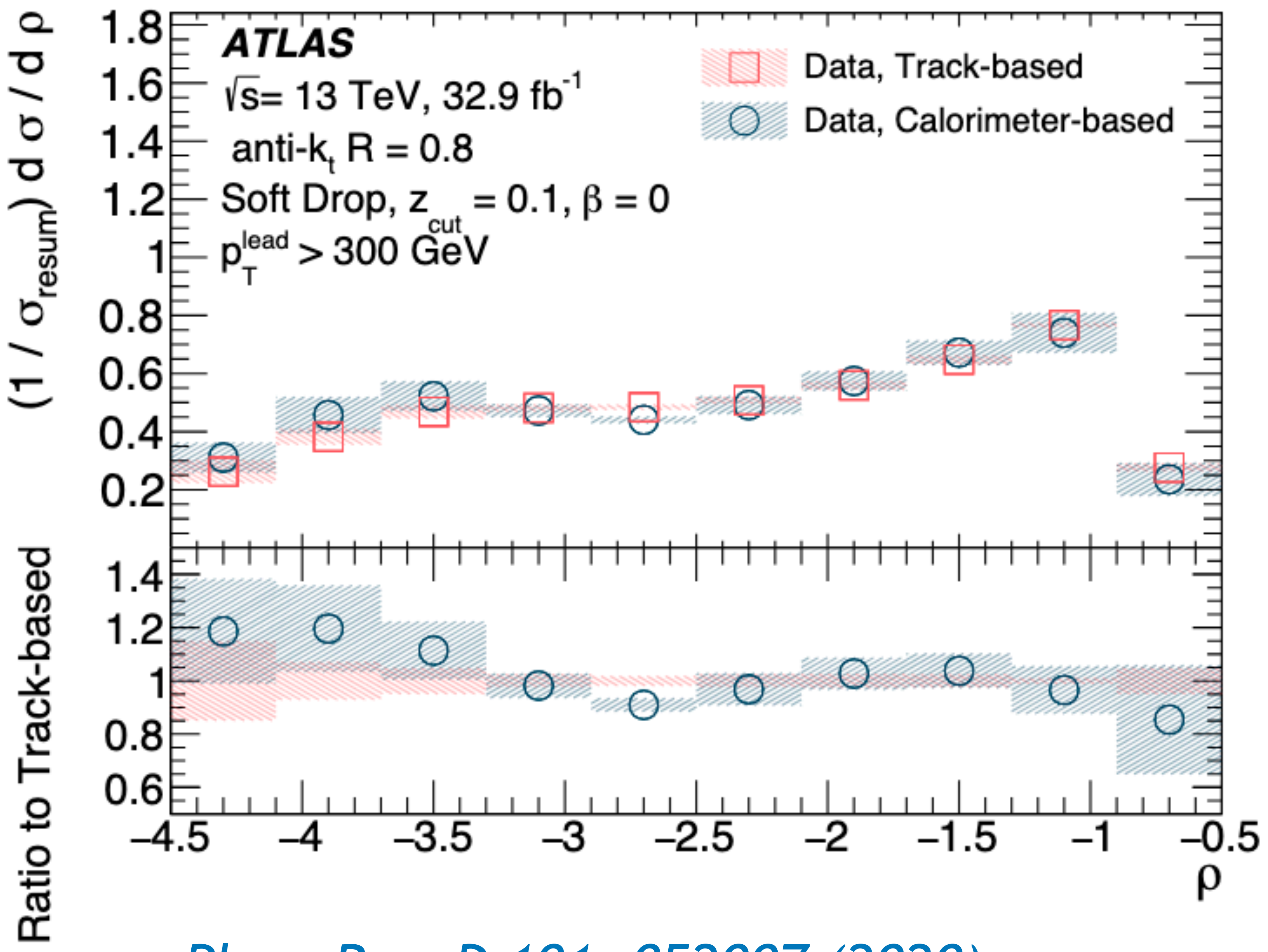

Phys. Rev. D 101, 052007 (2020)

Track-based measurements are more precise due to the angular resolution of tracks

Relevant question with substructure entering precision regime: can jet substructure be formulated in a manner that facilitates more precise calculations?

- Track functions: *Chan et al Phys.Rev.Lett. 111 (2013) 102002*
- Interesting proposal that incorporates non-perturbative info from tracks or charges into pert. calculation and connects to formal developments in QFT
  Chen et al, Phys. Rev. D 102, 054012 (2020)

The dead-cone effect in QCD

Gluon radiation by a particle of mass m and energy E is suppressed within a cone of angular size m/E around the emitter

$$\frac{\frac{dN_Q}{d\theta}}{\frac{dN_q}{d\theta}} \propto \frac{\theta^4}{(\theta^2+\theta_0^2)^2} \qquad \theta_0 = \frac{m_Q}{E_Q}$$

Parametric dependence of the dead cone effect

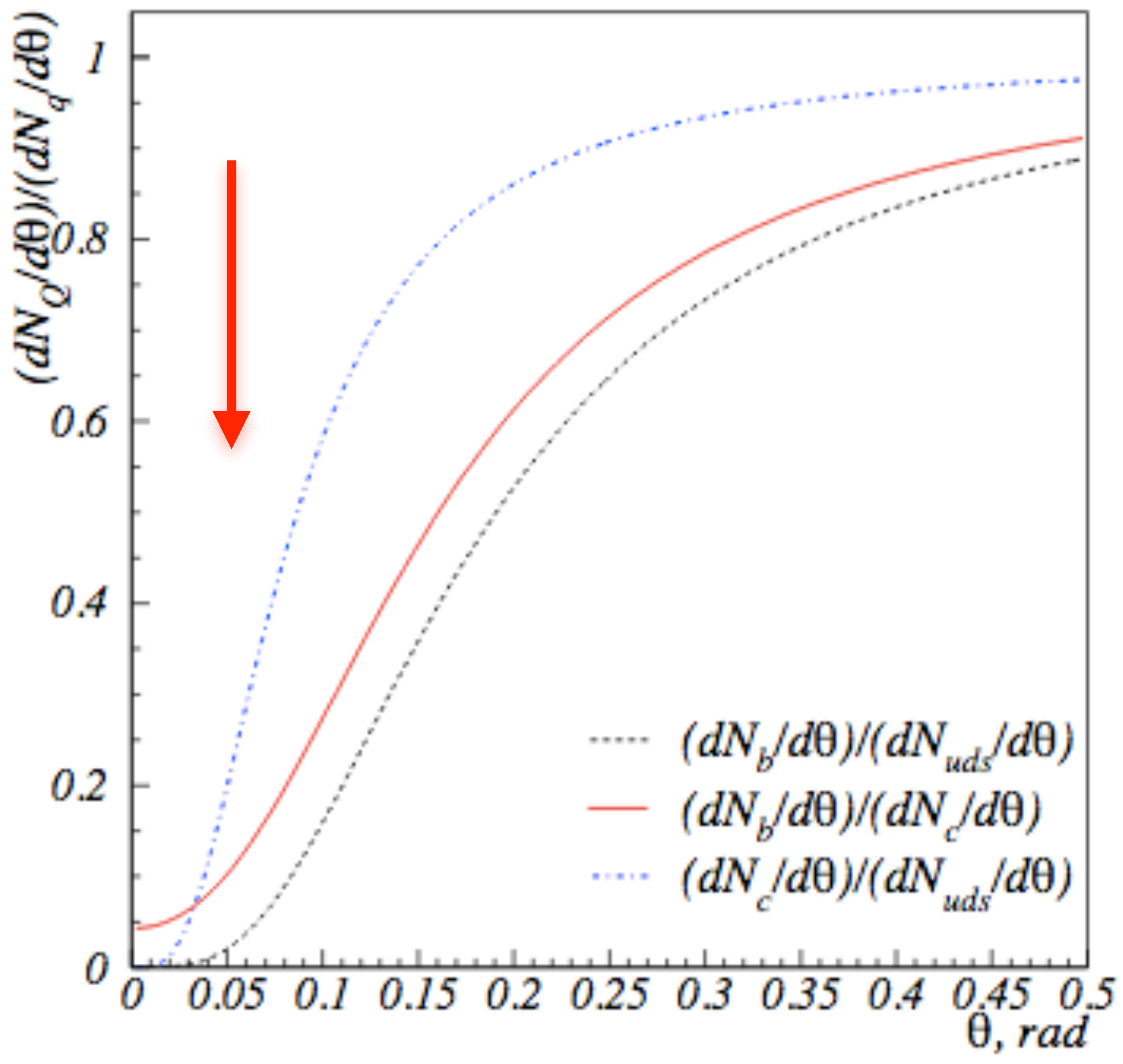

Battaglia et al, DELPHI-2004-037 CONF 712

Dokshitzer,V.A.Khoze and S.I.Troyan "On specific QCD properties of heavy quark fragmentation", J. Phys. G 17 (1991)

The dead-cone effect in QCD

Direct consequences of the dead cone:

- Restriction of hard gluons with small k_{T}
  —> reduction of emissions, FF peaked at larger z
- Lower intrajet multiplicities

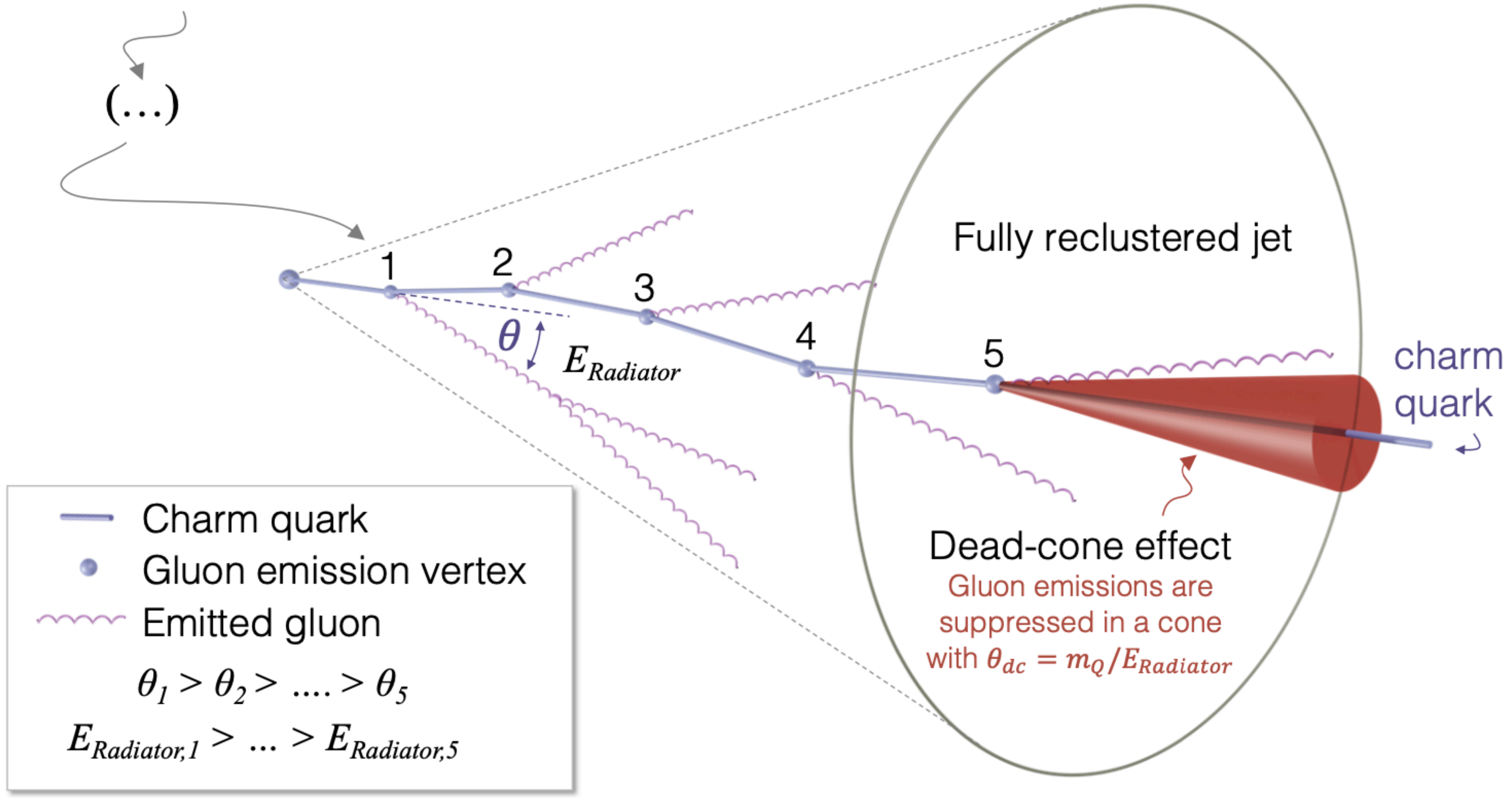

Experimental challenges for a direct measurement

- The decays of the heavy flavour particles happen at similar angular scales and fill the dead cone
- Accurate determination of the dynamically evolving direction of the heavy-flavour particle relative to which radiation is suppressed

The Lund plane of heavy-quark jets: exposing the dead cone

Inclusive jets

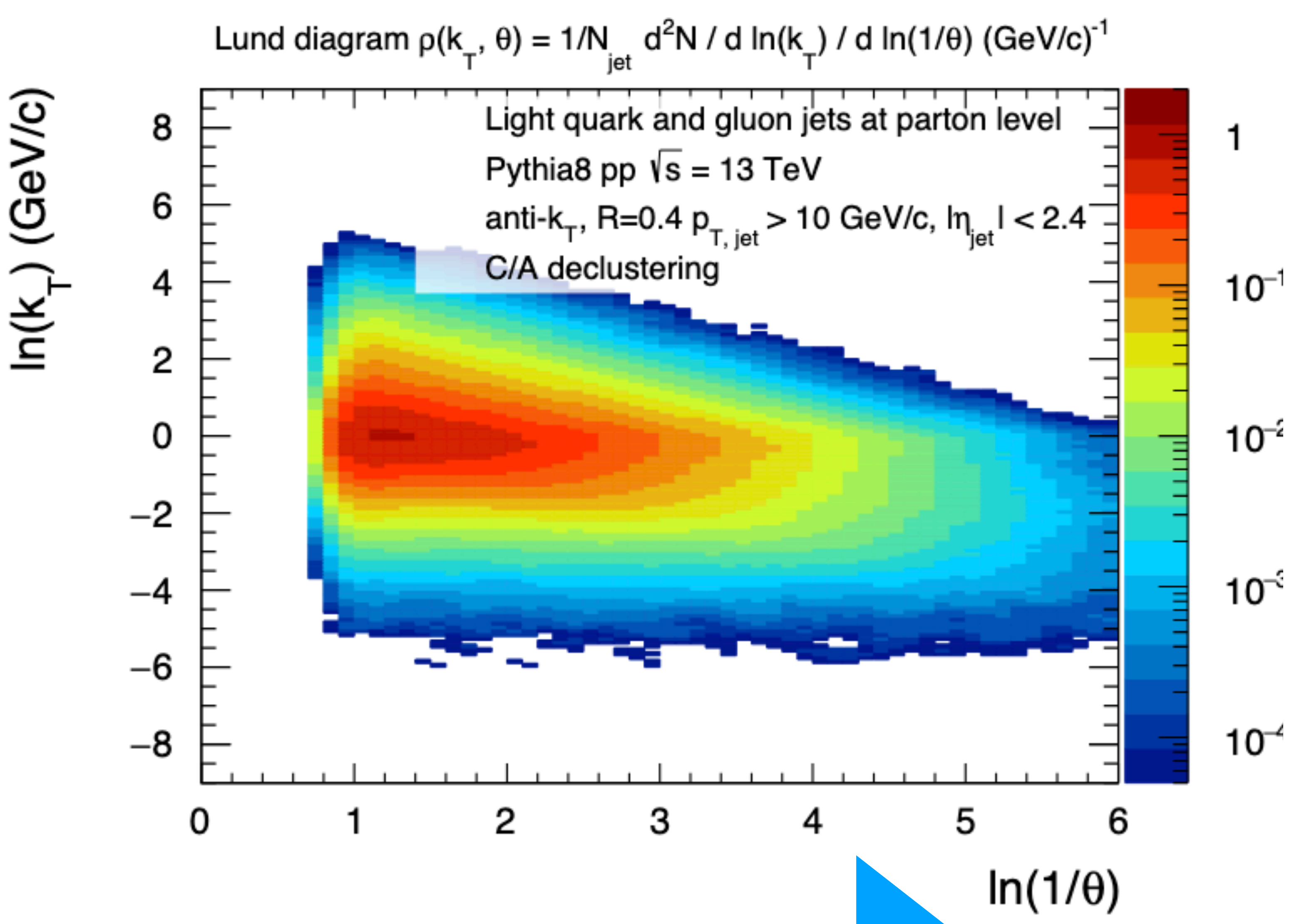

D jets

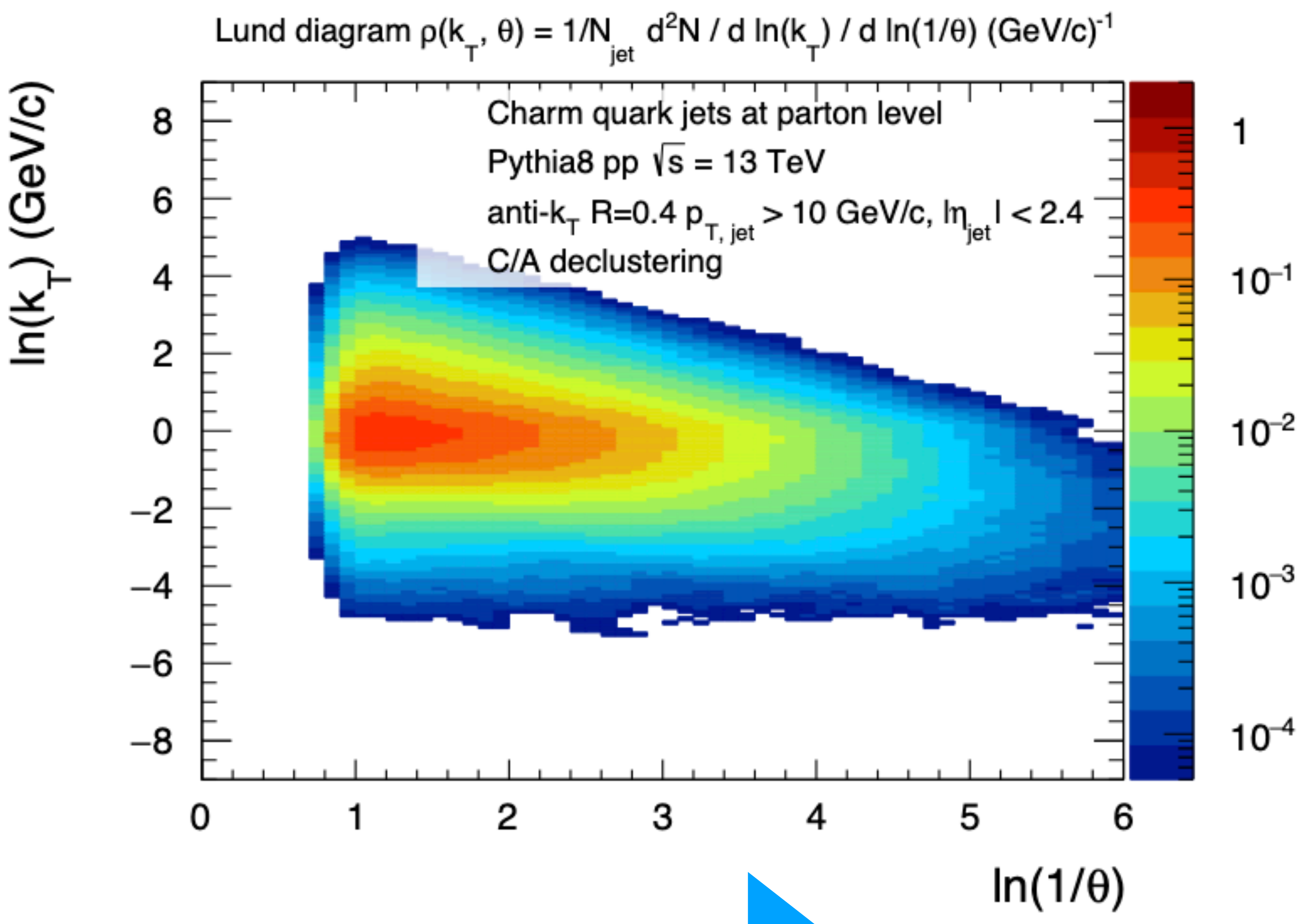

B jets

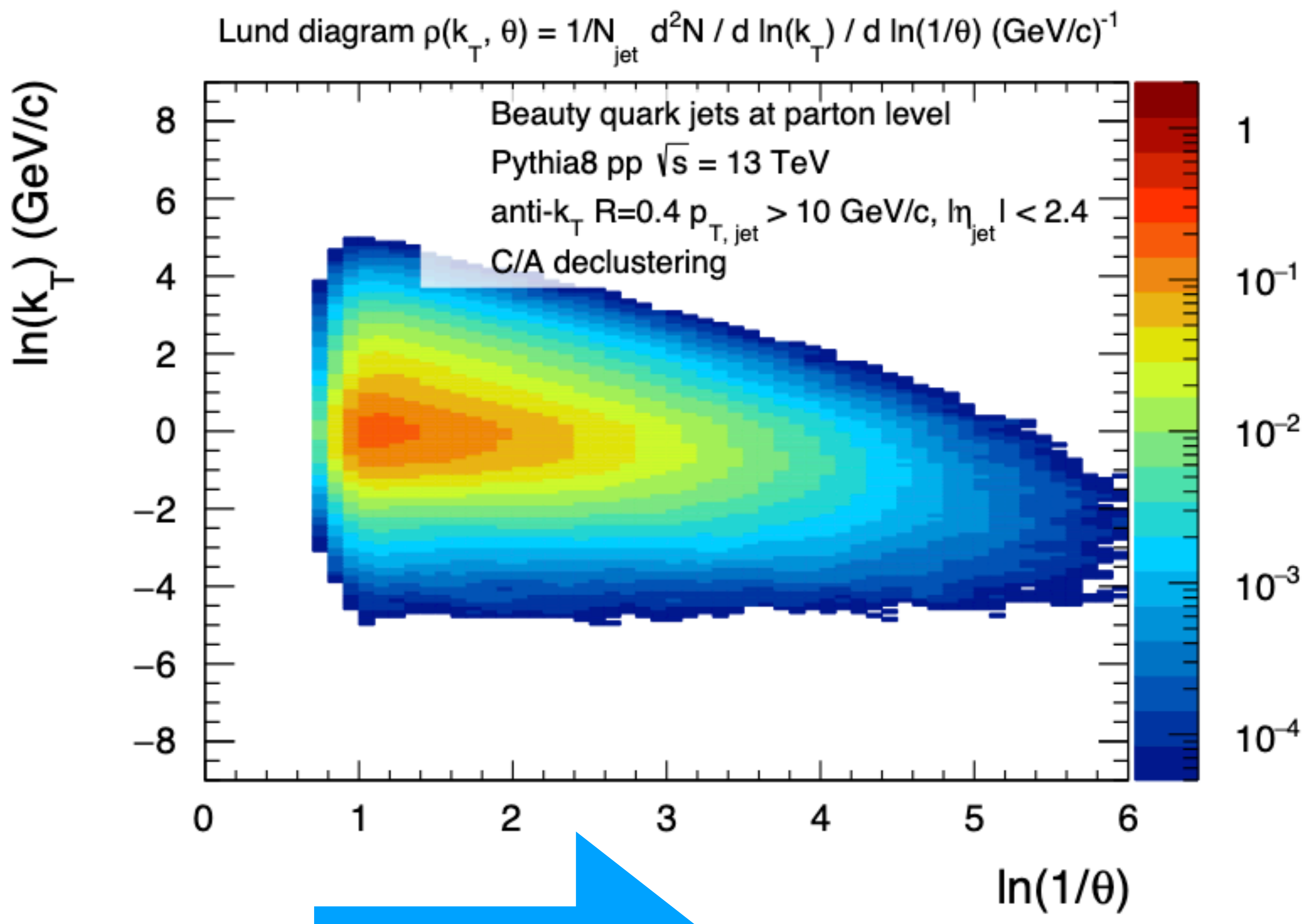

- Iteratively decluster jets with a fully reconstructed D or B meson among its constituents
- Follow always the prong containing the heavy flavour hadron
- At the deepest levels of the jet tree, splittings are at sufficiently small angles to be sensitive to quark mass

[Cunqueiro, Ploskon, Phys.Rev.D 99 (2019) 7, 074027]

The Lund plane of heavy-quark jets: exposing the dead cone

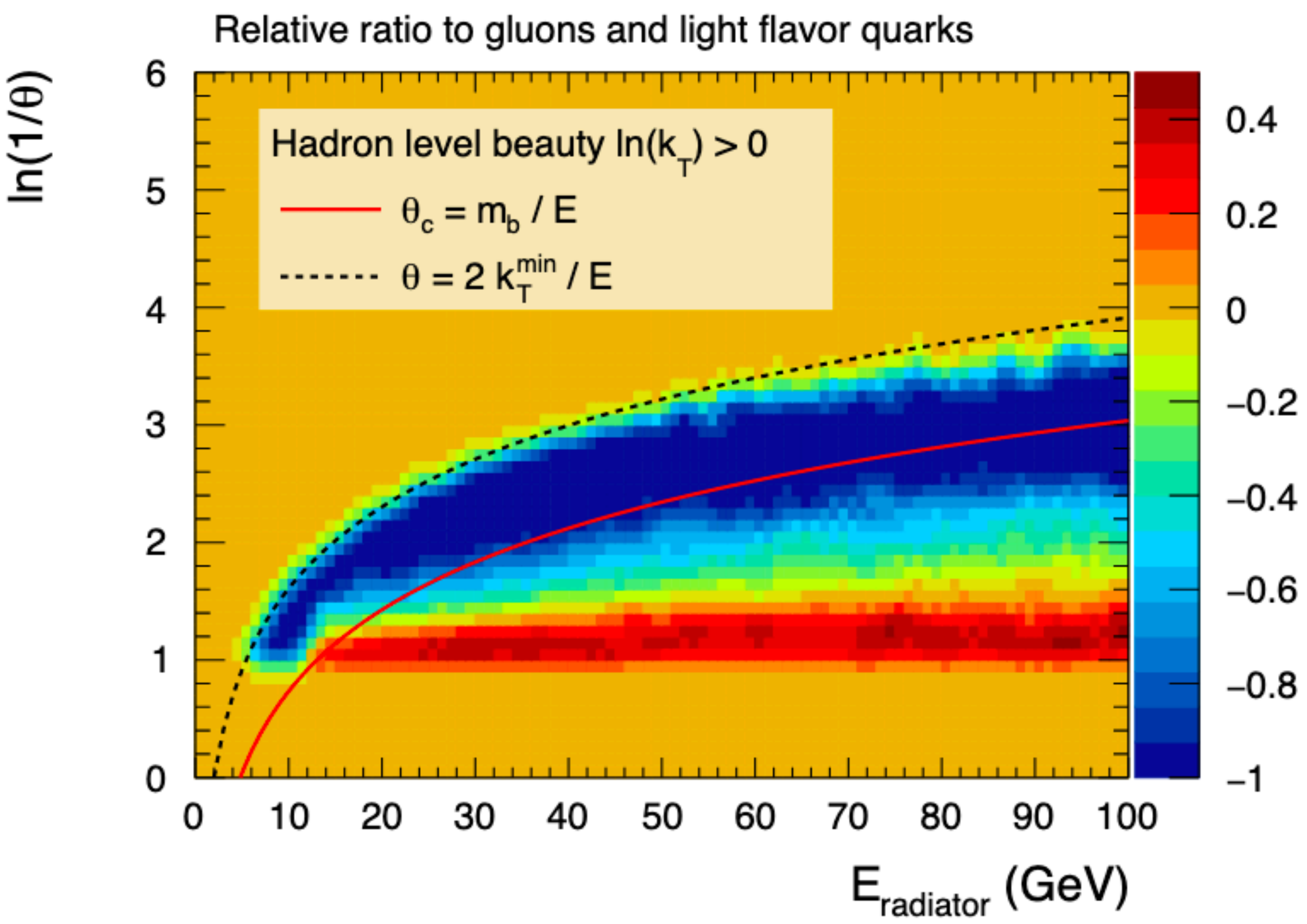

- Iteratively decluster jets with a fully reconstructed D^0 among its constituents
- Follow always the prong containing the D^0
- Register the splitting energy E_{radiator} and the splitting k_T at each step

Define:

$$R(\theta) = \frac{1}{N^{D^0\,\mathrm{jets}}} \frac{dn^{D^0\,\mathrm{jets}}}{d\ln(1/\theta)} \Bigg/ \frac{1}{N^{\mathrm{inclusive\,jets}}} \frac{dn^{\mathrm{inclusive\,jets}}}{d\ln(1/\theta)} \Bigg|_{k_T,\, E_{\mathrm{Radiator}}}$$

E_{radiator}=energy of the splitting prong at each declustering step

The deepest levels of the jet tree are splittings at small angles/lower energies
->most sensitive to mass and the dead cone effect

[Cunqueiro, Ploskon, Phys.Rev.D 99 (2019) 7, 074027](#)

The signal extraction

D jets (signal region)

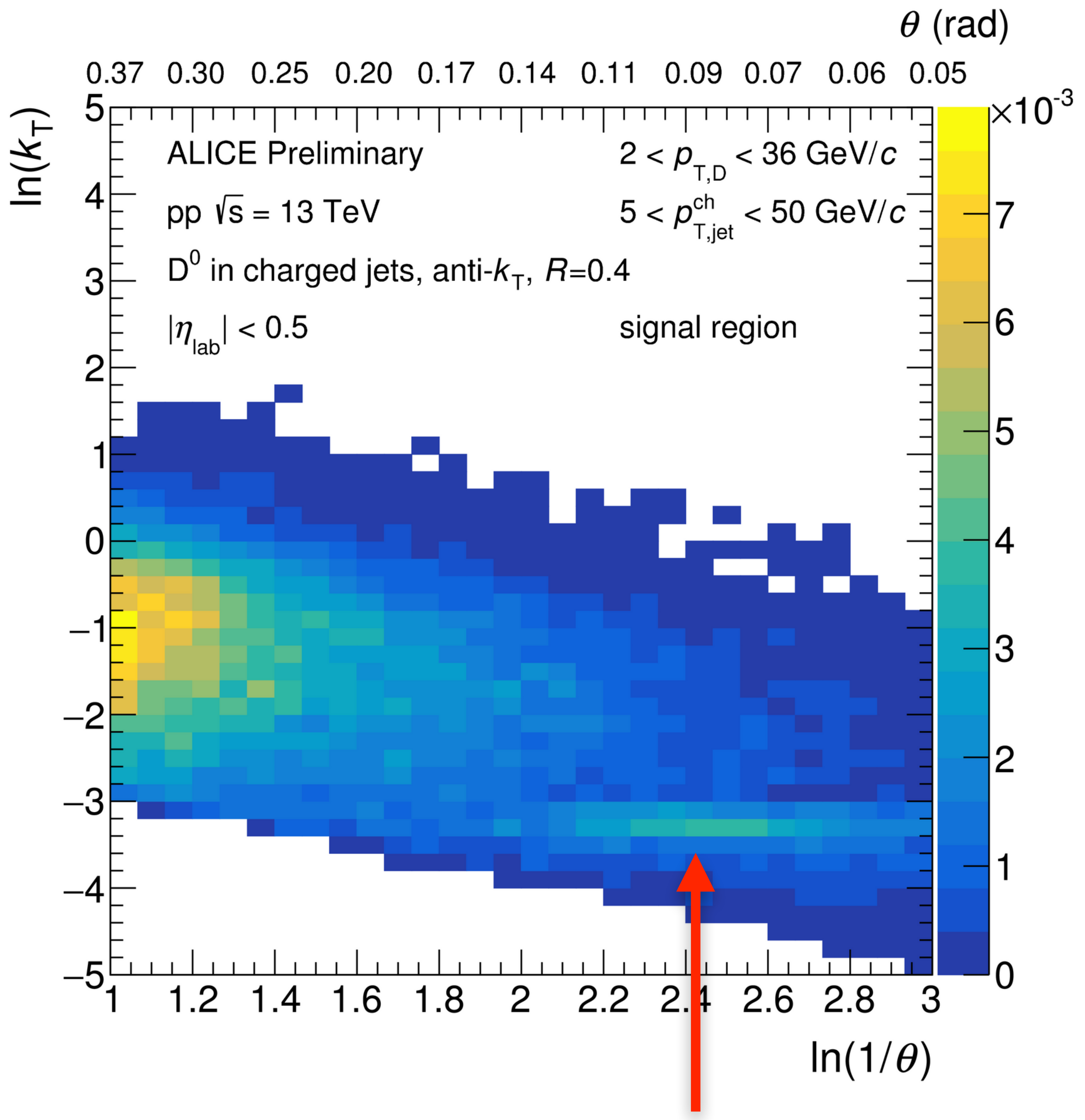

D jets (bkg region)

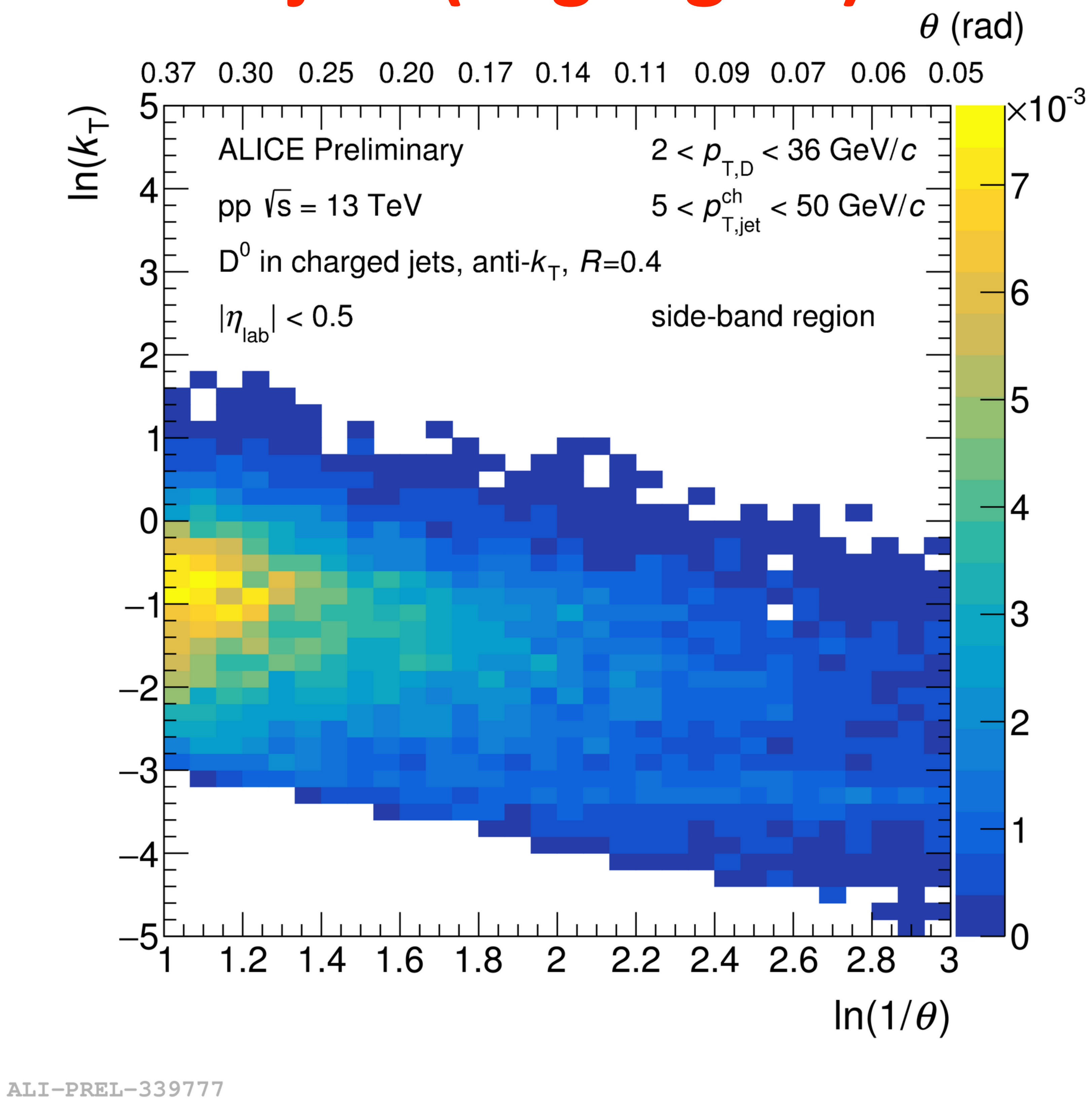

$D^0 \to K^{\pm}\pi^{\mp}$ (BR=3.8%)

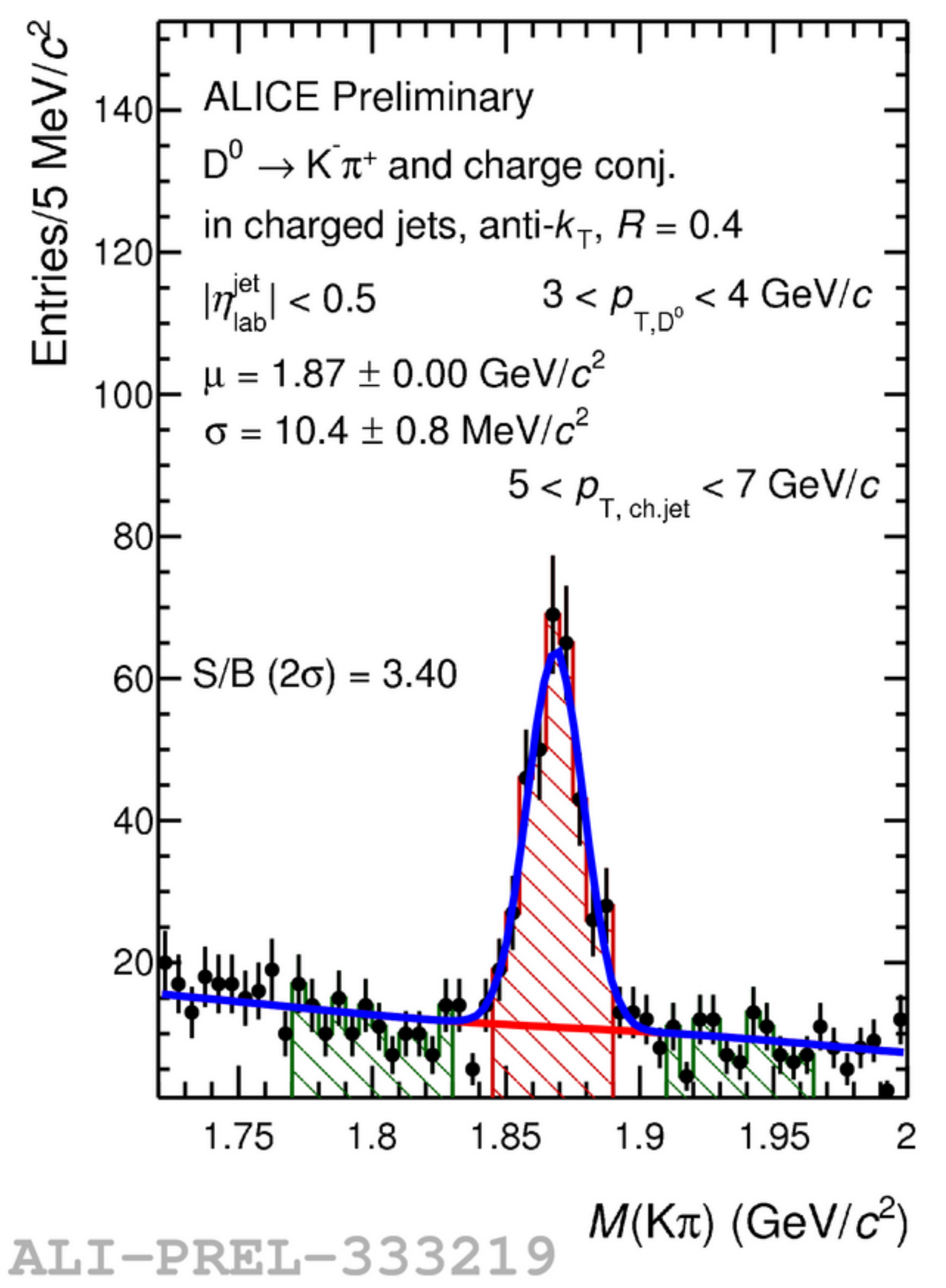

D^0 from D^* decays

$$\rho^{D^0\text{jet}} = \sum_i \frac{1}{\varepsilon_i}\left(\rho(\theta,E)_S^{D^0\text{jet candidate}} - \frac{A_S}{A_B}\rho(\theta,E)_B^{D^0\text{jet candidate}}\right)$$

- Invariant mass distribution of the K±, π∓ in bins of $p_{T,D}$
- Side-band subtraction procedure in 2D on Lund Maps
- Correction by D^0 reconstruction efficiency

The signal extraction

D jets (signal region)

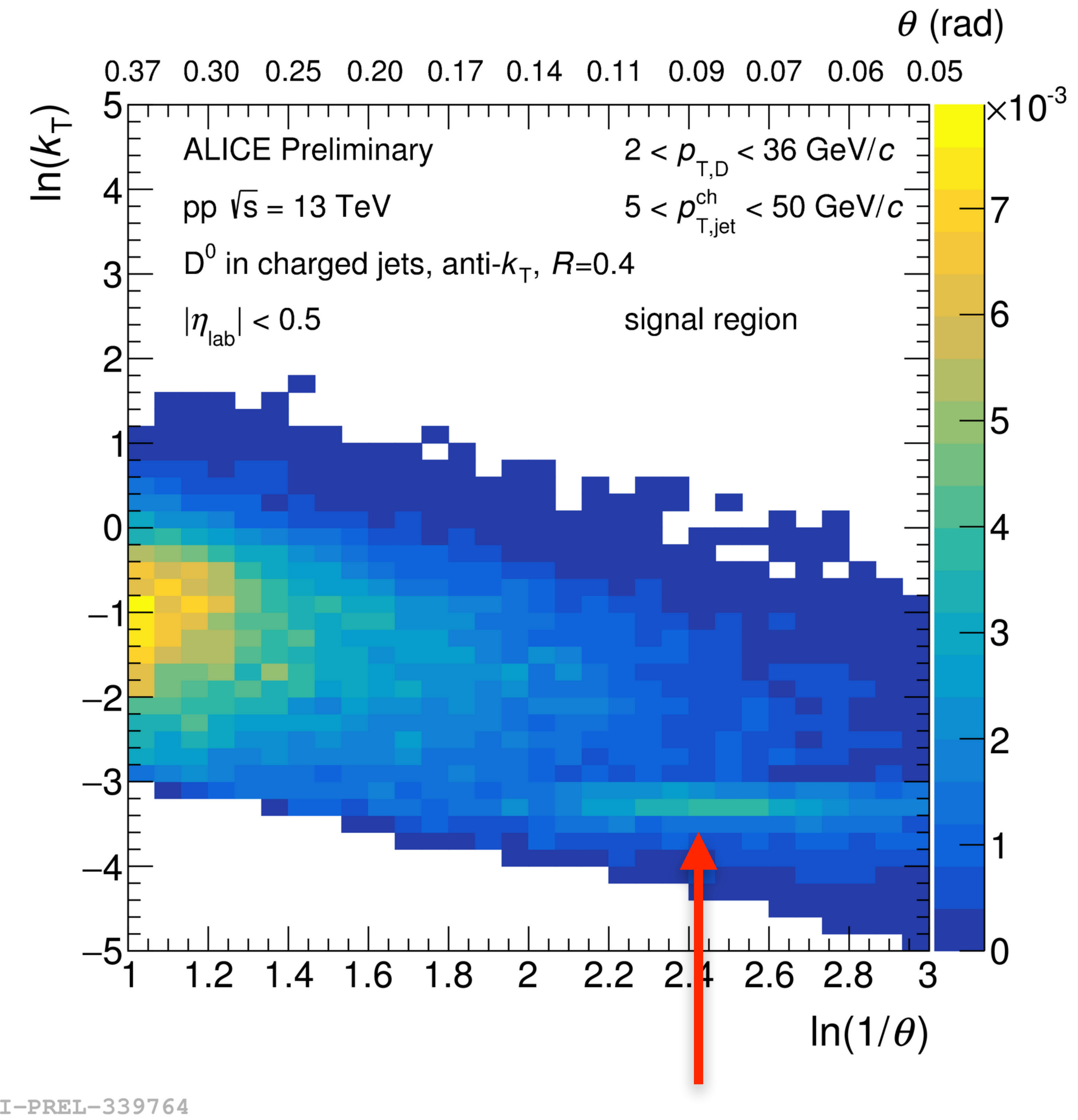

D jets (bkg region)

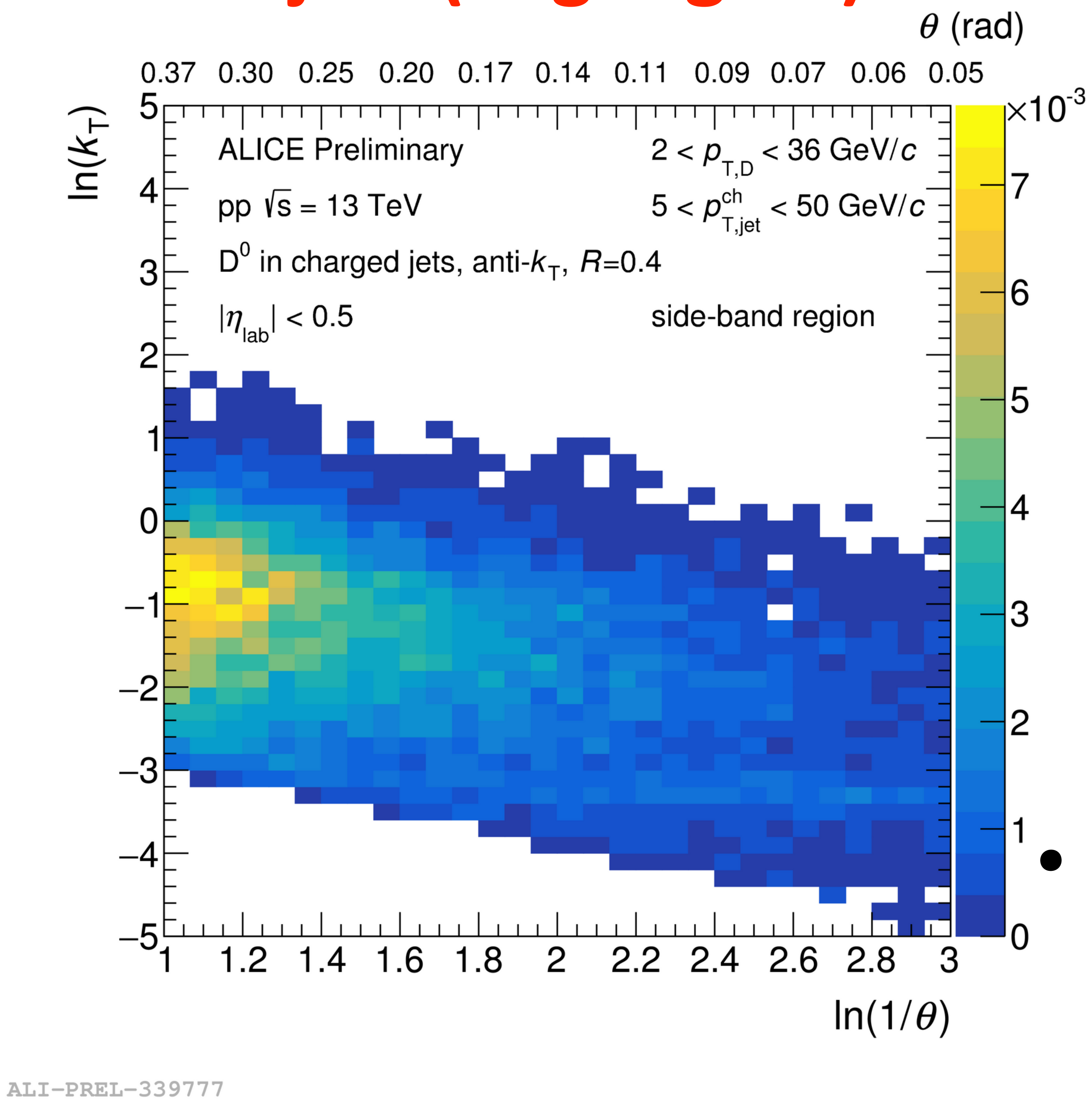

D^0 from D^* decays

$$\rho^{D^0\text{jet}} = \sum_i \frac{1}{\varepsilon_i}\left(\rho(\theta,E)_S^{D^0\text{jet candidate}} - \frac{A_S}{A_B}\rho(\theta,E)_B^{D^0\text{jet candidate}}\right)$$

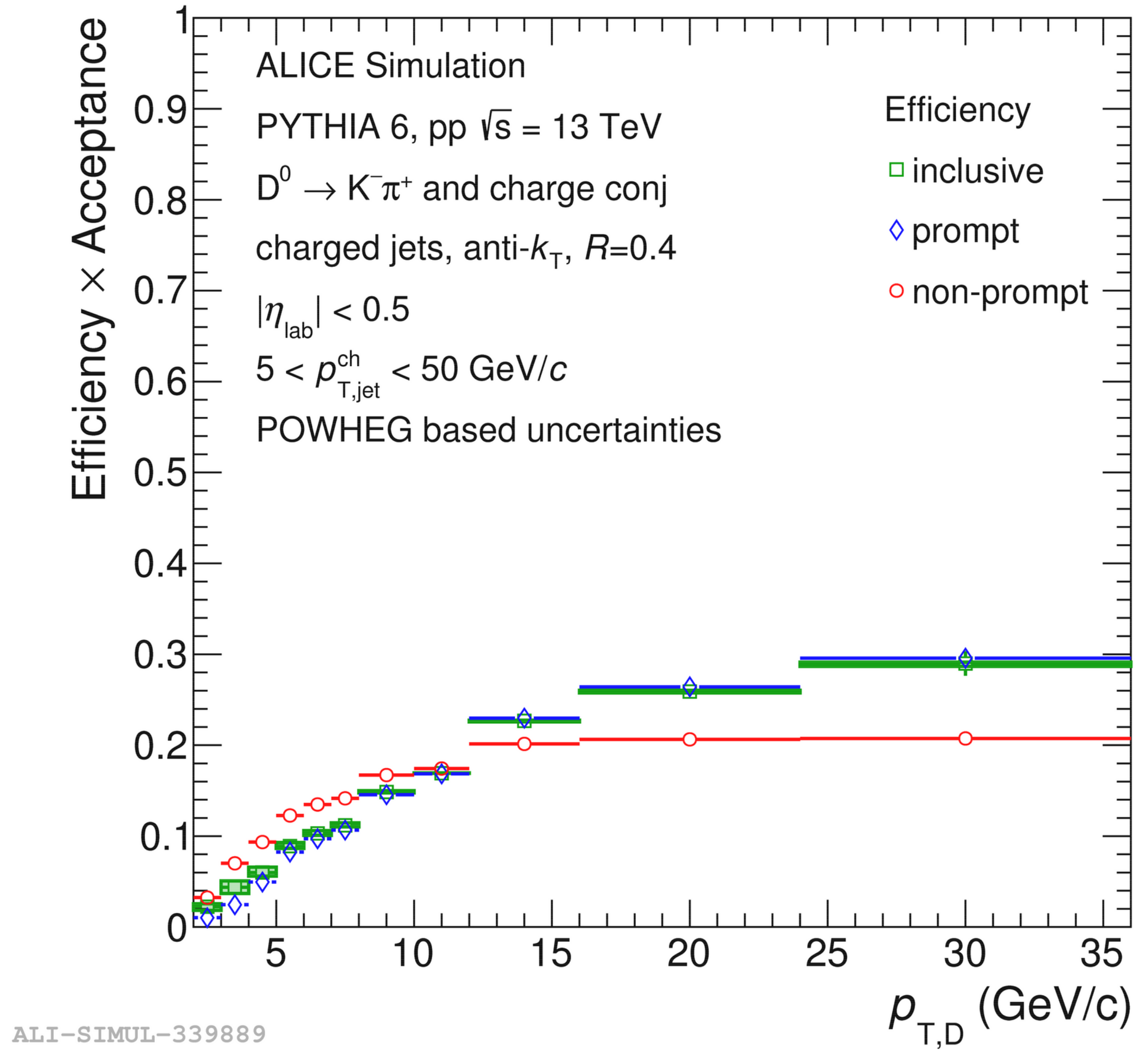

- The topological and PID cuts used for the D candidate selection have finite efficiency
- The prompt and non-prompt fractions at detector level are estimated by weighting POWHEG cross sections with the experimental efficiencies

The emission maps of HF and inclusive jets

D jets (side-band subtracted)

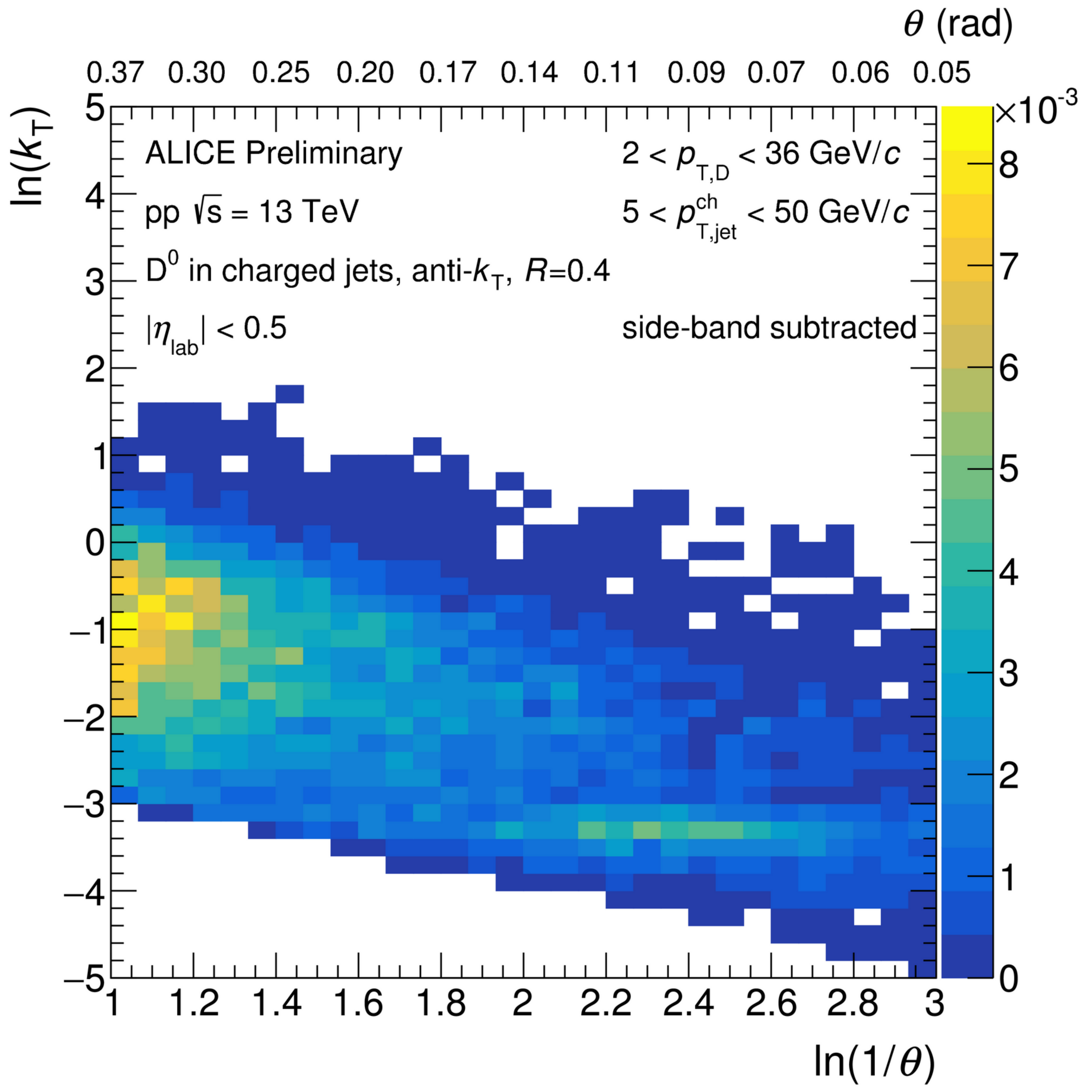

ALI-PREL-339746

Inclusive jets

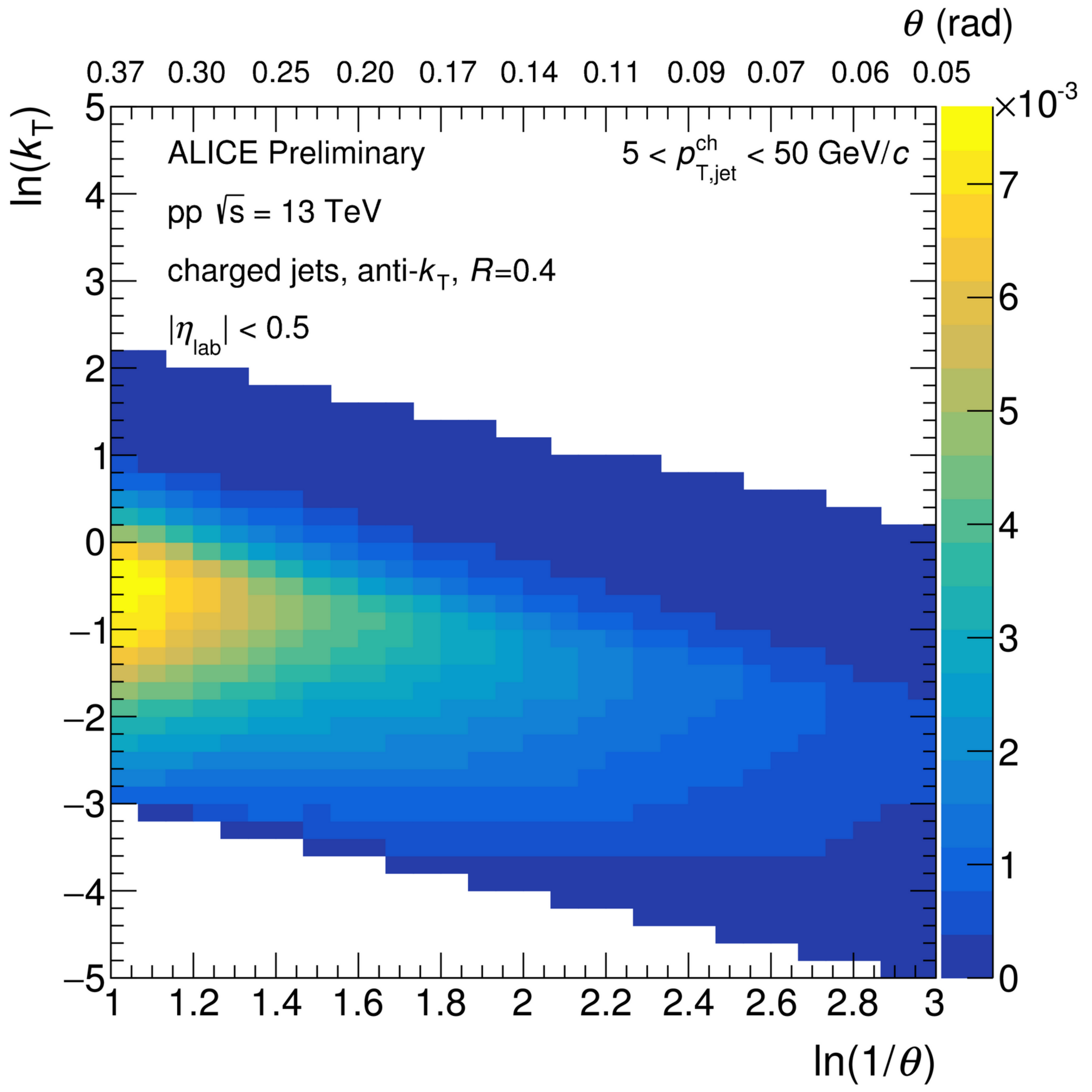

ALI-PREL-339786

Our main observable is the ratio of projections onto the θ axis for D and inclusive jets

The emission maps of HF and inclusive jets

D jets (side-band subtracted)

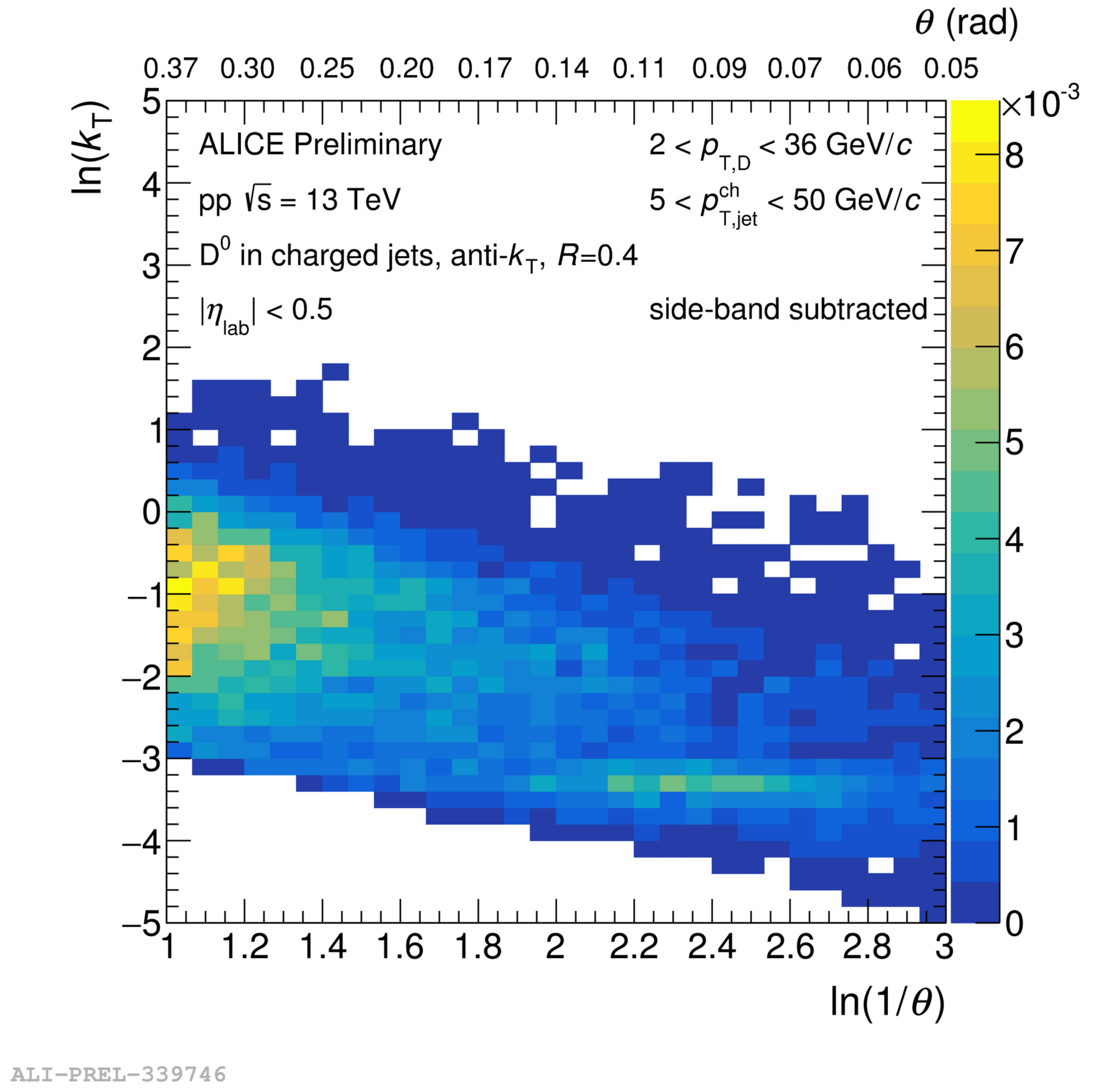

Inclusive jets

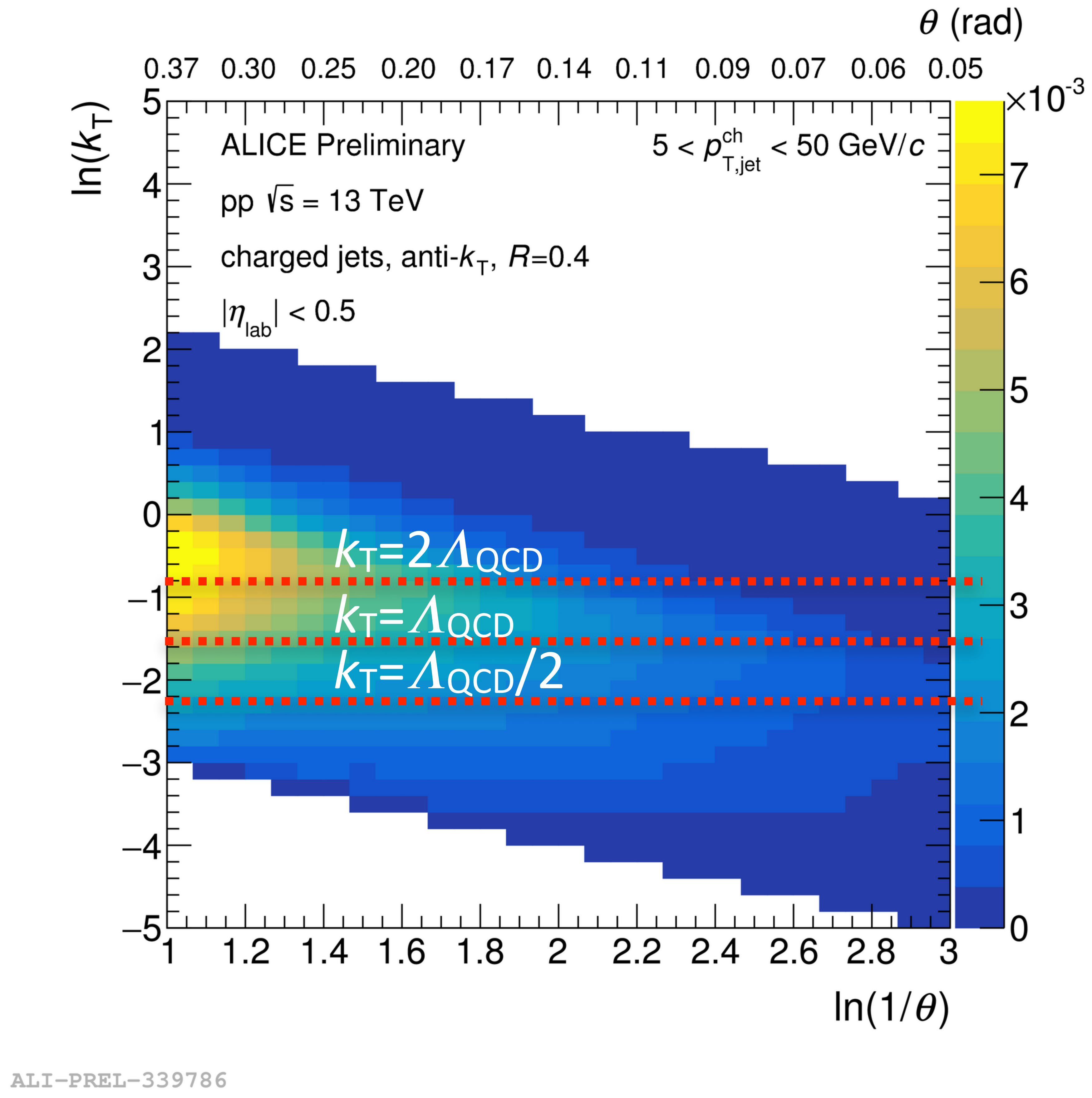

k_T cuts are applied to suppress hadronisation effects

Detector effects cancel out in the ratio

The dead-cone effect, exposed

ALICE, Nature 605, 440-446 (2022)

$$R(\theta) = \frac{1}{n^{D^0\text{jets}}} \frac{dn^{D^0\text{jets}}}{d\ln(1/\theta)} \Big/ \frac{1}{n^{\text{inclusive jets}}} \frac{dn^{\text{inclusive jets}}}{d\ln(1/\theta)} \Bigg|_{k_T > x\Lambda_{QCD}}$$

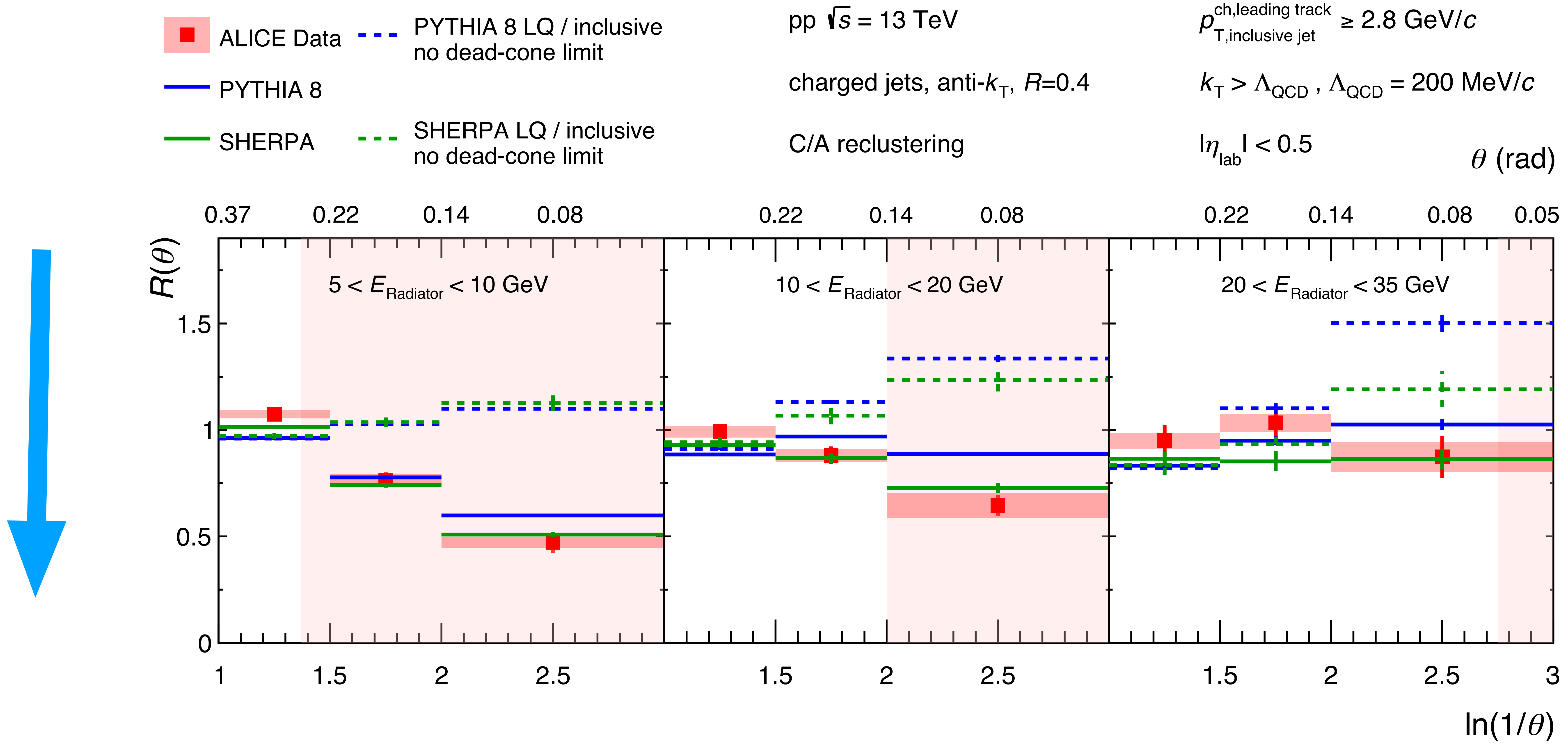

- Suppression of emissions at low angles for D^0 jets as compared to inclusive jets
- Smaller effects for higher splitting energy

Probing the Q->Qg splitting!

The dead-cone effect, exposed

[ALICE, Nature 605, 440-446 (2022)](#)

$$R(\theta) = \frac{1}{n^{D^0\text{jets}}}\frac{\mathrm{d}n^{D^0\text{jets}}}{\mathrm{d}\ln(1/\theta)} \Big/ \frac{1}{n^{\text{inclusive jets}}}\frac{\mathrm{d}n^{\text{inclusive jets}}}{\mathrm{d}\ln(1/\theta)}\Bigg|_{k_T > x\Lambda_{QCD}}$$

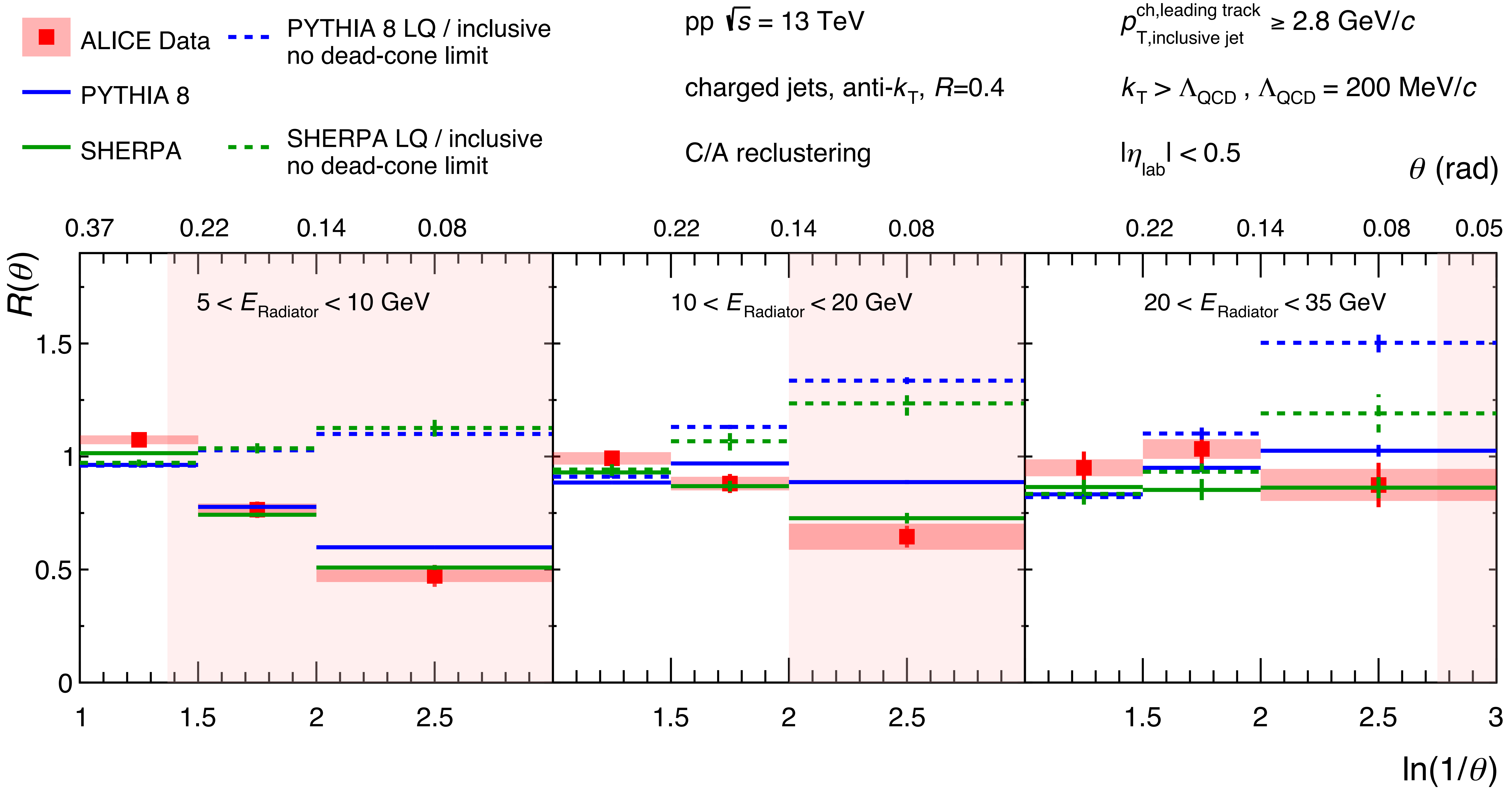

shaded regions are expected dead cone for charm mass of 1.275 GeV in each Erad bin

- Suppression of emissions at low angles for D^0 jets as compared to inclusive jets
- Smaller effects for higher splitting energy

Probing the Q->Qg splitting!

The dead-cone effect, exposed

[ALICE, Nature 605, 440-446 (2022)](#)

$$R(\theta) = \frac{1}{n^{D^0\text{jets}}}\frac{dn^{D^0\text{jets}}}{d\ln(1/\theta)} \Big/ \frac{1}{n^{\text{inclusive jets}}}\frac{dn^{\text{inclusive jets}}}{d\ln(1/\theta)}\Bigg|_{k_T > x\Lambda_{QCD}}$$

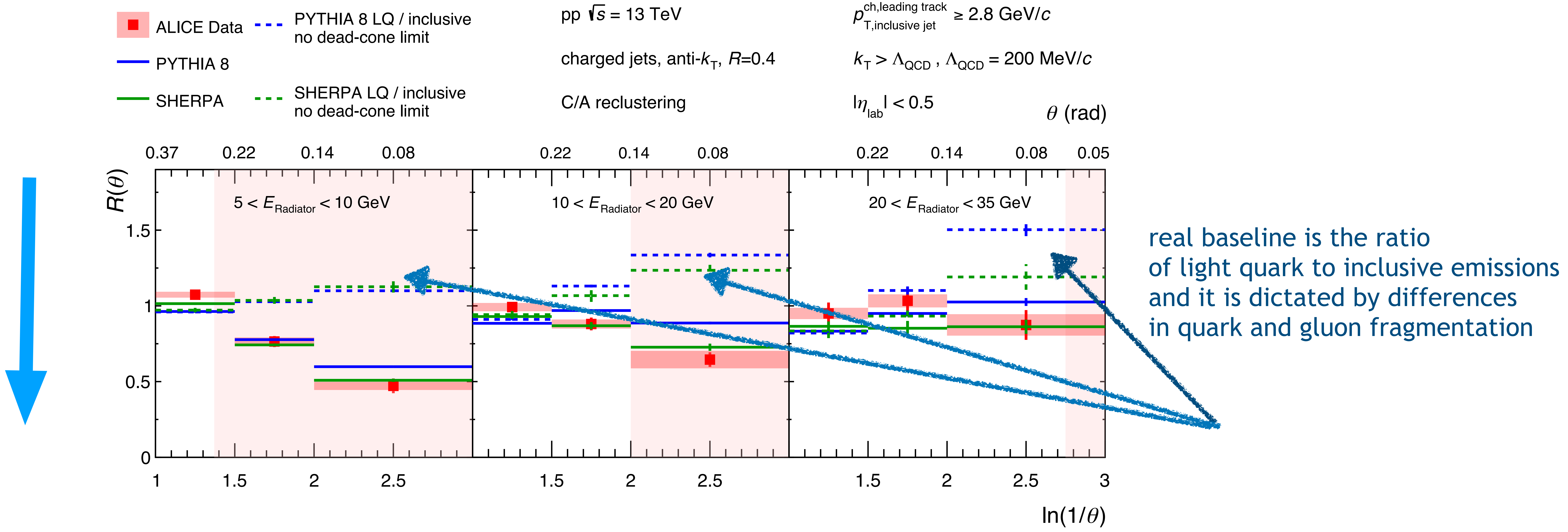

- Suppression of emissions at low angles for D^0 jets as compared to inclusive jets
- Smaller effects for higher splitting energy

Probing the Q->Qg splitting!

HF jet substructure prospects

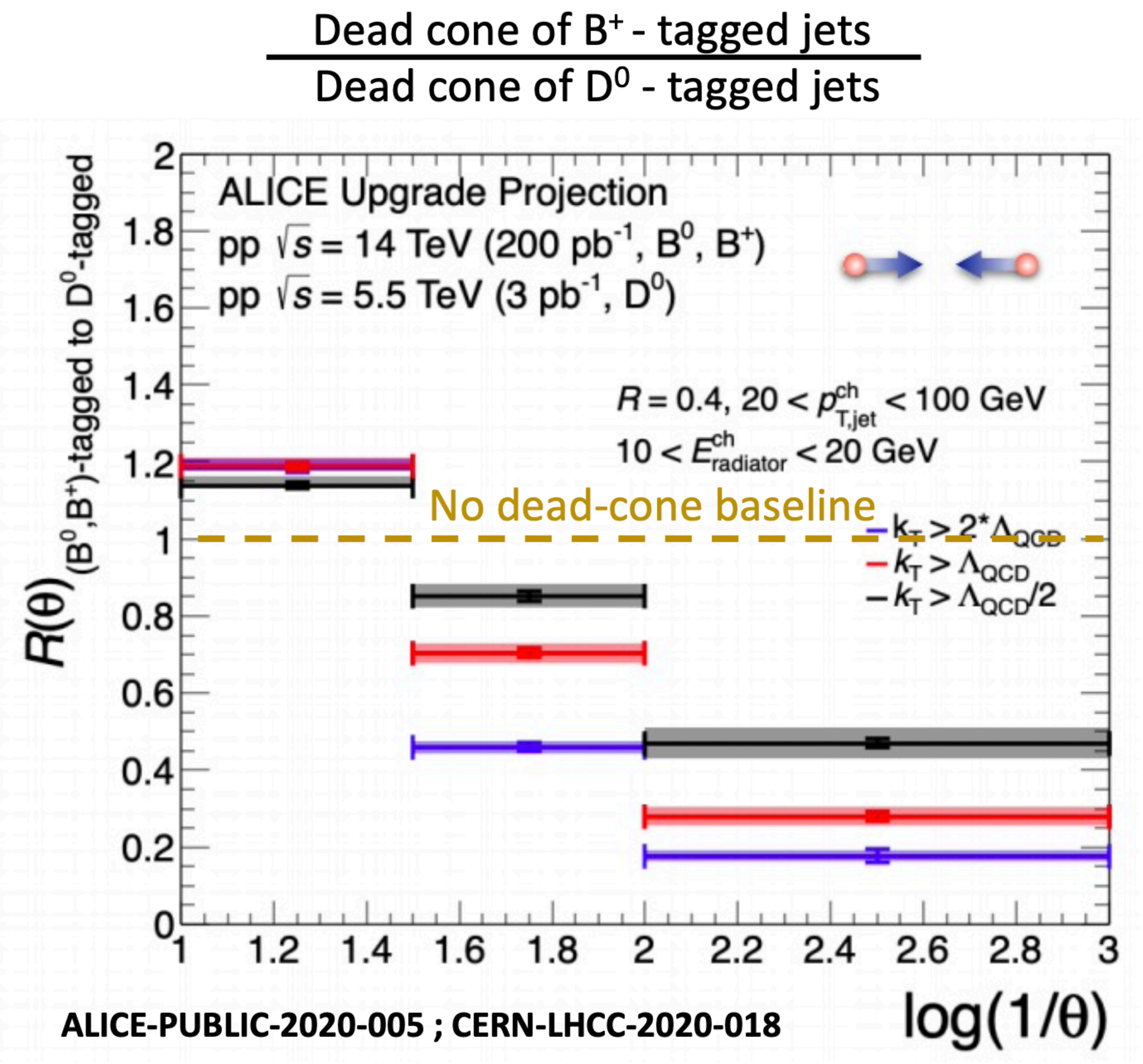

Mass scan: access to fully reconstructed beauty and charmed hadrons

Possibility to isolate mass effects by cancelling out color effects in B to D ratios, unambiguous baseline

Ideal: full reconstruction of heavy flavour hadrons. If not, deal with decay prongs

Very interesting scenario in PbPb where medium-induced radiation can fill the dead cone

Summary Lessons 1-2

Jet definitions allow us to access the parton kinematics

Modern algorithms used at colliders are IRC safe. Anti-k_T is used as default due to its resilience against soft background

New techniques like grooming or the iterative declustering allow to isolate different physics effects and constrain the parton shower ->prominent example is the Lund Jet Plane

Beyond utility for searches and constraining SM calculations, new techniques expose building blocks of QCD like the splitting function, or quantum properties like the dead cone effect or the color flow. This opens up a wide window of opportunities in the context of heavy ion collisions as we will see in the next lessons